MicroRNA and Epigenetic Controls of $CD4^+$ T Cells' Activation, Differentiation and Maintenance

by

Chaoran Li

Department of Immunology
Duke University

Date:_____

Approved:

_____
Qi-Jing Li, Supervisor

_____
Weiguo Zhang, Chair

_____
Thomas Tedder

_____
You-Wen He

_____
Xiao-Fan Wang

Dissertation submitted in partial fulfillment of
the requirements for the degree of Doctor
of Philosophy in the Department of
Immunology in the Graduate School
of Duke University

2014

ABSTRACT

MicroRNA and Epigenetic Controls of $CD4^+$ T Cells' Activation, Differentiation and Maintenance

by

Chaoran Li

Department of Immunology
Duke University

Date:_____

Approved:

_____
Qi-Jing Li, Supervisor

_____
Weiguo Zhang, Chair

_____
Thomas Tedder

_____
You-Wen He

_____
Xiao-Fan Wang

An abstract of a dissertation submitted in partial fulfillment of
the requirements for the degree of Doctor
of Philosophy in the Department of
Immunology in the Graduate School
of Duke University

2014

Abstract

As a major component of the adaptive immune system, $CD4^+$ T cells play a vital role in host defense and immune tolerance. The potency and accuracy of $CD4^+$ T cell-mediated protection lie in their ability to differentiate into distinct subsets that could carry out unique duties. In this dissertation, we dissected the roles and interplays between two emerging mechanisms, miRNAs and epigenetic processes, in regulating $CD4^+$ T cell-mediated responses. Using both gain- and loss-of-function genetic tools, we demonstrated that a miRNA cluster, miR-17-92, is critical to promote Th1 responses and suppress inducible Treg differentiation. Mechanistically, we found that through targeting Pten, miR-17-92 promotes PI3K activation. Strong TCR-PI3K activation leads to the accumulation of DNMT1, elevated CpG methylation in the *foxp3* promoter, and suppression of *foxp3* transcription. Furthermore, we demonstrated that an epigenetic regulator, methyl CpG binding protein 2 (MeCP2), is critical to sustain Foxp3 expression in Tregs, and to support Th1 and Th17 differentiation in conventional $CD4^+$ T cells (Tcons). In Tregs, MeCP2 directly binds to the CNS2 region of *foxp3* locus to promote its local histone H3 acetylation; while in Tcons, MeCP2 enhances the locus accessibility and transcription of *miR-124*, which negatively controls SOCS5 translation to support STAT1, STAT3 activation and Th1, Th17 differentiation. Overall, miRNAs and epigenetic processes may crosstalk to control $CD4^+$ T cell differentiation and function.

Contents

List of Figures

Acknowledgements

There are a number of people that I would like to thank for their support and help during my PhD training. First, I would like to thank my mentor, Dr. Qi-Jing Li, for everything that he had taught me, not just in research, but also in everyday life. I am extremely grateful for the time and effort he takes in training me on how to think critically, present clearly, and write logically. I could not have asked for a better mentor for my PhD training.

Next, I would like to thank every past and present members of the Li lab, Shan, Baojun, Erik, Regina, Siqi, Elizabeth, Jose, for their help, advice, and discussion. I want to show my special gratitude to Shan, who has been a great colleague and comrade to work with. Without her contributions, this dissertation would have been impossible.

I would also like to thank to my committee members, Drs. Weiguo Zhang, You-Wen He, Thomas Tedder, and Xiao-Fan Wang for keeping me on track and providing me with valuable suggestions throughout my graduate training. My fellow classmates Ian, Jacquelyn, Emily and Ashley have been my first friends in US and I am grateful for their support and kindness. I also want to thank the Duke Flow Cytometry Facility, especially Nancy Martin for the assistance on cell sorting.

Finally, I would like to thank my family for their love and support. My parents have been my role models throughout my life and they have given me incredible

encouragement when things were not working so well in graduate school. I want to thank my wife, Xiao-yu, for sharing every happy and sad moments in life with me, and for supporting me through every difficult decisions that I had to make in the past 6 years. At last, I want to say thank you to my son, Ben. You are the best thing that ever happened to me and I am grateful for every joy that you brought to me.

1. Introduction

1.1 Overview of T cell-mediated immune responses

T cell-mediated cellular immunity makes up an important component of the immune system and is critical to protect the host from infections and malignancies. To initiate a T cell response, foreign or altered self-antigens from pathogens and tumors are first taken, processed and displayed on the surfaces of antigen-presenting cells (APCs) in the form of a peptide-major histocompatibility complex (pMHC), which was then recognized by an antigen-specific T cell receptor (TCR) on the T cells. Antigen recognition initiates massive downstream signaling cascades, causing naïve T cells to undergo extensive expansion and functional differentiation for pathogen clearance. Upon resolution of primary responses, the majority of T cells undergo contraction via programmed cell death; however, a small population of antigen-specific T cells is maintained as a memory pool and is poised to respond rapidly upon secondary exposure to the same antigens[1]. Understanding the molecular mechanisms of how T cell responses are regulated is essential for the development of novel therapeutic strategies to treat infections, cancers, and autoimmunity. In this dissertation, I dissected the role of two regulatory machineries controlling $CD4^+$ T cell differentiation and function: microRNAs (miRNAs)[2] and epigenetic processes[3].

1.2 T helper cell differentiation and maintenance

In general, mature T cells can be divided into two groups: $CD4^+$ helper T cells and $CD8^+$ cytotoxic T cells. One interesting characteristic that separates helper T cells from cytotoxic T cells is their ability to differentiate into functional diverse sub-lineages that are capable of carrying out unique immune functions under different immunological settings[4]. Among these, Th1 cells are responsible for the clearance of intracellular infection and are implicated as the effectors in various malignancies and inflammations; Th2 cells control extracellular microbe infection as well as mediate chronic inflammation and allergic responses; Th17 cells contributes to host defense against extracellular bacterial and fungi and have also been linked to a growing list of autoimmune disorders; in addition, peripheral naïve $CD4^+$ T cells can convert to $Foxp3^+$ regulatory T cells (Tregs) that play an important role to maintain immune tolerance particularly in the mucosal barrier[5]. During malignancy, they can also be exploited by tumors to promote immune evasion[6]. In addition to the peripheral derived inducible Tregs (iTregs), Tregs can also develop from the thymus (called "tTreg or nTreg"). Because tTregs undergo a relatively distinct developmental process and possess several unique features[7], I will briefly introduce them in this section and discuss them in further detail in section 1.3.

1.2.1 T helper cell differentiation

1.2.1.1 Role of TCR signaling in T helper cell differentiation

The four T helper subsets mentioned above share a common feature: TCR signaling is an absolute requirement for their differentiation[8]. TCR-pMHC engagement and co-stimulation activate various downstream signaling pathways that eventually lead to the activation of several important transcription factors such as nuclear factor of activated T-cells (NFAT), activator protein 1 (AP-1), and nuclear factor kappa-light-chain-enhancer of activated B cells (NF-κB). Through direct binding to the promoters or enhancers of signature cytokine genes or by regulating the master regulators of each T helper subset, these transcription factors promote Th differentiation. However, since these factors are commonly employed during differentiation of all four Th lineages[8], how, then, do $CD4^+$ T cells determine to which fate they should commit? One way to achieve this is through sensing the specific cytokine milieu that is shaped by distinct inflammatory or tolerogenic conditions. This mechanism will be discussed in detail in section 1.2.1.2. Besides, accumulating evidence suggested that the density of antigens as well as the strength/duration of TCR signaling also dictate the fate determination of naïve $CD4^+$ T cells during Th differentiation[9]. This was first demonstrated in Th1/Th2 polarization by Bottomly and colleagues[10,11] and further confirmed by Paul's group[12]. By using natural and synthetic variants of the moth cytochrome C (88-103) peptide in the context of the MHC II molecule I-E^k, they showed that in general, weak signalling leads to Th2 differentiation while strong signalling favours Th1 commitment. This inhibition of Th2 differentiation by strong TCR stimulation was partially explained by the strong

and prolonged ERK activation that suppressed early GATA3 expression and IL-2R-mediated STAT5 activation, both of which are critical for Th2 differentiation[12]. Besides Th2 cells, it was recently reported that Th17 and iTregs also favour low-strength TCR stimulation for optimal differentiation[13-15]. The PI3K-Akt-mTOR axis downstream of TCR activation has been suggested to be critical for the inhibition of iTreg differentiation by strong TCR stimulation[14]. However, the underlying molecular mechanism and whether other pathways downstream of TCR signaling are also involved in this process are not fully understood. In Chapter 4, we attacked this question with a TCR transgenic system and showed that this is regulated through epigenetic mechanisms (See Chapter 4 for details).

1.2.1.2 Role of cytokine environment in T helper cell differentiation

As mentioned above, the cytokine milieu provides another layer of guidance for the unique lineage choice of naïve $CD4^+$ T cells during their fate specification[8]. In general, in response to infections or malignancy, innate immune cells become activated rapidly and secrete cytokines to quickly shape the microenvironment for Th differentiation. The unique set of cytokines generated under each condition then bind to their receptors on $CD4^+$ T cells and initiate the differentiation process by activating a distinct signal transducer and activator of transcription (STAT). These STAT proteins are central to shape a unique active enhancer landscape for individual Th lineage[16]. In addition, they could also drive the expression of master transcription factors, which in

turn take advantage of the enhancer landscape to specify and reinforce lineage fate determination.

Th1 differentiation is initiated by STAT1, which is activated by IL-27 produced from APCs and IFN-γ from NK cells. STAT1 induces the expression of T-bet, the master transcription factor for Th1 cells[17]. T-bet then directly drives IFN-γ production and opposes the inhibitory effect of GATA3 on Th1 differentiation[18]. At the same time, expression of IL-12Rβ2 was induced by T-bet to allow activation of STAT4 by IL-12 produced from APCs[19]. STAT4 then further promotes IFN-γ expression, which in turn boosts STAT1 activation through a positive-feedback loop to reinforce Th1 commitment.

Th2 differentiation is initiated by the induction of its master transcription factor GATA3[20]. GATA3 could be induced either through IL-4 mediated STAT6 activation[20], or through Notch-mediated, IL-4-independent pathway[21]. During this process, TCR stimulation also drives the production of IL-2 and upregulation of the IL-2R complex, which lead to STAT5 activation. Activated STAT5 then binds to *il4ra* locus and upregulate IL-4Rα expression to boost the IL-4R-STAT6 axis, and, in conjugation with GATA3, directly binds to *il4* locus to promote IL-4 expression. IL-4 then reinforces Th2 commitment through this autocrine feedback loop[20].

Both Th17 and iTreg differentiation require TGF-β, which promotes their lineage choice through at least two mechanisms: TGF-β may indirectly promote Th17 and iTreg commitment through inhibiting Th1 and Th2 differentiation; or, TGF-β could directly

drive the expression of the lineage specific transcription factors of Th17 and iTreg cells, RORγt and Foxp3, respectively[22]. RORγt and Foxp3 antagonize each other's function through direct and indirect mechanisms[23]. The divergence of these two lineages depends heavily on the distinct STATs that are activated during this process. In the presence of IL-6, STAT3 is activated and it directly upregulates RORγt and IL-17 expression through binding to their genomic loci. Activated STAT3 also suppresses iTreg differentiation by inhibiting the expression of Foxp3 and its interactions with RORγt. On the other hand, when IL-2 is present, it leads to the activation of STAT5, which potentiates iTreg differentiation through directly binding to *foxp3* locus and promoting Foxp3 expression[3]. Activated STAT5 also suppresses the Th17 lineage by competing with STAT3 for binding to the *il17* locus[24].

1.2.2 Maintenance and plasticity of T helper cell

Although different T helper subsets have been initially widely recognized as stable and "terminally differentiated" lineages, accumulating evidences have now favored that there are actually significant phenotypic flexibility and plasticity in these cells[25]. By definition, each distinct T helper subset was originally characterized by the expression of a unique cytokine signature. However, it was now clear that, under certain polarizing condition, a specified T helper subset could be induced to produce the signature cytokines from opposing subsets. For example, Th17 cells often co-express IFN-γ and IL-17 in a variety of autoimmune settings, and in some cases, they may even

completely convert to IFN-γ single producers[26]; also, during LCMV infection, *in vitro*-differentiated IL-4-producing Th2 cells could produce IFN-γ following adoptive transfer[27]; and although there are still some debates, Tregs (especially iTregs) could lose Foxp3 expression and produce inflammatory cytokines[28]. What adds up to the complexity of this issue is that T helper cells can also express more than one master regulator[29]. For instance, during myelin oligodendrocyte glycoprotein (MOG)- induced experimental autoimmune encephalomyelitis (EAE), a substantial portion of T cells that infiltrate into the central nervous system are T-bet$^+$RORγt$^+$, and these cells are highly pathogenic. In addition, besides Foxp3, Tregs can co-express T-bet, GATA3, or RORγt, all of which have functional relevance. During type I inflammation, Foxp3$^+$Tregs upregulate T-bet, which drives the expression of CXCR3 to guide Tregs to traffic to the site of inflammation. In barrier sites such as the GI tract and skin, Tregs express GATA3, and it is critical for the maintenance of Foxp3 expression during inflammation. In human peripheral blood and lymphoid tissues, a substantial portion of Tregs co-express Foxp3 and RORγt. These cells also express CCR6 and could strongly inhibit effector T cell proliferation. The remarkable plasticity in T helper cells may have some evolutionary benefit. For example, this would allow them to adapt to the new microenvironment when facing new threats and challenges, which will be extremely beneficial for the host defense[25].

1.3 Treg differentiation and maintenance

A hallmark of adaptive immunity is the ability to distinguish "self" and "non-self". T cells must quickly respond to invasions from foreign pathogens but at the same time refrain or tolerate from the detrimental responses against self and food antigens. Majority of this tolerance is thought to be achieved through negative selection in the thymus, in which most of the self-reactive T cells are deleted, and through anergy, in which lymphocytes become functionally inactivated in response to antigens when there is lack of co-stimulation. However, having these two tolerogenic mechanisms seem to be insufficient to provide full protection against immune-mediated pathology. Indeed, a specialized subset of T cells was required to act "in trans" to suppress pathogenic inflammation[30]. These cells are called regulatory T cells (Tregs). Tregs express the surface marker CD25 and the master transcription factor Foxp3[31]. Foxp3 is not only essential for the development of Tregs but also crucial for the maintenance of their lineage identity and suppressive function[5]. Consequently, mutation of Foxp3 in humans causes IPEX (immunodysregulation polyendocrinopathy enteropathy X-linked) syndrome, a fatal lymphoproliferative immune-mediated disorder, and targeted deletion of Foxp3 in mice led to similar lethal autoimmune syndrome[5]. In addition to restraining the deleterious response against self-antigens, Tregs were also crucial to limit excessive inflammatory responses against commensal microbiota, infections, and tumors. Therefore, understanding how Tregs are differentiated and maintained has a tremendous

therapeutic potential for various immune-mediated diseases. As mentioned earlier, Tregs can differentiate from both the thymus (tTreg or nTreg) and periphery (iTreg). Since the differentiation process of iTreg has been discussed in section 1.2, I will mainly focus on nTregs in this following section.

1.3.1 Treg differentiation

1.3.1.1 Role of TCR signaling in Treg differentiation

Similar to the differentiation of most T cell subsets, Treg development in the thymus also requires TCR signaling and CD28 mediated co-stimulation. TCR/CD28 signaling activates many transcription factors such as NFAT, NF-κB (C-Rel), AP-1, CREB1, which directly bind to *foxp3* locus and induce its expression[5]. Perturbation of these signaling pathways with genetic manipulations leads to significant reduction of Treg frequency and Foxp3 expression, demonstrating a crucial role of TCR/CD28 signaling in orchestrating nTreg development. In addition, nTreg differentiation also depends heavily on the strength of TCR signals that they receive[5]. The early observations that nTregs express higher level of CD25, CD5 and CTLA4, all induced by stronger TCR stimulation, suggested that nTregs are selected by TCR signals with increased strength. Analysis of TCR transgenic mice in the RAG-deficient background further supported this idea: Tregs bearing a transgene-encoded TCR that recognize a self-peptide can only develop when a high-affinity cognate ligand, but not a low-affinity ligand is co-introduced in the thymus by another transgene[32]. TCR repertoires studies

later suggested that Tregs are likely to be selected by TCR signals with strength range between those that mediate positive selection of conventional $CD4^+$ T cells and those that mediate negative selection of high-affinity self-reactive T cells[33].

1.3.1.2 Role of cytokine signaling in Treg differentiation

Although it is now commonly accepted that TCR signal plays an instructive function for Treg differentiation, it by itself is not sufficient to specify the Treg lineage in the thymus. Signals from the common gamma-chain (γc) cytokines (IL-2, and to a less extent, IL-7 and IL-15) and TGF-β are also required for nTreg differentiation. IL-2 or IL-2Rα deficient mice have a 50% reduction of the frequency and absolute number of Tregs in the thymus[34], and additional ablation of IL-7 and IL-15 signaling completely abrogate nTreg development[35]. IL-2 signaling leads to activation of transcription factor STAT5. Since STAT5 binds to *foxp3* promoter and CNS2 region, IL-2 signals may directly facilitate Foxp3 induction through STAT5 activation. Consistently, T cell specific deletion of STAT5 leads to a significant reduction of $Foxp3^+$ Tregs in the thymus[36]. However, IL-2-STAT5 pathway may also facilitate nTreg differentiation through other mechanisms, such as promoting the proliferation or survival of nTregs or their precursors. In agreement with this idea, forced expression of prosurvival molecules such as Bcl-2 in STAT5-deficient cells sufficiently rescued the defect of nTreg differentiation[37]. In addition to IL-2, TGF-β is another cytokine that was critical for nTreg differentiation. In neonatal mice with specific TGF-βRI deficiency in T cells, there is a substantial

impairment of nTregs development in the thymus[38]. It was then found that TGF-β signaling leads to the activation of Smads, which bind to the CNS1 region of *foxp3* locus and directly induces its expression[39]. However, there could also be other explanations. For example, it was recently found that TGFβRII deficient Tregs in the thymus express high level of proapoptotic proteins Bim and undergo extensive apoptosis during agonist antigen-mediated selection[40]. So TGF-β may also facilitate nTreg differentiation indirectly through promoting their survival during negative selection.

1.3.2 Treg stability and maintenance

It was recently reported that various T helper subsets have unexpected plasticity and could be induced to produce signature cytokines of other T helper subsets. This raises the question that whether the previously thought "stable" and "distinct" $Foxp3^+$ Treg lineage could also be "reprogrammed" into effector T cells in response to certain environmental cues. Recent studies have brought up a very complicated and controversial picture.

The first suggestions that Tregs are unstable came from studies using *in vitro* culture of sorted $Foxp3^+$ Tregs from several different Foxp3 reporter mice. When sorted $Foxp3^+$ Tregs were cultured with TCR stimulation and various T helper polarizing cytokines (such as IL-6, IL-4, TNF), a small fraction of them lose Foxp3 expression, and these "ex-Tregs" acquire ability to produce inflammatory cytokines such as IFN-γ, IL-2 and IL-17[41,42]. This was further confirmed later by *in vivo* experiments with adoptive

transfer of these sorted Foxp3$^+$ Tregs into lymphopenic recipients. Since these approaches all involve cell sorting, the potential outgrowth of few contaminating Foxp3$^-$ cells may contribute to the outcome of these experiments. However, this is less likely because Foxp3$^-$ cells spiked into Foxp3$^+$ cells fail to grow out in lymphopenic hosts, and even double sorted (>99.99% purity) Foxp3$^+$ cells will generate ex-Tregs in these settings[43]. Recently, genetic fate mapping approaches have been utilized to study the stability of Foxp3 expression in Tregs without involving cell sorting and adoptive transfers. Bluestone and colleagues generated a mouse model to label these ex-Tregs *in vivo* by crossing the BAC transgenic mice expressing GFP-Cre fusion protein under the control of the *foxp3* promoter with ROSA26-STOP-YFP reporter mice[44]. In these mice, cells that have a history of Foxp3 expression will be labelled with YFP and cells that are currently expressing Foxp3 will be GFP positive. Strikingly, in naïve mice, they found that around 10-15% of YFP$^+$ cells are Foxp3 and GFP negative, and this number increases significantly in mice under strong inflammation (such as in diabetic NOD mice). Collectively, these suggest that at least a small proportion of Tregs become unstable, particularly during inflammation.

Despite the above evidences for inflammation-induced Treg destabilization and reprogramming, this notion has evoked great controversy. First, the pivotal job of Tregs is to maintain immune tolerance. If Tregs could easily lose Foxp3 and convert to effectors, how can they suppress inflammation so effectively? From the immunotherapy

angle, given that many Foxp3$^+$ Tregs have self-reactive TCRs, it could be a catastrophe if these unstable Tregs are used to treat autoimmune disorders[43]. Against this "plasticity" model, Tregs have shown significant potency to treat various immune-mediated inflammatory diseases in both mouse and pre-clinial models (eg: IBD, RA). In addition, some recent studies have provided counter evidence against the "plasticity" model. Particularly, Rudensky and colleagues have used a different genetic lineage-tracing model to demonstrate that there is little or no conversion of Tregs into effectors during physiological and various inflammatory conditions[45]. In this model, DNA encoding a GFP-Cre-ERT2 fusion protein was knocked into the 3′ UTR of endogenous *foxp3* gene and these mice were then crossed with ROSA26-STOP-YFP reporter mice. This allows an inducible but heritable labelling of cells that are express Foxp3 during the tamoxifen treatment with YFP. When these mice were examined 2 weeks or 5 months after tamoxifen induced labelling, they found that very few (<5%) YFP$^+$ cells are negative for Foxp3 expression. Furthermore, this number is not increased under various inflammatory conditions such as sublethal irradiation and infection with *listeria monocytogenes.* Therefore, it was concluded that Tregs exhibit tremendous stability under both physiological and pathological conditions.

There could be at least several explanations for the discrepant data observed from these studies[43]. First, the different inflammatory conditions used (T helper polarizing conditions, adoptive transfer into lymphopenic recipients vs. infection and

irradiation model) may contribute to the different outcome. Also, the two lineage tracing models have different time window of labelling. Foxp3-GFP-Cre BAC transgenic model labels ex-Tregs that are accumulated from ontogeny till adulthood, while the Foxp3-GFP-Cre-ERT2 model only start to label these cells upon tamoxifen treatment. Although this controversy is far from reconciliation at this time, one common observation from these studies is that there seem to be certain heterogeneity within the Treg lineage: even in the "plasticity" models, only a relatively small proportion of Tregs (10% to 15%) may lose Foxp3 expression, while majority of mature Tregs seem to be highly committed and exhibit stable Foxp3 expression. This observed stability in most of Tregs implies the existence of dedicated machinery governing the maintenance of Foxp3 expression. Several transcription factors and epigenetic mechanisms have been implicated to be involved in this machinery. We will discuss these aspects in further detail in section 1.5.3.

1.4 The role of miRNAs in T cell activation and differentiation

While the signaling pathways and transcription factors controlling T cell activation and differentiation have been studied extensively over the past two decades, recent studies clearly pointed out an emerging role of a group of small non-coding RNAs in the regulatory networks governing this process. miRNAs are small (around 21-24 nucleotide long) endogenously expressed non-coding RNAs that regulate gene

expression post-transcriptionally[46]. They are first transcribed into a longer primary miRNAs (pri-miRNAs) and further processed by RNase III enzymes Drosha and Dicer into the mature form. These mature miRNAs are then loaded to the miRNA-induced silencing complex (miRISC) and guide it to specific target mRNAs through complementary base pairing. miRISC induces degradation of target mRNAs and/or inhibits their translation. The 2-8 nucleotides from the 5′ end of miRNA (seed sequence) are the major determinants of the specificity of target recognition and are thus used widely in target prediction. The miRNA-mediated regulatory network is highly complex. Each miRNA may have multiple mRNA targets; conversely, each mRNA may be targeted by multiple different miRNAs[47]. Adding to this complexity, the miRNA-mediated targeting is also context-dependent and the dominant functional target of a single miRNA may vary between different cell types and/or during different biological processes.

Recent studies suggest that miRNA-mediated gene regulation represents a fundamental layer of posttranscriptional genetic programs in immune cells and has broad effects on their development, activation, differentiation, and effector function[48]. An intact miRNA-mediated regulatory network is required for the maintenance of immune homeostasis and induction of immune activation against pathogens; and perturbation of this machinery may contribute to immunopathology during

autoimmunity and cancer. Thus, understanding how the miRNA-mediated network regulates immunity has great therapeutic potential.

1.4.1 Regulation of T cell activation by miRNAs

Early evidence of the involvement of miRNAs in T cell activation came from analysis of T cells lacking certain essential factors in the miRNA biogenesis pathway. These studies showed that global disruption of the miRNA machinery leads to incompetence of T cell proliferation and survival, as well as aberrant Th effector differentiation and cytokine production[49]. While these studies clearly indicated a critical role of miRNA-mediated regulation of T cell activation in general, it failed to provide a comprehensive picture of the miRNA regulatory network, because the phenotype observed in these T cells with global miRNA disruption might result from an integration of both the negative and positive effects of individual miRNAs regulating these processes. Therefore, it is important to dissect the role of individual miRNAs in T cell activation.

To screen for individual miRNAs that regulate T cell activation, Mark Ansel and colleagues took a systemic approach to transfect T cells that lack global miRNA expression with individual synthetic miRNA oligonucleotides, and screened for the miRNAs that could sufficiently rescue the proliferative defect in these cells[50]. Among the miRNAs that could promote proliferation, they found two miRNA seed families (miR-17 family and miR-92 family) that were significantly enriched. We also independently

identified that miRNAs from the miR-17-92 cluster were significantly increased upon T cell activation and were crucial to promote T cell proliferation and survival during T cell activation[51]. While this miRNA "add-back" approach is informative in determining the dominant miRNAs that contribute to the defects in T cells with global miRNA disruption, it also has its drawbacks. As mentioned above, because the hypoprolferation of T cells with global miRNA disruption could result from an "add up" of the loss of both pro-proliferative miRNAs and anti-proliferative miRNAs, many important miRNAs that regulate T cell responses might be overlooked by this approach. In this regard, expression profiling for miRNAs that are dynamically regulated during T cell development and activation is very informative and has led to the identification of many important miRNAs that regulate these processes.

miR-181a is one such regulator of T cell activation[52]. Expression analysis showed that expression of miR-181a is highly dynamically regulated during T cell maturation and activation. In the thymus, miR-181a expressed highly in the DP stage, but was reduced significantly as T cells matured to the CD4 and CD8 SP stages. Its level was further reduced to merely ~10 copies/cell when peripheral naïve $CD4^+$ T cells were activated by TCR stimulation. This sequential reduction of miR-181a level correlates well with the decreased sensitivity of T cells during these developmental and activation processes and suggested that it may play an important role in regulating TCR signaling strength. Indeed, further gain and loss-of-function studies showed that through

targeting multiple phosphatases that blunt TCR signals, miR-181a significantly augments TCR signaling strength and promotes T cell activation. In addition, the reduction of miR-181a upon TCR activation was proposed to be a negative feedback mechanism to fine-tune the TCR signaling strength against antigens[53].

Besides miR-181a, several other miRNAs have been suggested to regulate T cell activation by targeting key components of the pathways downstream of TCR engagement. We and others found that by targeting PTEN, miR-17-92 critically supports the activation of PI3K-Akt axis and T cell proliferation/survival[54]; NFAT and NF-κB activation induce the expression of miR-155, which targets Ship1 and Socs1 to promote T cell activation and expansion[55]; miR-146a is also upregulated by NF-κB activation and it inhibits T cell activation through a negative feedback loop that involves its targets Traf6 and Irak1[56].

1.4.2 Regulation of T helper cell differentiation by miRNAs

As introduced earlier, T helper cell differentiation is a highly regulated process when a T cell senses and interprets signals from antigens (TCR signal strength) and environmental cues (cytokine signaling). Therefore, it is not surprising that many of the key miRNAs that regulate T cell activation also influence T helper differentiation.

We identified miR-17-92 as a potent driver for Th1 mediated responses[54]. Naive T cells with genetic deletions of miR-17-92 showed a significant reduction in IFN-γ production under Th1 polarizing conditions *in vitro*. Conversely, Overexpression of

miR-17-92 in T cells with a transgene or a retrovirus encoding the miR-17-92 gene promotes Th1 differentiation. In addition, miR-17-92-deficient T cells are more prone to differentiate into Foxp3$^+$ iTregs when exposed to TGF-β *in vitro*. Because of its vigorous control over the Th1 cell iTreg balance, the loss of miR-17-92 in CD4$^+$ T cells results in tumor evasion in an allograft model of B16 melanoma. Recently, we found that miR-17-92 is also required for optimal Th17 responses during EAE. Reconstitution of T cells that lack miR-17-92 with individual miRNAs identified miR-17 and miR-19b as the functional representative of the whole cluster in regulating these processes. Mechanistically, the aberrant Th1, Th17 and iTreg differentiation with miR-17-92 deficiency could at least be in part explained by the accumulation of its *bona-fide* target PTEN and the subsequent blunted PI3K-Akt activation.

miR-155 is another miRNA that influences multiple aspects of T helper differentiation[47]. miR-155-deficient mice are highly resistant to EAE and had significantly reduced footpad inflammation during delayed-type hypersensitivity (DTH) response. Further *in vitro* and *in vivo* analysis showed that miR-155-deficient CD4$^+$ T cells have defective Th1 and Th17 differentiation, but showed a moderate bias toward Th2 differentiation and IL-4 production. In addition, some of the aged miR-155 mice developed spontaneous lung inflammation that showed characteristics of enhanced Th2 mediated immune pathology. Among the many identified miR-155 targets, Socs1, Ship1

could be responsible for its regulation on Th1 and Th17 differentiation, while cMaf contributes to the aberrant Th2 responses.

In addition to the aforementioned miRNAs that have broad effects on T helper cell activation and differentiation, several miRNAs were shown to specifically affect the differentiation of unique Th lineages. miR-29a and miR-29b were potent inhibitors of Th1 differentiation. Transfection of miR-29a and miR-29b into $CD4^+$ T cells that lack all mature miRNAs sufficiently reduced the aberrant elevated IFN-γ production from these cells[50]. Transgenic mice with a "miRNA sponge" that competes with endogenous miR-29 targets showed enhanced Th1 responses and greater resistance to infections with *Listeria monocytogenes* or *Mycobacterium tuberculosis*[57]. Further biochemical analysis revealed that Tbx21(T-bet), Eomes, and Ifng are functional relevant targets of miR-29 in its regulation of Th1 differentiation. miR-326 is an important regulator of Th17 differentiation[58]. Expression profiling experiments showed that the level of miR-326 is significantly elevated in patients with multiple sclerosis and in mice with aggressive EAE symptoms. $CD4^+$ T cells that overexpress miR-326 had enhanced Th17 differentiation while introduction of a miR-326 sponge reduced Th17 differentiation. The effects of miR-326 were attributed its *bona-fide* target, Ets1, which is a negative regulator of Th17 differentiation.

1.4.3 Regulation of Tregs by miRNAs

Early implications for miRNA's role in Tregs came from analysis of mice with T cell specific Dicer deficiency. It was shown that these mice lacking miRNAs in T cells had a significant block of Treg development in the thymus, as well as reduced iTreg differentiation *in vitro*. Consequently, many of these mice developed spontaneous inflammation and immunopathology as they aged[59]. In addition, restricted deletion of Dicer or Drosha in Foxp3$^+$ Tregs led to unstable Foxp3 expression in Tregs and early onset of spontaneous autoimmunity[60,61]. These studies suggested that miRNAs are not only important for Treg differentiation but also crucial for their maintenance and suppressive function.

Expression profiling experiments have identified several miRNAs that are differentially expressed between conventional CD4$^+$ T cells and Tregs, which play important roles in Treg differentiation and maintenance. Among these, miR-155 was shown to be a direct target of Foxp3 and was highly expressed in Tregs. miR-155 deficient mice had reduced percentages and numbers of Treg in the thymus and spleen. Mechanistically, miR-155 was shown to target Socs1 directly, which is a negative regulator of the IL-2-STAT5 signaling pathway. Therefore, miR-155 is critical for the competitive fitness of Tregs[62]. In addition, miR-146a was shown to play a critical role in regulating Treg suppressive function. miR-146a-deficient Tregs have elevated expression of Stat1, which contributes to IFN-γ mediated Th1 pathology[63].

1.5 The role of epigenetic mechanisms in CD4$^+$ T cell differentiation, plasticity, and maintenance

Activation of transcription factors downstream of receptor-mediated signaling is crucial to dictate the fate determination of CD4$^+$ T cell during differentiation. However, the ability of these factors to modulate gene transcription also depends on the state of chromatin and its underlying DNA, which is governed by epigenetic mechanisms[3]. Epigenetic processes are modifications that affect potentially heritable phenotypes and gene expression without altering the DNA sequences. In mammals, these epigenetic processes include, but are not limited to, DNA methylation, histone modifications, and higher-order chromatin structure. Through epigenetic processes, gene transcription programs in differentiating or differentiated cells can be faithfully inherited by progeny cells, but at the same time preserve the potential to be modified in response to altered environmental signals. Here in this section, we will discuss some of the major components of the epigenetic machinery and how they control the differentiation and maintenance of CD4$^+$ T cells.

1.5.1 Key components of the epigenetic machinery in CD4$^+$ T cells

1.5.1.1 DNA methylation

DNA methylation is a process that involves the addition of a methyl group to the cytosine nucleotide. In mammals, methylation mostly occurs in the cytosines in CpG dinucleotides. These CpG dinucleotides may form clusters that are typically 300-3000

base pairs long, termed CpG islands. Methylation of the CpG islands in the promoter and some important distal cis- regulatory elements can inhibit gene transcription in two major ways. DNA methylation could directly physically block the binding of transcription factors to the gene promoters or distal elements; or it may also provide docking sites for methyl-CpG-binding domain proteins (MBDs) that recruit other chromatin remodeling proteins to form a compact and inactive heterochromatin, thereby inhibiting transcription[3]. In mammalian cells, there are mainly two classes of DNA methyltransferases (DNMT) that catalyze DNA methylation: DNMT1, and DNMT3 (includes DNMT3a and DNMT3b). DNMT1 is mainly responsible for the maintenance of DNA methylation during DNA replication but it is suggested to also have *de novo* methyltransferase activity, while DNMT3 could methylate unmethylated DNA at a relatively high rate and it was shown to mainly function as *de novo* methyltransferase. Because of its fundamental regulation of gene induction, silencing, and maintenance, DNA methylation is involved in many biological processes, such as development, differentiation, and proliferation. Not surprisingly, aberrant DNA methylation and mutations in the DNA methylation machinery have been implicated in the pathogenesis of many diseases including cancer and autoimmunity.

1.5.1.2 Histone modifications

Besides DNA methylation, histone modifications are another type of epigenetic process that controls the accessibility of chromatins. The basic unit of chromatin is the

nucleosome, which consists of a piece of 146-base-pair DNA wrapping around an octamer of histone protein cores. The histone octamer contains two copies of each of the histones H2A, H2B, H3 and H4. In addition, the N-terminal tails of histone proteins can be modified posttranslationally through acetylation, methylation, phosphorylation, and ubiquitination[64]. These modifications may affect chromosome function either by (i) altering the electrostatic charge of the histone, thus leading to a structural change in chromatin accessibility, or (ii) by creating or removing certain binding sites for proteins that could regulate transcription. The association of various histone modifications with transcriptional activity has led to the "histone code" hypothesis[65], which states that histone modifications create a code that is recognized by regulatory proteins that contain certain protein domains, and this may dictate the potential of active transcription or silencing of genes. Recent genome-wide studies have identified several core histone modifications that are associated with and could faithfully predict genes and regulatory elements that are active, silenced, or inactive but poised[66]. For example, cis-elements of genes that are accessible or are actively transcribing can be characterized by the acetylation of various residues of histone H3 and H4, as well as by the mono-, di-, or tri-methylation of H3 lysine 4 (H3K4). In contrast, regulatory regions of genes that are silenced usually lack these active modifications, but are instead marked with di- or tri-methylation of H3K27 and H3K9. Finally, promoters and enhancers of genes that are poised for activation or silencing either lack both of these two types of modifications, or

have both permissive and repressive modifications. This poised state allows these genes to quickly "turn on" or "turn off" when the cells sense signals from altered environmental cues. In addition, it is worth emphasizing that although these histone marks were originally identified by their association with different transcription states, accumulating data confirmed that they do not merely mark "past events" but indeed have direct effect on the transcriptional competence of genes. For instance, treatment of cells with various inhibitors that block certain histone acetylations or DNA methylation could significantly alter gene expressions and cell phenotypes[67,68].

1.5.2 Role of epigenetic mechanisms in T helper cell differentiation and plasticity

1.5.2.1 Epigenetic regulation of T helper cell differentiation

Early indications of epigenetic regulation of T helper cell differentiation came from studies that identified multiple key cis-regulatory elements controlling the transcription of the genes encoding signature cytokines of each Th subset. Based on the sequence conservation among species and the presence of hallmark epigenetic modifications, multiple conserved non-coding sequences (CNS) were identified in the *ifng*, *il4*, and *il17* loci and were confirmed to have enhancer activity both *in vitro* and *in vivo*. These studies further showed that these cis-elements within the signature cytokine loci are associated with active epigenetic marks in featured lineages while exhibit repressive marks in the other lineages[3]. For example, in Th1 cells, the *ifng* locus exhibits high levels of permissive H3K4 dimethylation and H3 acetylation, and CpG islands in

the promoter and most CNS regions are completely unmethylated; in contrast, the *il4* locus is enriched with repressive H3K27 trimethylation and significant CpG methylation. On the other hand, in Th2 cells, the *il4* locus is permissive while the *ifng* locus is silenced. Importantly, disruption of the machinery of these modifications with small inhibitors or genetic tools has a tremendous effect on T helper cell differentiation, suggesting that there is a causal relationship between epigenetic mechanisms and cell phenotypes. Although it is now clear that epigenetic modifications of the signature gene loci play a critical role in T helper cell differentiation, how these chromatin modifications are regulated and their interplay with upstream signaling pathways are much less known. Recent global epigenome studies suggested that cytokine receptor signaling is central in shaping the chromatin landscape of T helper cells through activation of different STATs[16]. Particularly, a substantial proportion of the global active histone modifications in Th1 cells are dependent on STAT4 and STAT1, while STAT6 has a major role in generating the active enhancer landscape in Th2 cells. Importantly, expression of the lineage specific master regulators failed to fully re-establish the STAT-dependent enhancer landscape. These studies provide a potential mechanism by which differentiating $CD4^+$ T cells could sense environmental cues and translate them into modifications of the enhancer architecture. However, several important questions still remain. First, since these studies mainly focused on histone modifications, how DNA methylation is regulated in differentiating T helper cells is much less clear. Second, as

TCR signaling strength also plays an important role in determining the fate of T helper cells, whether and how it may influence the epigenetic modifications need to be addressed. Lastly, the previous studies focused on transcription factors that could recruit enzymes that directly catalyze the histone modification or DNA methylation reaction, but whether the availability of these enzymes is dynamically regulated during differentiation has been overlooked. For these purposes, we have examined the level of various DNMTs in $CD4^+$ T cells that received TCR signals with different strength and duration[69] (See Chapter 4). We found that the abundance of DNMT1 and DNMT3 proteins are positively regulated by high-affinity and prolonged TCR signals. This elevated abundance then leads to increased enrichment of DNMTs to the promoter of *foxp3* gene, and consequently causes enhanced CpG methylation and suppression of iTreg differentiation. This suggests that epigenetic regulation of $CD4^+$ T cell differentiation could also be enforced by TCR signaling, which calls for a further comprehensive investigation in the future.

1.5.2.2 Epigenetic regulation of T helper cell plasticity

In the absence of environmental perturbations, the unique epigenetic characteristics in the cytokine gene loci for different T helper subsets are in accordance with their relatively stable cytokine production. How, then, could we explain the substantial plasticity of T helper cells, especially when they are exposed to altered environmental cues? Several recent studies showed that in contrast to the cytokine genes,

the epigenetic features of the master transcription factors are less entrenched and may be more accessible to for chromatin remodeling[70]. For example, in Th1 cells, the *il4* gene is completely methylated and exhibits very little permissive H3K4 trimethylation but high levels of repressive H3K27 trimethylation, which is suggestive of gene silencing. However, looking at master transcription factors, in Th1 cells, the *gata3* (the Th2-specifying transcription factor) locus not only remains partially methylated, but is also associated with bivalent histone modifications that maintain accessibility. Such a strategy keeps the locus in a "poised" state, thereby preserving a certain degree of lineage plasticity. For further investigation, it will be critical to identify the pioneer factors that are able to bind to these bivalent features to initiate chromatin remodeling for "re-differentiation".

1.5.3 Role of epigenetic mechanisms in Treg differentiation and stability

Unlike the conventional T helper cells whose functions are mainly characterized by their ability to make one or two signature cytokines, the identity of Tregs is not only featured by the production of various immune-suppressive cytokines (eg: TGFβ, IL-10, IL-35), but also defined by the constitutive expression of many surface molecules (eg: CTLA-4, GITR, CD39) that could inhibit target cell proliferation or function. Expression of these Treg signature genes is mainly, if not all, controlled by the master transcription factor of Tregs, Foxp3[71]. Therefore, although several recent studies have started to assess the epigenetic aspects of these Foxp3-regulated genes, the majority of studies have

focused on dissecting the epigenetic mechanisms that regulate expression of the *foxp3* gene. Sequence conservation and specific epigenetic modification patterns have identified several important conserved non-coding regions, all of which were shown to be involved in the regulation of *foxp3* expression.

The *foxp3* promoter is a classic TATA and CAAT box-containing promoter that is located around 6kb upstream of the translational start site of *foxp3* gene. It contains a CpG island, which is completely demethylated in Tregs and heavily methylated in opposing lineages such as Th1 cells[72]. Interestingly, in resting conventional $CD4^+$ T cells, this region is still largely demethylated, suggesting that naïve $CD4^+$ T cells are poised for Foxp3 induction. The *foxp3* promoter contains six binding sites for NFAT and AP-1, which promote the transcription of *foxp3* in response to TCR signaling[73]. This agrees with the absolute requirement of TCR stimulation for both nTreg and iTreg differentiation. However, it was also very clear that TCR signaling with enhanced strength actually inhibits Foxp3 induction during iTreg differentiation. This suggests that strong TCR stimulation must also negatively control Foxp3 expression through a more dominant pathway. Indeed, we found that extensive TCR activation could limit the chromatin accessibility of *foxp3* locus through enhancing the CpG methylation of *foxp3* promoter, thereby preventing the binding of transcription factors such as NFAT and AP-1 and blocking *foxp3* transcription[69] (See Chapter 4 for further details).

The second important conserved region controlling *foxp3* expression is a TGF-β sensitive region (CNS1) that contains binding sites for SMADs. The chromatin region of CNS1 is also more accessible in Tregs than other T helper subsets and naïve conventional $CD4^+$ T cells, as indicated by increased histone acetylation[74]. Moreover, mice with genetic deletion of CNS1 contain a normal nTreg compartment, but exhibit a 50% reduction in TGF-β-dependent iTreg differentiation[75]. This partial reduction clearly shows that SMADs-mediated chromatin remodeling of CNS1 upon TGF-β treatment is required for Foxp3 induction from conventional $CD4^+$ T cells; nevertheless, since neutralization of TGF-β could completely abolish iTreg differentiation[76], it also indicates that other pathways downstream of TGF-β signaling may also be involved. We recently found that through activation of the p38 pathway, TGF-β could decrease the abundance of DNMT1 and subsequently reduce CpG methylation of the *foxp3* promoter[69], thereby providing a SMADs-independent mechanism for TGF-β-induced Foxp3 expression.

CNS2 is the third highly conserved non-coding region that regulates Foxp3 expression. It contains a CpG island, which is completely demethylated in nTregs but is fully methylated in conventional $CD4^+$ T cells[72]. The enhancer activity of CNS2 depends highly on its demethylation state, as methylation of CNS2 significantly inhibits the binding of transcription factors to this region[77]. Interestingly, as opposed to CNS1, CNS2 seems to be irrelevant for the induction of Foxp3 but instead is important for the maintenance of Foxp3: mice with a specific deletion of CNS2 have normal nTreg and

iTreg development, but they cannot stably maintain Foxp3 expression in the progeny of mature nTregs[75]. This suggests that factors that bind to CNS2 are potential regulators of Treg stability. Indeed, it was recently reported that a protein complex containing transcription factors Runx1/CBFβ and Foxp3 itself binds to CNS2 in a demethylation-dependent manner and this is critical for the maintenance of high level of Foxp3 in nTregs[75]. This "autoregulatory loop" enforced by Foxp3 provides an intriguing model for the remarkable stability of nTregs under homeostatic conditions. However, it might not be sufficient to explain how the majority of nTregs are still able to maintain Foxp3 expression even during inflammation (see section 1.3.2). We and others have recently found that inflammatory stimulation could prone the silencing of Foxp3 expression by inducing CpG methylation in the CNS2 region. Since this silencing epigenetic modification disfavors the binding of transcription factors known to regulate *foxp3*, there must be additional factors that are able to resist such modifications to safeguard *foxp3* expression. Indeed, we recently identified methyl CpG binding protein 2 (MeCP2) as such a unique rescuer (See Chapter 5 for details). Unlike other traditional transcription activators such as Runx1 and Foxp3, MeCP2 favors binding to methylated DNA and was therefore enriched in the partially methylated CNS2 region, where it promoted local histone H3 acetylation to counteract the silencing modification. We further demonstrated that the transactivation role of MeCP2 for *foxp3* during inflammation is dependent on CREB1, a well-known partner for the acetyltransferase complex CBP/p300:

in the absence of MeCP2, the binding of CREB1 to CNS2 was completely abolished; and when the activation of CREB1 was blocked, the stabilizing influence of MeCP2 on the local chromatin structure and *foxp3* expression was largely reversed. Thus, in addition to the Runx1/CBPβ/Foxp3 complex, MeCP2 provides an additional layer of protection for *foxp3* stability, especially under inflammatory conditions.

A fourth regulatory cis-element in the *foxp3* locus (CNS3) was identified recently. CNS3 was proposed to act as a pioneer element for *de novo foxp3* expression, because the accessible histone modifications in CNS3 were present not only in Tregs that are actively expressing Foxp3, but also in thymic and peripheral Treg precursors[75]. A NF-κB family member, c-Rel, was shown to bind to CNS3 and critically supports early Foxp3 induction during Treg differentiation. Consistently, mice with specific deletion of CNS3 or c-Rel have a severe block in nTreg development in the thymus. It remains to be determined whether c-Rel is sufficient to induce the epigenetic modifications in CNS3 and whether other factors are also involved in this process.

2. Materials and methods

2.1 Mice

Mice homozygous for the floxed *mir-17-92* allele (Mir17-92$^{tm1.1Tyj/J}$) and *mecp2* allele (B6.129P2-MeCP2$^{tm1Bird/J}$) were purchased from The Jackson Laboratory. Lck-cre (B6.Cg-Tg(*lck-cre*)1Cwi N9) and Cd4-cre mice(C57BL/6Tac-Tg(*cd4-cre*)N9) were from Taconic. Foxp3-GFP-Cre BAC transgenic mice were kindly provided by Dr. Xiaoping Zhong from the Duke University Medical Center. T cell-specific miR-17-92 or MeCP2 deficient mice were generated by crossing floxed *mir-17-92* mice or floxed *mecp2* mice with the cd4-cre or lck-cre mice. Treg-specific MeCP2 deficient C57BL/6 mice were generated by crossing floxed *mecp2* mice with Foxp3-GFP-Cre mice. With speed congenic service provided by The Jackson Laboratory, mice carrying MeCP2$^{f/f}$ alleles were back-crossed to NOD mice carrying Foxp3-GFP-Cre BAC transgenes. With genome-wide marker-assisted selection protocol, after eight generation of back-crossing, the conditioned MeCP2$^{f/f}$ alleles resides in mice with pure NOD background. 5C.C7 TCR transgenic mice were from Taconic (B10.A$^{Rag2tm1Fwa\ H2\text{-}T18a}$ Tg (Tcra5CC7, Tcrb5CC7)lwep). WT B10.A mice were also from Taconic. All mice were maintained under pathogen-free conditions, and animal experimentation was conducted in accordance with institutional guidelines.

2.2 Quantitative PCR

Total RNA was isolated with miRVana extraction kit (Ambion) according to the manufacturer's instructions. For mRNAs, reverse transcription was performed with qScript™ Flex cDNA Kit (Quanta Biosciences) and gene expression was quantified by SYBR Green based qPCR analysis and normalized to the level of SDHA as internal control. For miRNAs, *E. coli* polyA polymerase was employed to add adenines at the 3' end of RNA molecules lacking a polyA tail. Following oligodT annealing, a universal tag was attached to the 3′ end of cDNAs during the cDNA synthesis using retro-transcriptase superscript III (Invitrogen). With miRNA-specific forward primers and a reverse universal primer mix, the expression of individual miRNAs was quantified by SYBR Green based qPCR analysis and normalized to the level of U6 as internal control.

2.3 Western Blots

Total cell extracts were collected by lysing cells in RIPA buffer in the presence of protease inhibitor cocktail (Roche) and phosphatase inhibitor mix I and II (Sigma). Samples were fractionated by electrophoresis on a 10% SDS polyacrylamide gel (Invitrogen) and electroblotted on to a PVDF membrane. Western blot was performed according to standard protocols with the following primary antibodies: anti-STAT1, anti-STAT3, anti-pSTAT1 (Y701), anti-pSTAT3 (Y705), anti-SOCS1, anti-SOCS3, anti-SOCS5, anti-JAK1, anti-JAK2, anti-JAK3, anti-MeCP2, anti-DNMT1, anti-PTEN, anti-

TGFβRII, anti-CREB1, anti-Bim, anti-p-Smad3 (S423/425), anti-Smad3 (Cell Signaling Technology), anti-DNMT3b (Abgent), and anti-β-Actin (Sigma). Anti-rabbit-Alexa680 and anti-goat-Alexa680 (Invitrogen) were used as secondary antibodies and the fluorescence intensity was measured on an Odyssey system (Licor).

2.4 Cell sorting, staining and flow cytometry analysis

Cell sorting was performed using a MoFlo Legacy sorter, and purity of sorted cells was determined by post-sorting to be at least 98 percent for each experiment. For intracellular cytokine staining, cells were stimulated with 0.9nM PdBU (Phorbol 12,13-dibutyrate) and 0.5μg/mL ionomycin (Sigma-Aldrich) in the presence of 5μg/mL brefeldin A and 2μM monensin (eBioscience) for 4 hours. Cells were fixed with 2% paraformaldehyde, followed by permeabilization with 0.1% saponin (Sigma-Aldrich) and antibody staining. Foxp3 staining was performed using Foxp3 / Transcription Factor Staining Buffer Set and Anti-Mouse/Rat Foxp3 antibody (clone FJK-16s) from eBioscience based on the suggested protocol. For DNMT1, STAT1, pSTAT1 (Y701), STAT3, pSTAT3 (Y705) staining, cells were fixed with 2% paraformaldehyde in PBS, permeabilized with 90% methanol in PBS, and stained with the appropriate primary antibodies or isotype control followed staining with a Pacific Blue secondary antibody. Fluorescence-conjugated antibodies for CD4, CD8, CD25, CD44, CD62L, IL-17A, IFN-γ, IL-2, CD90.1(Thy1.1), CD90.2(Thy1.2) were purchased from Biolegend. The survival of

cells was assessed by staining with the Annexin V, 7AAD (biolegend), and LIVE/DEAD® Fixable Violet Dead Cell Stain Kit (Invitrogen). The proliferation of cells was assessed by CFSE (Invitrogen) dilution and Edu (Invitrogen) incorporation.

2.5 In vitro $CD4^+$ T cell differentiation

Conventional $CD4^+$ T cells from the lymph nodes and spleens of different mice were stimulated by TCR specific peptides or plate bound anti-CD3/CD28 antibodies and cultured under various Th-skewing conditions for 4-7 days. Th1 skewing condition: 50ng/ml recombinant mouse IL-12 (Peprotech), 10μg/ml purified anti-IL-4 (11B11), and 50U/ml recombinant mouse IL-2 (Peprotech)). Th2 skewing condition: 50U/ml recombinant mouse IL-2, 50ng/ml recombinant mouse IL-4 (Peprotech), 10μg/ml purified anti-IFNγ (XNG1.2) and 5μg/ml anti-IL-12 (BD). Th17 skewing condition: 20ng/ml recombinant mouse IL-6 (Peprotech), 4ng/ml recombinant TGFβ (Peprotech), 10μg/ml purified anti-IFNγ (XNG1.2) and 10μg/ml purified anti-IL-4 (11B11). iTreg skewing condition: 0.2 -5.0ng/ml recombinant human TGFβ, 50U/ml recombinant mouse IL-2, 10μg/ml anti-IL-4 (11B11), 10μg/ml anti-IFN-γ (XMG1.2), and 10μg/ml anti-IL-6 (BD). Cytokine production and Foxp3 expression by differentiated $CD4^+$ T cells were determined by intracellular staining.

2.6 Plasmids and retrovirus transduction

The retroviral Foxp3 expression plasmid (Addgene plasmid 24067) was kindly provided by Dr. Dan Littman from New York University. The Vectors expressing miRNAs were cloned by inserting the fragments containing the "pre-" form of miRNAs into the MSCV-PIG-Mock vector. For retrovirus transduction, Tcons or Tregs were stimulated with TCR specific peptides or plate bound anti-CD3/CD28. 18 hours later, cells were transduced with retrovirus in a 24-well plate by spin inoculation at a speed of 1258g for 90 minutes at 37°C.

2.7 miRNA target predictions and luciferase assays

The miRNA target candidates were predicted using multiple methods assembled on the miRecords website (*http://mirecords.biolead.org/*). The 3'UTRs of mouse *pten, tgfbr2, creb1, dnmt1, and socs5* containing predicted binding sites of miR-19b, miR-17, miR-148a, and miR-124 were amplified from a 3' RACE-ready cDNA library generated from mouse T cell total RNAs, and cloned into a luciferase reporter right downstream of the firefly luciferase gene. For normalization, 3T3 cell lines that overexpress individual miRNAs were co-transfected with a renilla luciferase vector (pRL-TK) whose expression is not affected by miRNA targeting. Luciferase activity was determined 48 hours post transfection using a dual luciferase assay kit (Promega). To assess *foxp3* promoter and enhancer activity, we acquired the PGL4, PGL4-Pro and PGL4-Pro-CNS2 constructs[78]

from Dr. Yisong Wan at the University of North Carolina at Chapel Hill. Jurkat T cells were transfected by Nucleofector Device (Lonza) with a non-targeting control siRNA or siRNA against human MeCP2 (150pmol per sample) (Thermo Scientific Dharmacon), together with1μg reporter plasmid or 1μg of pRL-TK plasmid as an internal control. 48 hours after transfection, cells were either untreated, or treated with 0.9 nM PdBU and 0.5 μg/ml ionomycin (Sigma) for an additional 16-24 hours. Firefly and Renilla Luciferase activities were then determined.

2.8 DNA methylation and chromatin immunoprecipitation (ChIP) analysis

Genomic DNA was purified with GenElute™ Mammalian Genomic DNA Miniprep Kit (Sigma). Methylation analysis was quantified by sequencing of genomic DNA after bisulfite conversion using the MethylDetector kit (Active Motif), PCR amplification and cloning. Chromatin immunoprecipitation was done based on a standard protocol with anti-H3Ac, anti-H3K4me2, anti-H3K4me3, anti-H3K27me3 Rabbit polyclonal antibody (Millipore), MeCP2 (D4F3) XP® Rabbit monoclonal antibody, CREB1 (48H2) Rabbit monoclonal antibody (Cell Signaling), rabbit anti-DNMT1 (H300) antibody, mouse anti-DNMT3b mAb (52A1018) (Santa Cruz Biotechnology), or a nonspecific rabbit anti-mouse IgG (Jackson ImmunoResearch Laboratories). The amount of DNA immunoprecipitated by antibodies was quantified

by qPCR using primers specific for the indicated gene-regulatory regions and normalized to the input prior to immunoprecipitation.

2.9 B16 melanoma tumor model and anti-tumor responses assay

B16/F10 melanoma cell line was a gift from Dr. Thomas Tedder (Duke University). The OVA-secreting B16/F0/OVA cell line was kindly provided by Dr. Edith Lord (University of Rochester). In the subcutaneous melanoma tumor model, different mice were anesthetized and injected s.c. on the shaved right lateral flank with $2x10^5$ B16/F10 tumor cells or $3x10^5$ B16/F0/OVA cells in 200 μl sterile PBS. Tumor volumes were monitored and calculated using the equation: $V = 4 (L1 \times L2^2)/3$, where V = volume (mm^3), L1 = the longest radius (mm), L2 = the shortest radius (mm). For the detailed analysis of adaptive anti-tumor responses, lymphocytes from the tumor draining lymph node were isolated 16 days after tumor cell injection and activated with 1 μg/ml plate-bound anti-CD3 and anti-CD28 antibodies for 24 hrs or stimulated with LB27.4 APCs loaded with 10 μM OVA (323-339) for 48 hrs. Cell proliferation, AICD, and cytokine production were measured with CFSE staining, Annexin-V/7AAD staining, and cytokine beads array, respectively.

2.10 Mouse model of delayed-type hypersensitivity reaction (DTH)

Mice were subcutaneously immunized with KLH protein (100μg/mouse) in CFA. 7 days after immunization, mice were rechallenged with KLH (50μg/mouse) or PBS in each lateral footpad. 48 hours later, footpad swelling was measured prior to euthanasia for immunological and histological analysis.

2.11 Mouse model of inflammatory bowel disease (IBD)

Naïve T cells ($CD4^+CD25^-CD45Rb^{high}$) from different mice were mixed with nTregs ($CD4^+CD25^+$) from different mice at various ratios, and injected intraperitoneally into $Rag2^{-/-}$ recipients. Recipients were weighed throughout the course of the experiments and were euthanized at the experimental endpoints for immunological and histological analysis.

2.12 Mouse model of Experimental autoimmune encephalomyelitis (EAE)

For the induction of EAE, 6-10 week old mice were injected with 200ng pertussis toxin in 200ul PBS per mouse i.p. on day0 and day2. On day 0, each mouse was immunized with 100ug MOG peptide emulsified in CFA subcutaneously. Mice were then monitored closely for disease severity using the standard scale: 0, no clinical signs; 1, limp tail; 2, weak paraparesis (weak and incomplete paralysis of one or two hind limbs); 3,

paraplegia (complete paralysis of two hind limbs); 4, paraplegia with forelimb weakness or paralysis; 5, death.

2.13 In vitro Treg suppression assay

1.0×10^5 $CD4^+CD25^-$ conventional T cells from LNs and spleens of $Thy1.1^+$ B6 mice were FACS sorted, labeled with CFSE (Invitrogen) at a concentration of 10μM, and then mixed with sorted $Thy1.2^+$ $CD4^+CD25^+$ Tregs from LNs and spleen of $MeCP2^{fl/fl}$ Lck-Cre or littermate control mice at different ratios. The mixture of cells was then stimulated for 72 hours with 0.5ug/mL soluble anti-CD3 (BioXCell) and 0.5ug/mL soluble anti-CD28 (BioXCell) in the presence of 1×10^5 T cell depleted-splenocytes from B6 mice, which had been pre-treated with 50ug/ml mitomycin C (Sigma) at 37 degrees for 1 hour to serve as APCs. The proliferation of conventional T cells were analysed by CFSE dilution. Cytokine production from conventional T cells or Tregs was analysed by intracellular staining following 4 hours of PdBU and ionomycin stimulation.

2.14 Microarray sample preparation and data analysis

$Thy1.2^+$ $CD4^+CD25^+$ Tregs from LNs and spleen of 6-8 week old $MeCP2^{fl/fl}$ Lck-Cre or littermate control mice were sorted and mixed with $CD4^+CD25^-$ conventional T cells from LNs and spleens of $Thy1.1^+$ B6 mice at ratio of 1 to 4, and stimulated for 72 hours with 0.5ug/mL anti-CD3 and 0.5ug/mL anti-CD28 in the presence of T cell

depleted splenocytes from B6 mice that served as APCs. At the end of culture, viable Thy1.2^{+} wild type and MeCP2-deficient Treg cells were sorted and lysed for RNA. Two rounds of samples from different mice were independently collected. The global gene expression was assessed by GeneChip Mouse Genome 430 2.0 Array from affymetrix using service from the Duke DNA Microarray Core Facility. Microarray data was analyzed using the Partek Genomics Suite, with RMA background correction and mean probeset summarization analysis parameters used. Only non-cross-hybridizing probes that were declared present or marginal in at least one sample (according to the MAS5 file) were considered for analysis. The normalized expression levels were then compared between WT Tregs and MeCP2 KO Tregs. An average fold-change of 1.5 was used as a threshold for differential expression between the two samples. For genes with multiple probes, the fold changes were averaged, resulting in 154 unique, differentially expressed genes.

2.15 Fluorescence microscopy

5C.C7 T cells that were stimulated with different peptides for defined durations were fixed with 4% paraformaldehyde on coverslips, permeabilized with 0.5% Triton X-100 in PBS, and stained with anti-DNMT1 mAb (Cell signaling). A Cy3 Donkey anti-rabbit antibody was used as secondary antibody for fluorescence microscopy**.** Imaging was performed on a Zeiss Axiovert-100TV station equipped with a Zeiss 40X EC Plan-

Neofluar objective lens (NA=1.30), a CoolSNAPHQ CCD camera (Roper Scientific) and a high-speed piezzo Z-motor for Z stack recording.

2.16 Histology

Footpads and colons was excised, inflated with 4% paraformaldehyde in PBS, fixed overnight at room temperature, placed in 70% ethanol, embedded with paraffin, and sent for H&E staining. The histologic scores of colon in IBD model were assessed as previously described[79] in a double-blinded setting.

2.17 Statistics

Two-tailed Student t tests were utilized to determine whether the difference between a given set of means was statistically significant unless otherwise mentioned. Differences with p values of less than 0.05 were considered statistically significant. n.s. : non significant.

3. Dissecting miR-17-92 cluster's critical roles in supporting Th1 mediated immune responses and preventing inducible Treg differentiation: A miRNA modulator of T cell anti-tumor response

The contents of this dissertation chapter have been slightly modified from the following publication:

Shan Jiang*, Chaoran Li*, Virginie Olive, Erik Lykken, Feng Feng, Jose Sevilla, Ying wan, Lin He & Qi-Jing Li (* equal contribution and listed in an alphabetic order). Molecular dissection of the miR-17-92 cluster's critical dual roles in promoting Th1 responses and preventing inducible Treg differentiation. *Blood* 118, 5487-5497 (2011)

3.1 Introduction

$CD4^+$ T cells are essential components of the adaptive immune system that regulate immune responses against foreign pathogens and tumors. Upon antigen recognition, naïve $CD4^+$ T cells undergo activation and expansion, and then contract via programmed cell death[1]. Specific antigen challenges also induce $CD4^+$ T cells to differentiate into distinct T helper lineages characterized by unique cytokine production profiles[8]. Among these lineages, Th1 cells, whose differentiation is controlled by the master transcription factor T-bet[80], are specialized for the clearance of intracellular infections and implicated as the major effectors against tumors[81]. The production of IFN-γ by these cells directly eliminates the tumor cell[82], induces cytotoxic effects indirectly through the activation of macrophages[83], enhance the immunogenicity of tumor cells

and tumor antigen presentation[84], and inhibits angiogenesis[85] , which collectively constitutes the bulk of the effector function of Th1 cells against tumors. Supporting the key role of Th1 cells in the anti-tumor response, mice that lack IFN-γ or are insensitive to IFN-γ-mediated signaling were more vulnerable to carcinoma-induced and spontaneous tumors[86-88]. Additionally, T cell survival and expansion are also essential for the clearance or inhibition of tumor growth *in vivo*, a fact highlighted by the observation that tumors utilize various strategies to suppress T cell proliferation, and to induce their apoptosis[89]. Another remarkable immune evasion mechanism is tumor-induced conversion of effector T cells into inducible $Foxp3^+$ regulatory T cells (iTregs) and subsequent accumulation of Treg cells to transform the tumor microenvironment[6]. Due to their ability to negatively regulate immune responses through inhibiting APCs and effector T cell function[90], Treg cells are suggested to be one of the major barriers to applying anti-tumor immune therapies[91,92]. As a result, enhancing effector T cell expansion, survival, Th1 cytokine production, and blocking iTreg induction are currently the central concerns when conducting anti-tumor T cell immunotherapy. While the protein-based regulatory machinery that operates during the T cell response has been vigorously explored, we have recently become aware of a novel and crucial element modulating T cell function – miRNA [48,52].

miRNAs are 21-24 nucleotide non-coding RNAs that regulate gene expression by destabilizing target mRNAs, leading to degradation or by blocking translation[46]. Recent

studies suggest that miRNA-mediated gene regulation represents a fundamental layer of posttranscriptional genetic programs in metazoan genomes that has broad effects on gene expression[2]. Global disruption of miRNAs caused by deletion of their biogenesis machinery had profound effects on the development of B cells[93], and recent studies indicate that they were also critical for Th1/Th2 differentiation[49,94] and regulatory T cell function[60,95]. In addition to these demonstrations of the importance of miRNA biogenesis in general, accumulating evidence shows that many specific miRNAs are differentially regulated in hematopoietic lineages and suggests that they play an important role in controlling the development and function of immune cells[48,52]. One such regulator is the miR-17-92 cluster. This cluster of miRNAs is encoded by a polycistronic miRNA gene located on human chromosome 13 and has two paralogs: miR-106b-25 on chromosome 7 and miR-106a-363 on the X chromosome[96]. Unlike most miRNAs, which are usually processed from an independent primary transcript, the miR-17-92 cluster gene generates a single transcript that yields six individual mature miRNAs, which can be further grouped into three families based on the similarity of their "seed" regions (nucleotides 2-8): the miR-17 family (miRs-17, 20, and 18a), the miR-19 family (miRs -19a and 19b), and the miR-25 family (miR-92a). miR-17-92 is well recognized as an "oncomiR" due to its potent acceleration of c-Myc-induced lymphoma[97]. Genetic ablation has clearly established miR-17-92's critical roles in embryonic development[98]. This cluster was also shown to promote angiogenesis in endothelial cells during both normal development

and tumor growth[99]. In immune cells, miR-17-92 plays an integral part in the development of myeloid cells and B cells[98,100]. Mice with germ-line deletion of miR-17-92 exhibit a severe defect in adult B cell development with an augmentation of apoptosis in the pro-B cell fraction and consequently a blockade at the pro-B to pre-B transition[98]. Additionally, transgenic mice with ectopic expression of the miR-17-92 cluster in lymphocytes developed lymphoproliferative disease and autoimmunity as early as 18 weeks of age. It was suggested that the overexpression of miR-17-92 unbalances lymphocyte homeostasis via control of the tumor suppressor PTEN and the proapoptotic protein Bim[101].

Due to its extensive roles in promoting malignant transformation in hematologic tumors[102], the miR-17-92 cluster has been put forward as a potential candidate for miRNA-based anti-tumor therapy. However, the global inhibition of miR-17-92 for cancer therapy is largely limited by the lack of knowledge regarding the physiological function of endogenous miR-17-92 in normal tissues, especially in patients' immune systems, which may compromise the efficacy of the therapy. Furthermore, even less is known about the differences or similarities in the functions of individual miRNAs within the cluster during antigen responses. Here, combining both gain- and loss-of-function approaches, we analyzed the physiological roles of individual miRNAs within the miR-17-92 cluster in the regulation of T cells' effector function. Our data establish the miR-17-92 cluster as a multifaceted and indispensible positive regulator of $CD4^+$ T cells'

antigen responses, particularly in the context of Th1 T cell-mediated tumor rejection, suggesting that global inhibition of miR-17-92 is likely to subvert the immune response against tumors. Furthermore, we demonstrate profound functional divergence among the individual miRNAs in this cluster, with miR-19b and miR-17 accounting almost entirely for mir-17-92's pro-Th1 influence, while miR-18a acts as an internal antagonist of the cluster's function.

3.2 Results

3.2.1 miR-19b facilitates T cell proliferation upon antigen challenge

Upon antigen challenge, we observed a rapid decline in the levels of most miRNA species in $CD4^+$ T cells. Among the few miRNAs showing significant augmentation, the miRNAs comprising the miR-17-92 cluster form a distinct group, although the dynamics of mature miRNA elevation varies individually (Figure 1). These phenomena prompted us to explore the intrinsic function of the miR-17-92 cluster during the effector T cell response and to further analyze the individual functions of the component miRNAs.

To characterize miR-17-92's role in $CD4^+$ T cells' proliferation during the expansion phase after antigen engagement, we first infected lymph node T cells from 5C.C7 TCR transgenic mice with a retrovirus encoding the whole primary miR-17-92 transcript. In addition to the cluster, our vector also encoded a puromycin resistance

gene for drug selection and *gfp* as the transduction marker. This resulted in a 5- to 20-fold increase of expression of each of the six miRNAs in $CD4^+$ T cells, in comparison to cells infected with mock virus lacking the miRNA expression cassette (Figure 2A). T cells were then stimulated with CH27 APCs preloaded with the agonist peptide moth cytochrome-c (MCC) for 24 hours, and the proliferation of $CD4^+$ T cells was analyzed by EdU staining. As reported previously[101], we noted a higher percentage of $CD4^+$ T cells in S phase for those cells overexpressing miR-17-92 as compared to cells expressing the mock vector (Figure 2B). We then examined the impact of reduced miR-17-92 expression on $CD4^+$ T cell proliferation by analyzing *mir-17-92* conditional knockout mice, in which the *mir-17-92* locus is flanked by two loxp sites[98] and CD4-Cre expression drove T cell specific deletion (Figure 2C). $CD4^+CD25^-$ conventional T cells from the lymph nodes and spleen were sorted by FACS and stained with CFSE dye, stimulated by plate-bound anti-CD3/CD28, and cell proliferation was examined in terms of CFSE dilution. Reciprocal to the enhanced proliferation of $CD4^+$ T cells overexpressing miR-17-92, the proliferation of $CD4^+$ T cells heterozygous or null for *mir-17-92* was decreased in a gene-dosage-dependent manner (Figure 2D). These results suggested that miR-17-92 is essential for $CD4^+$ T cells' proliferation *in vitro*.

To determine the contribution of each individual miRNA of the miR-17-92 cluster in promoting $CD4^+$ T cell proliferation, we retrovirally transduced either the whole cluster or individual miRNAs back into miR-17-92 deficient $CD4^+$ T cells, and

analyzed $CD4^+$ T cell proliferation via EdU staining. As expected, reconstitution with the miR-17-92 cluster rescued the proliferation defect of miR-17-92 deficient $CD4^+$ T cells. Moreover, we found that miR-19b alone was functionally equivalent to the whole cluster in enhancing $CD4^+$ T cell proliferation (Figure 2E). To our surprise, although it only differs from its family member miR-19b by one nucleotide at position 11, miR-19a failed to promote the proliferation of $CD4^+$ T cells. Also surprisingly, the expression of miR-18a exerted an inhibitory effect on proliferation. These data suggested that miR-19b is the functional representative of miR-17-92 in regulating $CD4^+$ T cells' proliferation upon antigen stimulation.

3.2.2 miR-17 and miR-19b protect $CD4^+$ T cells from activation induced cell death

During the course of an immune response, antigen-reactive T cells clonally expand and then apoptotically contract to maintain immune homeostasis[1]. To determine whether miR-17-92 affected activation-induced cell death (AICD) for $CD4^+$ T cells, we challenged 5C.C7 T cells overexpressing miR-17-92 with MCC peptide as described above and measured AICD via Annexin V/7AAD staining. We noted that miR-17-92 overexpression reduced the proportion of Annexin V^+ $CD4^+$ T cells compared to cells expressing the mock vector (Figure 3A). Reciprocally, peripheral $CD4^+$ T cells from the miR-17-$92^{f/f}$ CD4-Cre^+ and miR-17-$92^{f/+}$ CD4-Cre^+ mice showed reduced survival after anti-CD3 /CD28 stimulation (Figure 3B).

To assess which miRNAs were functionally responsible for the cluster's apparent protective effect, AICD was measured for $CD4^+$ T cells retrovirally transduced with individual miRNAs. miR-19b was responsible for enhancing $CD4^+$ T cell survival following stimulation and miR-17 was also observed to rescue miR-17-92 deficient $CD4^+$ T cells from intense AICD. miR-18a exhibited antagonizing behavior, driving massive apoptosis of $CD4^+$ T cells (Figure 3C).

3.2.3 miR-19b promotes IFN-γ production

The diversity of pathogens demands discrete cytokine combinations from T helper cells, and so an effective adaptive immune response requires appropriate $CD4^+$ T cell functional differentiation. To test whether miR-17-92 is involved in this process, we cultured naïve $CD4^+$ T cells from miR-17-92 deficient mice under Th1 conditions *in vitro*. While around half of the wild type $CD4^+$ T cells were IFN-γ^+, only 10% of miR-17-92-deficient $CD4^+$ T cells produced IFN-γ, which they also produced at much lower levels (Figure 4A). In line with the above observations, while the expression levels of *gata3* and *il4* at Th2 condition were largely unaltered, miR-17-92-deficient Th1 cells exhibited significantly reduced transcription levels of *ifng* and the key Th1 lineage specific factor *tbx21* (Figure 4B). As before, we dissected the individual contributions of the miRNAs in supporting IFN-γ production. Only miR-19b was able to rescue the capacity of IFN-γ production in miR-17-92 deficient Th1 cells (Figure 4C). Collectively, these results

demonstrated an indispensible role for miR-19b in promoting effector T cells' IFN-γ production.

3.2.4 miR-17 and miR-19b promote the *in vivo* Th1 response during delayed type hypersensitivity (DTH)

To investigate whether miR-17-92 facilitates Th1 responses *in vivo*, we assessed the ability of miR-17-92 deficient mice to mount DTH responses. WT and miR-17-92$^{f/f}$ CD4-Cre^{+} mice were immunized with keyhole limpet hemocyanin (KLH) emulsified in complete Freund's adjuvant (CFA), and then re-challenged in one footpad with KLH and with PBS in the contralateral footpad. In agreement with a critical role for miR-17-92 in promoting Th1 mediated effector function, miR-17-92 deficient mice have significantly reduced footpad swelling compared to WT mice (Figure 5A). To determine the function of individual miRNAs *in vivo*, 5C.C7 T cells were transduced with retrovirus encoding miR-17 or miR-19b and then adoptively transferred into B10A recipients. These mice were then immunized with MCC peptide in CFA, and DTH was assessed following footpad re-challenge. With transferred T cells expressing miR-17 and miR-19b, we observed intensified footpad swelling, augmented numbers of lymphocytes in the draining lymph node (dLN), as well as enhanced infiltration in the footpad (Figure 5B, 5C, and 5E). In addition, consistent with its IFN-γ-promoting function *in vitro*, miR-19b substantially enhanced T cells' capacity for IFN-γ production during the DTH response when examined *ex vivo* (Figure 5D). These data supported a general role for miR-17 and miR-19b in facilitating Th1 mediated inflammatory responses *in vivo*.

3.2.5 miR-17 and miR-19b inhibit iTreg differentiation

We further examined the role of the miR-17-92 cluster in the development and homeostasis of Treg cells. We observed no reduction in the percentage of natural Treg (nTreg) cells in the thymus, spleen, or lymph nodes in miR-17-92$^{f/f}$ Lck-Cre^{+} mice (Figure 6A). Foxp3^{+} inducible Treg (iTreg) cells are generated through the conversion of CD4^{+}CD25^{-} conventional T cells in the periphery. We used an *in vitro* differentiation assay[103] to examine the role of miR-17-92. Overexpression of miR-17-92 significantly impaired the induction of Foxp3^{+}CD25^{+} cells (Figure 6B), while ablation of the miR-17-92 cluster in CD4^{+} conventional T cells dramatically enhanced Foxp3 induction for various dosages of TGF-β treatment in this *in vitro* differentiation assay (Figure 6C&D). When the six miRNAs were expressed individually, miR-17 and 19b again emerged as the functional representatives, inhibiting iTreg differentiation (Figure 6E).

3.2.6 miR-17-92 is essential for effective CD4^{+} T cell anti-tumor responses

As presented above, the phenotypic and mechanistic studies of miR-17-92 indicate that this cluster is a multifaceted promoter of Th1 effector responses. As Th1-guided effector T cell function has been well established as a critical defense mechanism for immune surveillance and rejection of tumors, we therefore hypothesized that miR-17-92 might be an important component in the adaptive immune system's attempt to control tumor progression. We subcutaneously transplanted 2×10^{5} B16/F10 melanoma tumor cells into miR17-92$^{f/f}$ CD4-Cre^{+} mice and monitored tumor growth. In mice

homozygous or heterozygous for miR-17-92 deletion, the B16 tumors formed faster and had significantly accelerated growth in comparison to the tumors in wild type mice. At day 16, tumor volumes at the site of injection were 2-3 folds greater in mice lacking miR-17-92. The loss of a single copy of this gene is sufficient to impair tumor protection (Figure 7A). To detail the functional failure of T cells in the anti-tumor response, lymphocytes from tumor dLNs were stimulated with plate-bound anti-CD3/CD28 antibodies for 24 hours to measure the secretion of the inflammatory cytokines. We found that both Th1 and Th2 cytokines were dramatically reduced in the lymphocyte culture from the dLNs of miR-17-92 deficient mice (Figure 7B). Although there was a declining trend of IL-17 production in the same assay, the change was not statistically significant (Figure 7B). To confirm the critical role of $CD4^+$ T cells in the anti-B16 tumor responses, we collected $CD4^+$ T cells from WT or KO miR-17-92 mice and $CD8^+$ T cells from the tumor antigen specific Pmel TCR transgenic mice, and co-transferred them into $Rag2^{-/-}$ mice that were then challenged with B16/F10 cells. T cell responses in the dLNs were analyzed 18 days after tumor transplantation. We found that deficiency of miR-17-92 in $CD4^+$ T cells alone significantly impairs the Th1 response to B16 tumor cells, including a decrease in cell number (Figure 7C) and IFN-γ production of $CD4^+$ T cells (Figure 7D) in the dLN. In addition, the ability of miR-17-92 deficient $CD4^+$ T cells to help the $CD8^+$ T cells was also inhibited (Figure 7E).

To further demonstrate that this deficiency of immune protection is due to the weakness of antigen-specific T cell responses against the tumor, we inoculated mice subcutaneously with 3×10^5 B16/F0/OVA cells that ectopically secrete OVA protein. Sixteen days after transplantation, T cells were enriched from the dLNs, labeled with CFSE, and restimulated with OVAII peptide (a.a. 323-339) loaded APCs for 48 hours. Upon antigen-specific recall, ova-specific $CD4^+$ T cells exhibited a significant defect in proliferation and IFN-γ secretion and showed enhanced apoptosis, all of which correspond to the function of miR-17-92 as revealed *in vitro* (Figure 7F). Collectively, these results suggest that miR-17-92 profoundly regulates T cells' anti-tumor responses through strict enforcement on their Th1-lineage specific functions.

3.2.7 miR-17 facilitates effector T cell responses by targeting TGFβRII and CREB1

As presented above, miR-17 played a key role in inhibiting AICD of $CD4^+$ T cells and in blocking iTreg differentiation. To explore the molecular mechanism of miR-17 regulation, microarray analysis was performed to characterize the gene expression patterns among wild type T cells, T cells with miR-17-92 deletion, and T cells from the knockout background with miR-17 added back by retrovirus transduction. From the analysis, 122 genes were up-regulated in the miR-17-92 deficient $CD4^+$ T cells and reciprocally repressed when miR-17 was reintroduced. We next searched these mRNAs for sequence complementary to miR-17's seed region. Twenty-two genes were selected as candidates that might be directly controlled by miR-17. Based on the phenotypic

impact of miR-17 in T cells, two genes in this group attracted our attention: transforming growth factor, beta receptor II (*tgfbr2*) and cAMP responsive element binding protein 1 (*creb1*), both of which have been previously implicated in the Treg differentiation pathway[72,104]. In addition, C/EBP-β, a CREB1 transcriptional target, has been reported to promote apoptosis of macrophages following IFN-γ stimulation[105]. Through bioinformatics approaches, one conserved miR-17 binding site was identified in the 3'UTR of *tgfbr2* and two sites were found for *creb1* (Figure 8A). We verified that miR-17 can directly bind to the 3'UTR of *tgfbr2* (Position 2388) and *creb1* (position 6984) mRNAs (Figure 8B&C) using luciferase reporter assays. In $CD4^+$ T cells lacking *mir-17-92*, the expression levels of TGFbRII and CREB1 were significantly elevated at both the mRNA and protein level, and these elevations were completely abolished when the *mir-17* gene was re-introduced (Figure 8D&E).

To validate its functional relevance, we examined whether the moderate reduction of TGFβRII by miR-17 was sufficient to alter TGF-β signaling. TGF-b binds to TGFβRII, which initiates the signaling cascade by recruiting and phosphorylating the type I receptor. During Treg differentiation, this receptor activation leads to Smad3 Ser423/425 phosphorylation and translocation to its binding sites within the *foxp3* gene enhancer region[39,104]. We found that Smad3 was hyperphosphorylated upon TGFβ treatment in miR-17-92 deficient T cells, and this was diminished by miR-17 ectopic expression (Figure 8F).

The transcription factor CREB1 was shown to bind to the CNS2 region of the *foxp3* gene in a DNA-methylation-sensitive manner[72]. To demonstrate the functional importance of targeted CREB1 suppression by miR-17, we restored CREB1 expression in the presence of miR-17 expression using a bicistronic expression vector (Figure 8G). In $CD4^+$ T cells, the epichromosomal expression of CREB1 reversed the phenotype of miR-17 expression: there was loss of protection from AICD (Figure 8H) and rescue of iTreg differentiation at both the population and single cell levels (Figure 8I). Collectively, we concluded that the moderate inhibition of TGFβRII and CREB1 by miR-17 results in the diminution of iTreg lineage commitment; and that the dampened CREB1 expression by miR-17 is sufficient to aid T cell survival against excessive contraction.

3.2.8 miR-19b directly targets Pten to promote PI3K-Akt activation and to regulate $CD4^+$ T cell function

Previous reports have identified Pten, a negative regulator of PI3 kinase signaling, as a target of the miR-17-92 cluster[101]. The ability of Pten to suppress T cell proliferation and survival through its antagonizing effect on the PI3K-Akt pathway is well documented[106]. In addition, the PI3K-Akt pathway has also been shown to be critical for facilitating Th1 differentiation and supporting IFN-γ production[107,108], and the PI3K-AKT-mTOR axis was shown to inhibit iTreg differentiation[14,109]. Therefore, all of observed phenotypic aspects of miR-19b in effector T cells can be potentially explained by the diminution of Pten expression. Computational prediction revealed, the 3'UTR of *pten* mRNA contains two miR-19b and two miR-17 binding sites highly conserved

between mouse and human (Figure 9A). To assess miRNA binding to the 3'UTR, we constructed luciferase reporters with the full length *pten* 3'UTR. The reporter was tested in NIH3T3 cell lines stably overexpressing miR-19b, miR-19a, or miR-17. We observed significant suppression of luciferase production by miR-19b, but not miR-17 or miR-19a (Figure 9B). Additionally, site-directed mutagenesis of the miR-19 binding motifs within *pten*'s 3' UTR[110] completely abolished this suppression (Figure 9B), suggesting that miR-19b directly binds to these two sites. Consistently, overexpression of miR-19b in T cells down-regulated endogenous Pten mRNA and protein levels (Figure 9C). Reciprocally, mRNA and protein levels of Pten are significantly increased in $CD4^+$ T cells lacking the miR-17-92 gene (Figure 9D).

To directly assess the biochemical consequence of miR-19b targeting, we performed live cell imaging to visualize its perturbation on PI3K signaling initiated by TCR antigen recognition. The PH domain of Akt kinase was fused with GFP as a probe to monitor the local production of PIP3 through PI3K activation. miR-19b and this PH-GFP probe were simultaneously expressed in 5C.C7 T cells, which were then challenged with MCC peptide loaded on APCs. Within 10 seconds, agonist engagement of the TCR led to PI3K activation, which was sustained for hours inside the gradually assembled immunological synapse[111]. When we expressed miR-19b in 5C.C7 T cells and followed the dynamics of PH-GFP probe recruitment upon stimulation, we did not detect any enhancement of PI3K activation during the initiation stage (i.e. within 10 mins of T:APC

engagement, Figure 9E&F); however, when measured at 1 hour post T:APC engagement, there was a significant enhancement of sustained PI3K activity (Figure 9E&G). Taken together, these single cell assays strongly suggest that the Pten-mediated opposition of PI3K signalling was weakened by miR-19b expression.

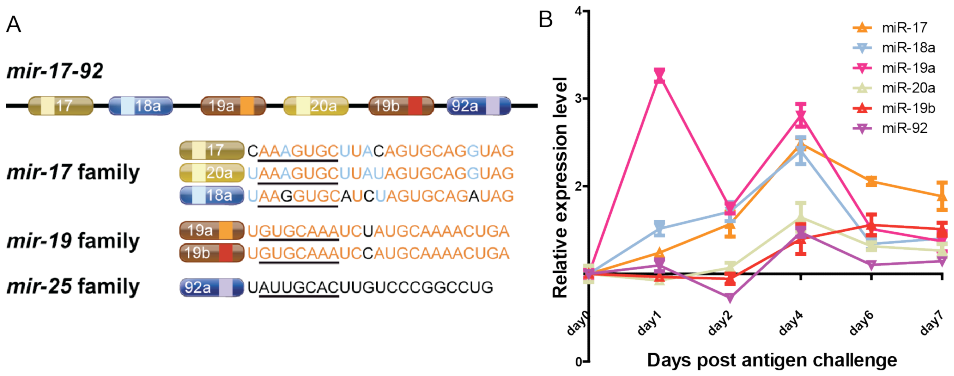

Figure 1: Dynamic regulation of miR-17-92 expression upon antigen challenge.

(A) Members of the miR-17-92 cluster. (B) $CD4^+$ T cells from the 5C.C7 TCR transgenic mice were stimulated with plate bound anti-CD3/CD28 for 7 days. Expression levels of individual miRNAs from the miR-17-92 cluster at indicated time points were quantified by qPCR analysis.

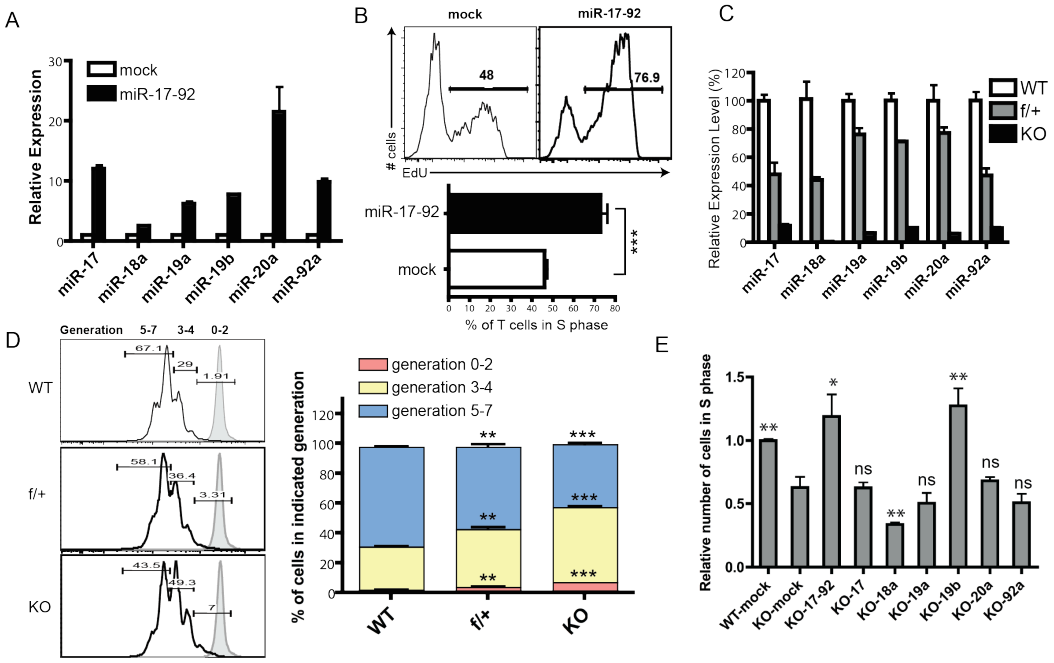

Figure 2: miR-19b promotes proliferation of CD4⁺ T cells upon antigen challenge.

(A & C) Assessment of miR-17-92 relative expression in CD4⁺ T cells by quantitative real-time PCR (qPCR). Data were normalized to a reference small RNA U6. Bar graph shows mean ± SEM from 3 independent experiments. (A) LN T cells from 5C.C7 TCR transgenic mice were primed by syngeneic APCs loaded with agonist peptide MCC (10 μM) and transduced with retrovirus encoding GFP alone (mock) or *mir-17-92* gene with GFP. Three days later, CD4⁺GFP⁺ T cells were FACS sorted, and the expression of miRNA was analyzed by qPCR. Data was normalized to the mock group. (B) *mir-17-92* genes were introduced into 5C.C7 T cells as described in (A). Cells were selected by puromycin for 48 hours, and restimulated with MCC-loaded CH27 APCs (10 μM) for 24 hours. EdU was supplied into the culture media 3 hours prior to cell fixation.

Percentage of $CD4^+GFP^+$ T cells in S phase was measured by by the Click-iT EdU flow cytometry assay. Top: representative FACS plot; Bottom: statistical analysis of 5 independent experiments. (C) Expression of miRNAs in $CD4^+$ T cells from LNs and spleens of miR-17-$92^{f/f}$CD4-Cre^- (WT), miR-17-$92^{f/+}$CD4-Cre^+(f/+), and miR-17-$92^{f/f}$CD4-Cre^+ (KO) littermates. Data was normalized to WT. (D) $CD4^+CD25^-$ T cells from LNs and spleens of WT, f/+ and KO littermates were labeled for 10 min at 37°C with carboxyfluorescein diacetate succinimidyl diester (CFSE) at a ratio of $3x10^6$ cells/4 mM chemical, followed by washes with complete culture medium, then activated by 1 μg/ml plate-bound anti-CD3 and anti-D28 antibodies for 72hrs. Left: representative FACS plot showing CFSE dilution. Tinted peaks represent CFSE stained T cells without stimulation; Right: statistical analysis of 3 independent experiments. (E) $CD4^+CD25^-$ T cells from WT or KO mice were primed and transduced with indicated retroviruses. After 2 days of puromycin selection, cells were restimulated with anti-CD3/CD28 for 24 hours, and T cells in S phase were determined by staining of pulsed EdU. Bar graphs summarize means ± SEM from 4 independent experiments and data were normalized to WT-mock. The statistical significance was assessed in comparison to the KO-mock group.

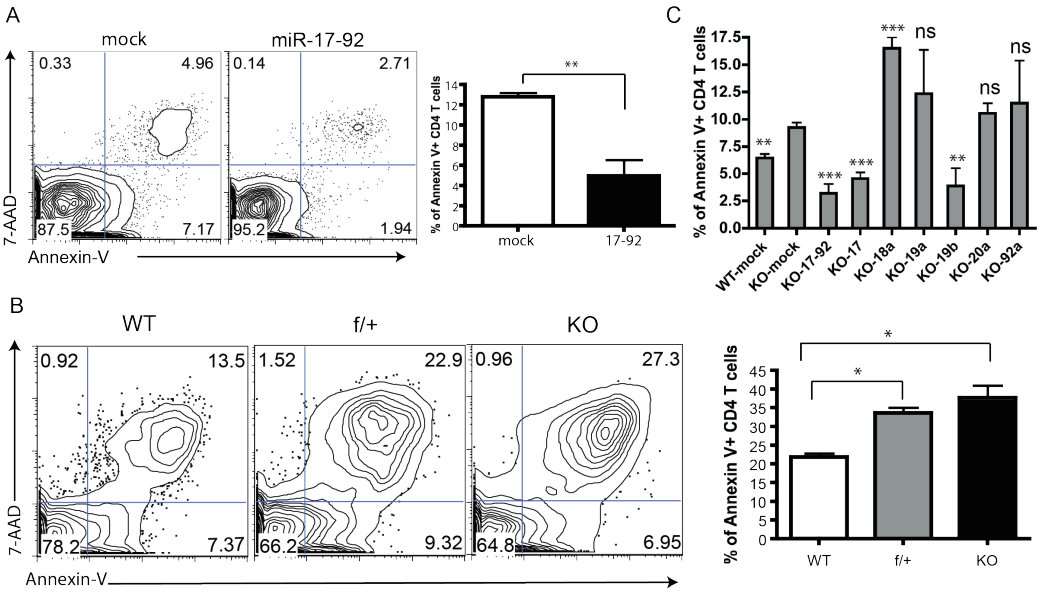

Figure 3: miR-17 and miR-19b inhibit activation-induced cell death of CD4⁺ T cells upon antigen challenge.

(A) Lymph node T cells from 5C.C7 TCR transgenic mice were primed and transduced with retrovirus encoding GFP or miR-17-92 as described in Figure 2A. Three days later, viable cells were enriched by density gradient centrifugation and then restimulated with CH27 loaded with MCC (10 μM) for 24 hours, and the status of AICD was assessed by Annexin V and 7AAD staining. The bar graph summarizes the means ± SEM from 4 independent experiments. (B) $CD4^+CD25^-$ T cells from LNs and spleens of WT, f/+, and KO littermates were stimulated with anti-CD3/CD28 antibodies for 72 hours, and the percentages of $CD4^+$ T cells undergoing apoptosis were assessed by Annexin V and 7AAD staining. The bar graph summarizes means ± SEM from 3 independent experiments. (C) $CD4^+CD25^-$ T cells from LN and spleen of KO mice were primed and transduced with retrovirus encoding individual miRNAs of miR-17-92 as

described in Figure 2E. Three days post transduction, viable $CD4^+$ T cells were enriched and restimulated with anti-CD3/CD28 for 24 hours. The profiles of restimulation induced apoptosis were measured by Annexin-V staining. Bar graphs summarize the means ± SEM from 3-5 independent experiments. The statistical significance was assessed in comparison to the KO-mock group. *: $p<0.05$; **: $P<0.01$; ***: $P<0.001$; ns: no significance.

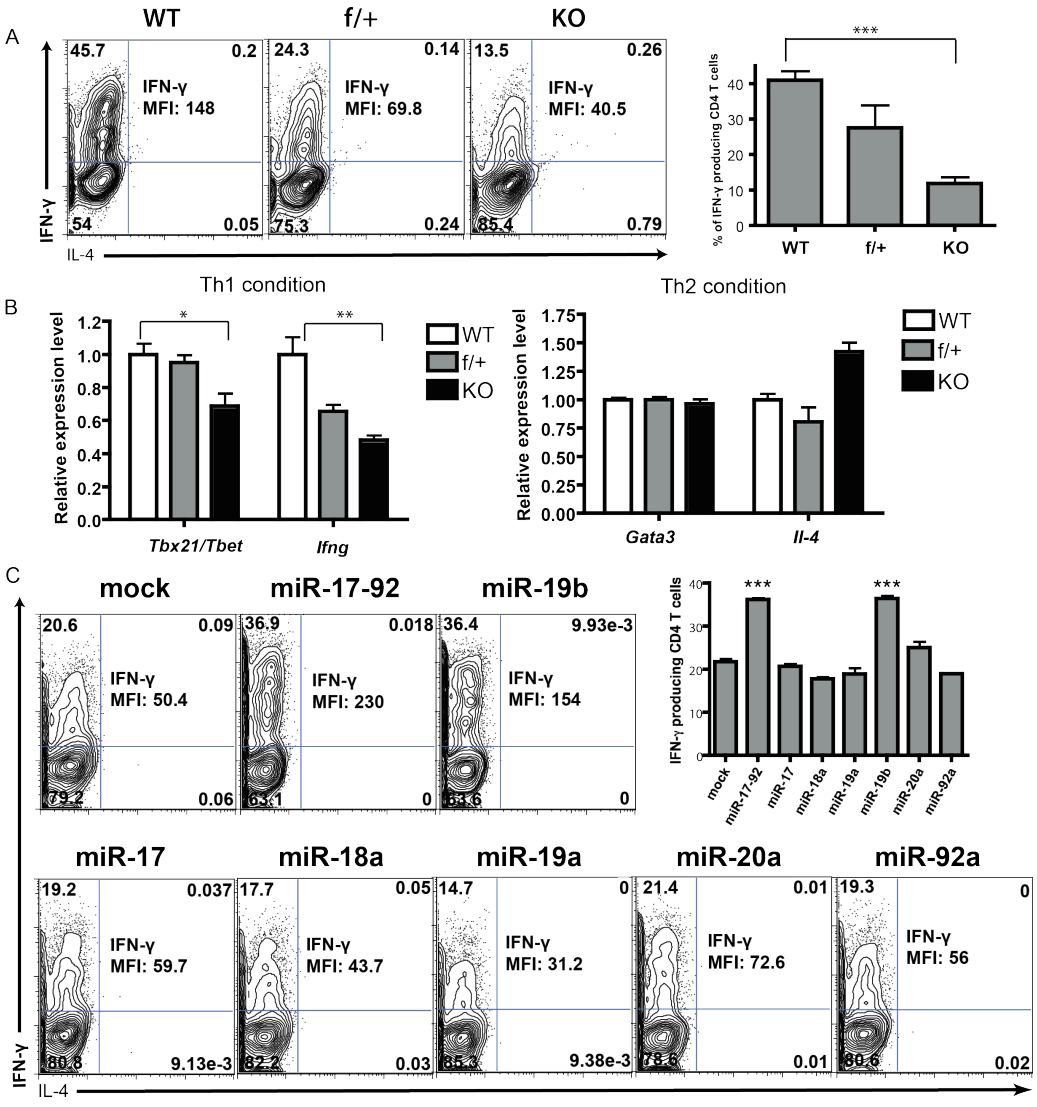

Figure 4: miR-19b is indispensible for IFNγ production from differentiated Th1 cells.

(A & B) $CD4^{+}CD25^{-}$ T cells were sorted from LNs and spleens of WT, f/+, and KO littermates, activated by anti-CD3/CD28 antibodies under Th1 or Th2 skewing conditions for 4 days. (A) The percentage of viable cells producing IFN-γ and the mean florescence intensity (MFI) of IFN-γ under Th1 condition were determined by intracellular staining following 4 hours of stimulation with 0.9 nM PMA and 0.5 μg/ml

ionomycin in the presence of 5 μg/ml brefeldin A and 2 μM monensin. The bar graph summarizes the means ± SEM from 3 independent experiments. (B) The mRNA levels of T-bet and IFN-γ or Gata3 and IL-4 from $CD4^+$ T cells differentiated under the Th1 or Th2 skewing conditions were quantified by qPCR. Data were normalized to a reference gene SDHA and shown as relative to WT. The bar graph shows means ± SEM from 3 independent experiments. (C) As described in Figure 2E, $CD4^+CD25^-$ conventional T cells of KO mice were primed and transduced with retrovirus encoding individual miRNAs within the miR-17-92 cluster, and then cultured under the Th1 skewing condition for 4 days. The percentages of IFN-γ or IL-4 producing cells and the MFI of IFN-γ signal were measured by intracellular cytokine staining. Left: representative FACS plot; Right: means ± SEM from 3 independent experiments. Statistic analysis was done by comparing to mock. ***, $P<0.001$.

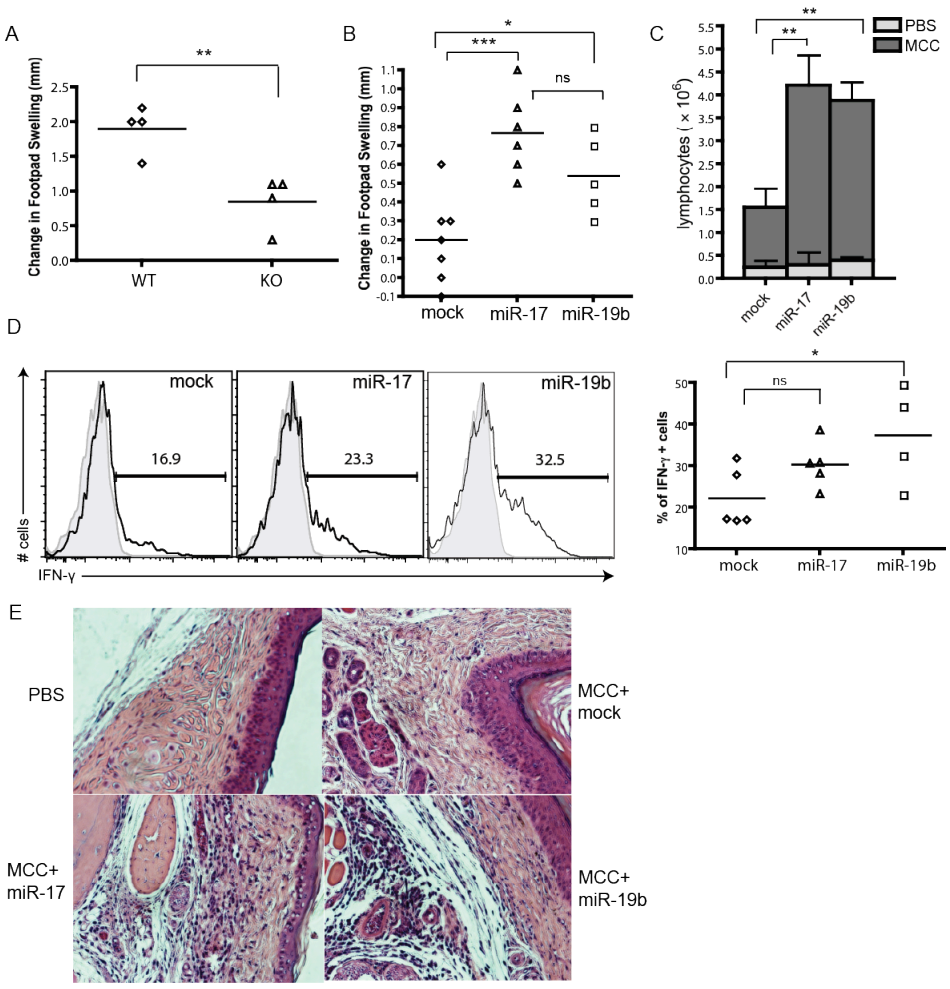

Figure 5: miR-19b and miR-17 enhance DTH responses *in vivo*.

(A) WT and KO mice were immunized s.c. with 100μg KLH in CFA (Sigma) and 8 days later injected with 50μg of KLH in one footpad and PBS in the contralateral footpad. Increase in footpad thickness was measured for both groups at 48 hours after secondary challenge (n=4). (B-E) WT B.10A mice were transferred through tail vein with 0.5×10^6 $CD4^+$ T cells from 5C.C7 $Rag2^{-/-}$ mice infected with GFP, miR-17 or miR-19b expressing retrovirus and immunized s.c. with 20μg of MCC peptide in CFA. Five days post immunization, mice were injected with 20μg MCC and PBS in each lateral footpad.

Seventy-two hours later, the swelling of footpads (in B) and the number of total lymphocytes from the popliteal LN (in C) were measured ($n \geq 5$). The percentage of IFN-γ producing cells within the GFP^+ $CD4^+$ population in the DLN was assayed (in D) by intracellular staining ($n \geq 4$). Representative images of footpad tissues with hematoxylin and eosin (H&E) staining were shown in E. *, $P<0.05$; **, $P<0.01$; ***, $P<0.001$, ns: no significance. Each experiment was repeated 3 times.

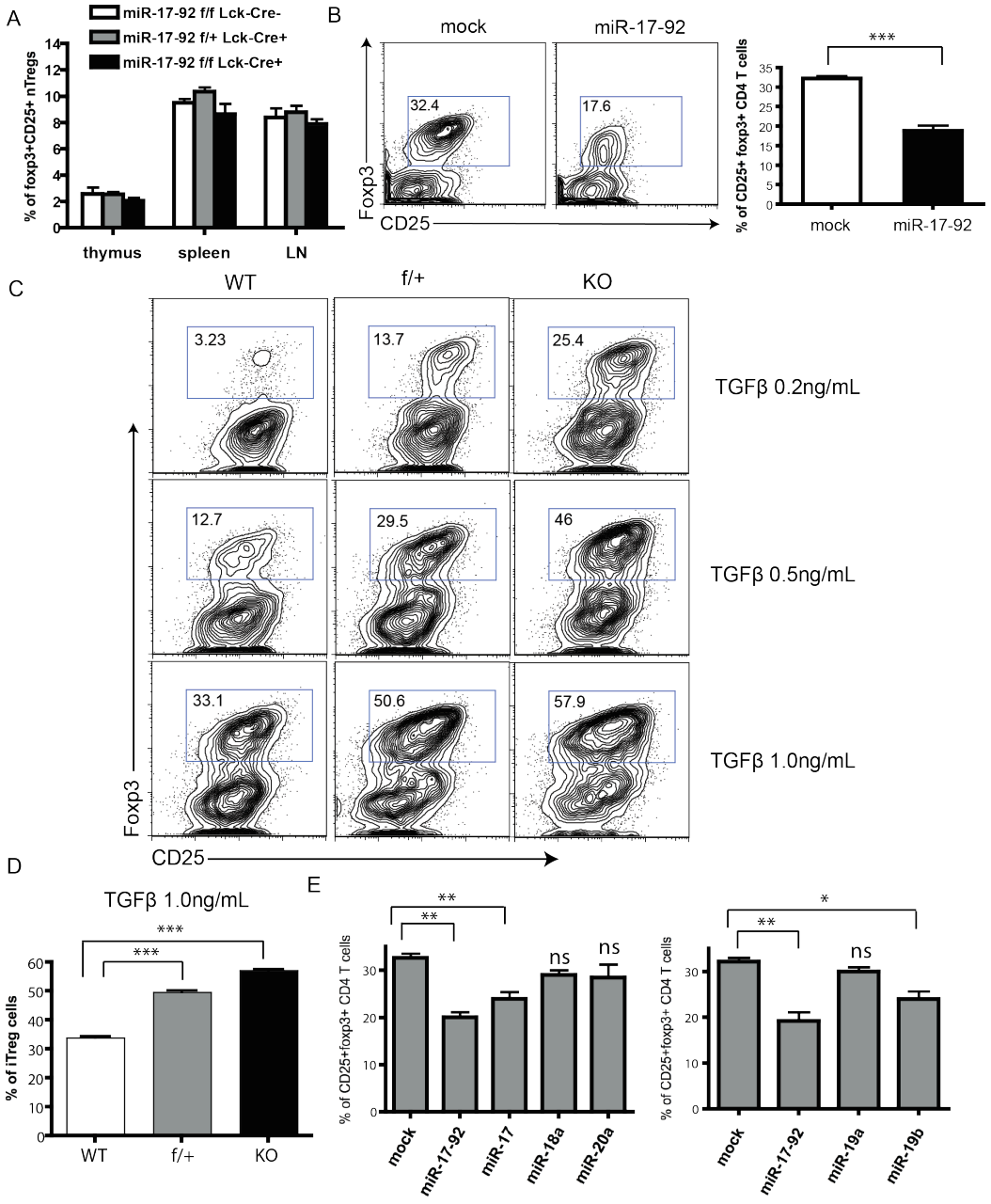

Figure 6: miR-19b and miR-17 suppress iTreg differentiation.

(A) Percentage of nTregs in the thymus, spleen, and lymph nodes of miR-17-92$^{f/f}$Lck-Cre^{-}, miR-17-92$^{f/+}$Lck-Cre^{+}, and miR-17-92$^{f/f}$Lck-Cre^{+} mice. (B) 5C.C7 T cells were primed, transduced with retrovirus encoding GFP alone or miR-17-92/GFP, and cultured

under iTreg differentiation conditions for 6 days. The percentage of Treg cells within the $CD4^+GFP^+$ population was measured by Foxp3 staining. The bar graph summarizes means ± SEM from 4 independent experiments. (C-D) $CD4^+CD25^-$ T cells sorted from LNs and spleens of WT, f/+, and KO littermates were cultured under iTreg differentiation conditions for 6 days with indicated TGF-β doses, and the percentage of $CD25^+Foxp3^+$ Treg cells was assessed. (C) Representative FACS plots. (D) Statistical analysis of 4 independent experiments at the indicated TGF-β dose. (E) 5C.C7 T cells were transduced with individual miRNAs from the miR-17 or miR-19 families, and cultured under iTreg differentiation conditions for 6 days. The percentage of $CD25^+Foxp3^+$ cells was measured by flow cytometry. Bar graphs summarize the means ± SEM of 3 independent experiments. *, $P<0.05$; **, $P<0.01$; ***, $P<0.001$, ns: no significance.

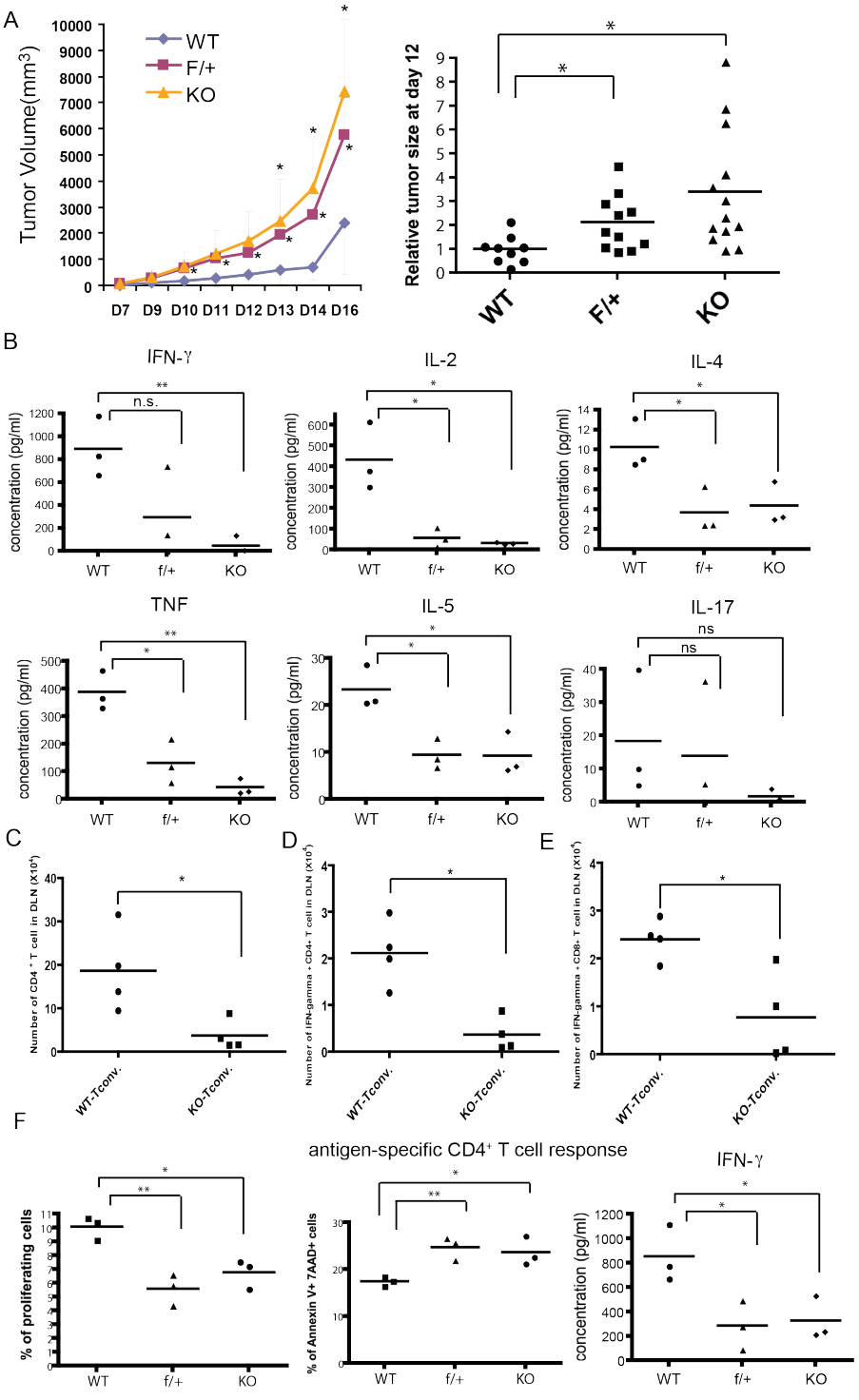

Figure 7: ***In vivo,*** **the miR-17-92 cluster is essential for the T cell mediated anti-tumor response.**

(A) WT (n=5), f/+ (n=8) and KO (n=7) littermates were injected s.c. with 2 x 10^5 B16/F10 melanoma cells. The tumor volume was measured each day from 7 days post injection up to 16 days and plotted against time. Left panel: the representative tumor growth curve; right panel: compiled data from three independent experiments. Individual dot represents the relative tumor volume normalized to that of the WT at 12 days after melanoma cells injection. (B) Lymphocytes from the draining lymph nodes of tumor carrying mice were isolated 16 days post B16/F10 melanoma inoculation and stimulated with 1 μg/ml anti-CD3/CD28 antibodies for 24 hours. Supernatants from the cultures were assayed for the concentration of indicated Th1, Th2 and Th17 cytokines by the cytokine beads array. Each dot represents data obtained from an individual mouse (n=3). (C-E) Sorted $CD4^+CD25^-$ T cells from WT or KO mice were mixed with Pmel TCR transgenic CD8+ T cells and then transferred into RAG2 deficient mice ($CD4^+CD25^-$: $1X10^6$, $CD8^+$: $0.5X10^6$/mouse) through i.v. After 24 hours, the mice were challenged with B16/F10 cells ($0.5X10^6$/mouse) through s.c. At day18, the cells from DLN were analyzed. The numbers of $CD4^+$ T (C), IFN-γ^+CD4^+ (D) and IFN-γ^+CD8^+ (E) cells in DLN were shown (n=4). (F) WT, f/+, and KO littermates were injected with 3×10^5 OVA-secreting B16/F0 cells. Sixteen days after injection, T cells were enriched from the DLN, labeled with CFSE, and stimulated with LB27.4 APCs loaded with 10 μM OVA peptide (323-339) for 48 hours. Antigen-specific responses (proliferation, AICD, IFN-γ production) were measured as described above. *, $P<0.05$; **, $P<0.01$, ns, no significance.

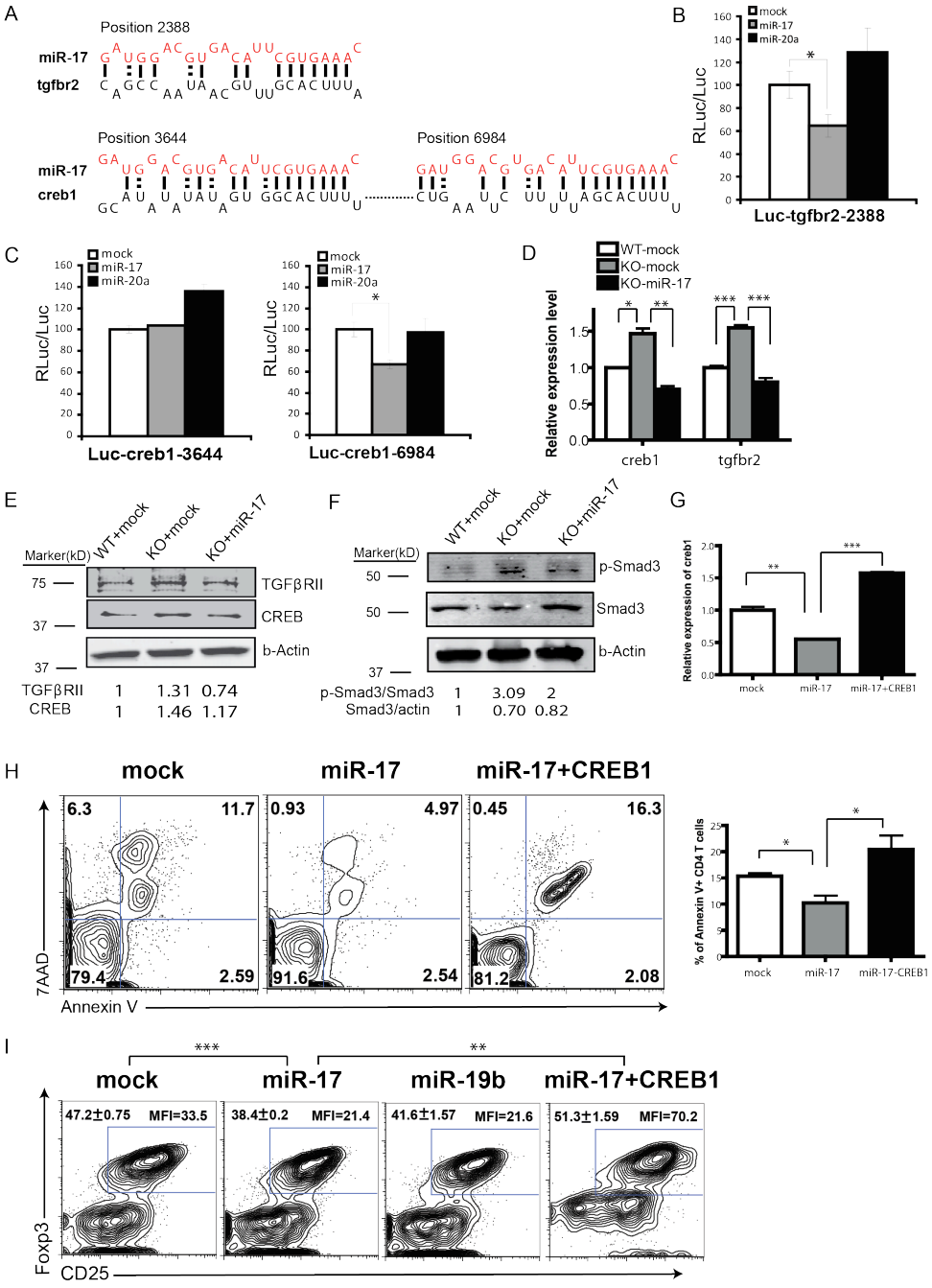

Figure 8: miR-17 modulates CD4⁺ T cells' effector responses by targeting TGFbRII and CREB1.

(A) Schematic representation of the putative miR-17-binding sites in the 3'UTR of *tgfbr2* and *creb1*. (B&C) A portion of the 3'UTR of *tgfbr2* or *creb1* was cloned downstream

of a luciferase reporter and transfected into an NIH3T3 cell line stably expressing miR-17, miR-20a or mock control. The luciferase activity was measured 72 hours after transfection. Bar graphs show the means ± SD of 3 (B) or 6 (C) independent experiments. (D&E) $CD4^+CD25^-$ T cells from WT or KO mice were transduced with indicated retrovirus, and $CD4^+GFP^+$ T cells were FACS sorted and total RNA and protein were extracted for qPCR (D) and western blot (E). The bar graph shows means ± SEM from 3 independent experiments. (F) T cells were transduced with indicated virus and cultured under iTreg differentiation conditions for 5 days. $CD4^+GFP^+$ T cells were then sorted, lysed, and analyzed for Smad3 Ser423/425 phosphorylation by western blot. (G-I) 5C.C7 T cells were primed and transduced with retrovirus containing both the CREB1-IRES-GFP expression cassette and the indicated miR-17 expression cassette, or miR-17 alone with GFP marker, or GFP only. (G) Assessment of CREB1 expression in 5C.C7 T cells by q-PCR. The graph shows means ± SEM from 3 independent experiments. (H) Death profile of $CD4^+GFP^+$ T cells following restimulation with anti-CD3/CD28 antibodies. Left: representative FACS plot; Right: Bar graphs showing means ± SEM from 3 independent experiments. (I) 5C.C7 T cells were transduced as indicated and cultured under the iTreg differentiation condition for 5 days. The percentage of $CD25^+Foxp3^+$ cells inside of $CD4^+$ T cell populations and the MFI of the intracellular Foxp3 staining were measured. The numbers on the left corner show the means ± SEM of the percentage of iTreg cells from three independent experiments. *, $P<0.05$; **, $P<0.01$; ***, $P<0.001$.

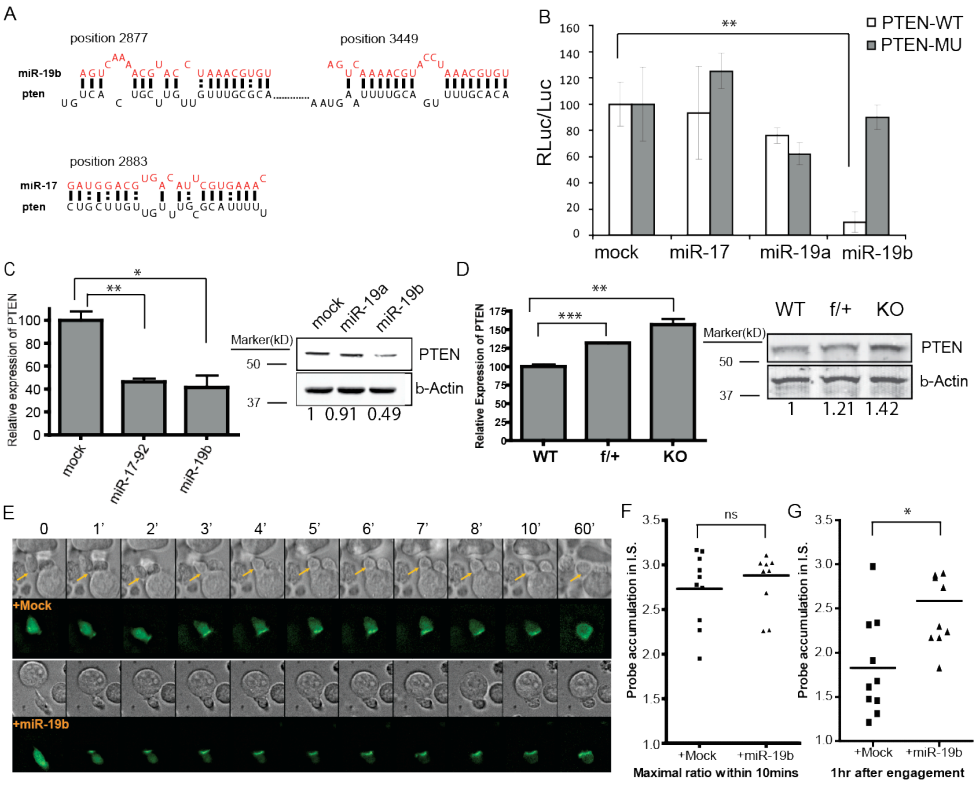

Figure 9: Pten is the primary target of miR-19b in regulating CD4⁺ T cells' effector functions.

(A) Schematic illustration of the predicted targeting sites for miR-19b and miR-17 within the 3'UTR of *pten* mRNA. (B) The full length 3'UTR of *pten* (Pten-WT) or 3'UTR with mutations at the two miR-19b target sites (Pten-MU) were cloned downstream of a luciferase reporter and transfected into NIH3T3 cell lines stably expressing the indicated miRNAs. The luciferase activity was measured 72 hours post transfection. Bar graphs show the mean ± SD of 3 independent experiments. (C) 5C.C7 T cells transduced with mock, *mir-17-92*, or *mir-19b* were sorted by FACS, and total RNA and protein were extracted for qPCR and western blot. (D) Relative expression of Pten mRNA in $CD4^{+}CD25^{-}$ T cells from LNs and spleens of WT, f/+ and KO mice was measured by

qPCR. T cells activated with plate-bound anti-CD3/CD28 antibodies for 72 hours were lysed for protein quantification. qPCR data were normalized to SDHA and shown as relative to mock or WT, and the graph shows means ± SEM for 3 independent experiments. (E) miR-19b mediated regulation on PI3K signaling upon antigen engagement was visualized by fluorescence video microscopy. As described previously[111], the PH domain of Akt kinase was fused with GFP as an imaging probe to monitor the production of PIP3 through PI_3K activation. miR-19b or mock vectors were expressed simultaneously with this PH-GFP imaging probe in 5C.C7 T cells, which were challenged by CH27 APCs pre-loaded with MCC agonist peptide. Live cell imaging was performed to monitor the initial signaling strength and the duration of PI3K activation. The activity of PI3K was represented by measuring the ratio of the average probe fluorescent intensity in the synaptic region versus the average intensity in the rest cell area. Top panels: representative montages from the DIC channel; Bottom panels: representative montages from the GFP channel. (F) The highest level of probe synaptic accumulation within the first 10 minutes of T:APC contact was used as the mark for the maximal activity of PI3K activation in the initiation stage (prior to the formation of mature immunological synapse) of TCR signaling. (G) A similar measurement was performed at 1 hour post the initiation of TCR signaling. *, $P<0.05$; **, $P<0.01$; ***, $P<0.001$.

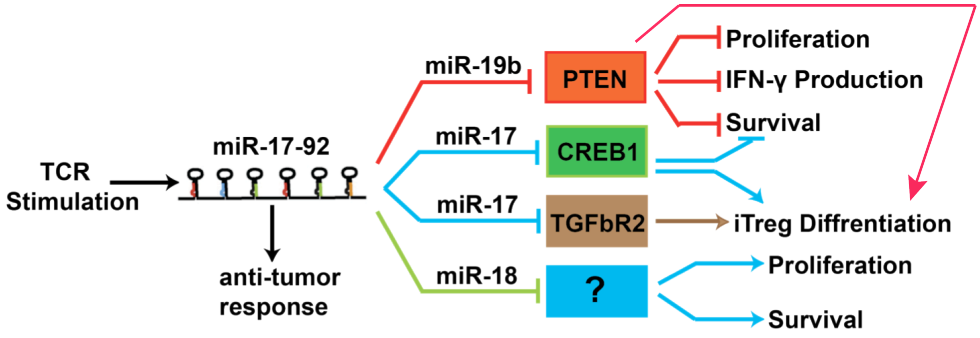

Figure 10: Model for miR-17-92 in regulating CD4⁺ T cell response.

Upon TCR activation, the abundance of miR-17-92 was upregulated to promote CD4⁺ T cell-mediated Th1 response. Through targeting PTEN, miR-19b promotes CD4⁺ T cell proliferation, survival, IFN-γ production, and inhibits iTreg differentiation. miR-17 also promote T cell survival and inhibits iTreg differentiation through directly inhibiting CREB1 and TGFbR2. On the other hand, through a still unknown mechanism, miR-18 antagonizes the whole cluster's function and suppresses T cell proliferation and survival.

3.3 Discussion

Our studies through gain- and loss-of-function analysis demonstrate that the miR-17-92 cluster is a multicomponent potentiator that governs T cells' responses to antigen challenge (Figure 10). Specifically, this cluster manages the efficacy of Th1 responses by protecting T cells from AICD, enhancing T cells' proliferation, facilitating IFN-γ production, and obstructing iTreg differentiation. The extensiveness of miR-17-92's regulation was especially evident during T cell-dependent tumor rejection, since local Th1-guided cytotoxicity is crucial for direct tumor elimination and indirect galvanization of macrophage activation[81,112]. Mice with a T cell-specific single allele ablation of miR-17-92 were extremely vulnerable to B16 melanoma transplantation, and further analysis revealed that $CD4^+$ T cells from these recipients' draining lymph nodes were defective in all aforementioned aspects of Th1 responses upon tumor antigen challenge.

The miR-17-92 cluster is produced from a single transcript, designated C13orf25[96]. Taking this cluster as a single entity, miR-17-92 provides cohesive guidance for T cells' antigen responses. However, our data indicate that the individual miRNAs within the cluster are quite diversified in terms of their functions. Previously, we and others independently identified miR-19 as the key components of this cluster in promoting Myc-induced B cell lymphomas[110,113]. In T cells, miR-19b is also critical, as it comprehensively drives the antigen response in every tested aspect. Furthermore, the

regulation provided by miR-19b is greatly facilitated by miR-17 in protecting cells from AICD and especially in suppressing iTreg differentiation. Surprisingly, we noted that miR-18a opposes the cluster's pro-Th1 function, primarily through elevation of AICD and inhibition of proliferation. Given that miR-17-92 has been well recognized as an oncomiR, we suspect that miR-18a might act as a brake on the pro-proliferation and anti-apoptosis functions of the cluster, which is a common phenomenon for proteinaceous oncogenes[114-116].

The miRNAs comprising the miR-17-92 cluster can be grouped based on the similarity of their seed regions (nucleotides 2-8), which are thought to be especially critical for the specificity of mRNA targeting. Our current, limited knowledge predicts that a majority of targets should be shared between family members. However, inside primary $CD4^+$ T cells, and despite the very high degree of homology within the miR-17 family, miR-20a is not capable of performing any of miR-17's pro-Th1 functions, and miR-18 clearly exerts an antagonistic effect. Similar distinction was also observed between miR-19a and miR-19b. One explanation is that the diversity of functionality might simply reflect the differences in their expression levels. Expression levels between miR-19a and miR-19b were significantly different in T cells (data not shown), which therefore prevents us from drawing any solid conclusions about the functional diversity inside this family. Nevertheless, our data does suggest a potential difference in the endogenous processing or maintenance of these two miRNAs in effector T cells, with

miR-19a being disadvantaged. On the other hand, inside the miR-17 family, the overexpression level and the absolute copy number of miR-20a was equal to or even higher than that of miR-17 (data not shown). Although our quantification determined that miR-18a is expressed at a lower level, the antagonist effect is so evident that distinctions of mRNA targeting become a more conceivable explanation. In mature miRNAs, only few nucleotides differ between miR-17 and miR-20a/-18a; and these differences reside outside the seed region. We suspect that these subtle differences are sufficient to result in a significant affinity difference between the miRNAs and their targets to produce the observed differential targeting. Alternatively, as reported[117], the loop sequence of the pre-miRNA may participate in the process of target recognition. In that case, the distinct mRNA targeting activities of miR-181a and miR-181c were largely determined by their divergent pre-miRNA loop sequences, but not by the one-nucleotide alteration in the mature miRNAs. As the pre-miRNA loops also differ between miR-17 and miR-20a/-18a, it is possible that the targeting preference between them is caused by differences of their pre-miRNA loops. Regardless, our results do argue that the sequences outside the seed region can also be an indispensible component of the miRNA targeting machinery.

The other novel pathway identified in this study is that miR-17 functions through targeting CREB1. By restoring CREB1 levels in miR-17-coexpressing T cells, we demonstrated that the subtle increase of this protein diminished the protection from

AICD afforded by miR-17. This functionally confirmed CREB1 as a target of miR-17, and, more importantly, provided the first evidence that CREB1 is a pro-apoptotic factor during AICD in $CD4^+$ T cells. The ability to restrain iTreg differentiation was an unexpected role for miR-17. In accordance with previous findings[118,119], we found that miR-17 inhibits TGF-β signaling through targeting TGFβRII. Biochemically, the reduction of either CREB1 or TGFβRII is not dramatic; but impacts from these moderate adjustments on T cell function are not negligible. However, despite its clear role during iTreg differentiation, the loss of miR-17-92 did not influence the development of nTregs in our mouse models. One possibility is that the moderate protein level changes of TGF-bRII, CREB1 and Pten caused by the loss of miR-17/-19b, while critical for Foxp3 induction in peripheral conventional T cells, are not sufficient to affect thymic nTreg development. Alternatively, miR-17 and miR-19b do affect the thymic selection of the nTreg population, but in a more subtle way (e.g. TCR repertoire changes within the mature nTreg pool).

4. TCR and TGF-β signaling converge on DNMT to control *foxp3* locus methylation and iTreg differentiation: An epigenetic node that links environmental cues to DNA methylation

The contents of this dissertation chapter have been slightly modified from the following publication:

Chaoran Li, Peter J.R. Ebert & Qi-Jing Li. T Cell Receptor (TCR) and Transforming Growth Factor β (TGF-β) Signaling Converge on DNA (Cytosine-5)-methyltransferase to Control forkhead box protein 3 (foxp3) Locus Methylation and Inducible Regulatory T Cell Differentiation. *J Biol Chem*. 288(26):19127-392012. (2013).

4.1 Introduction

Recognition of a peptide-major histocompatibility complex (pMHC) displayed on the surface of antigen-presenting cells (APCs) by a specific T cell receptor (TCR) initiates the T cell response. Upon pMHC:TCR engagement, coordinated downstream signaling cascades promote naïve $CD4^+$ T cells to undergo massive expansion and differentiation into distinct T helper (Th) subsets, such as Th1, Th2, Th17, and inducible regulatory T cells (iTreg)[4]. Although the requirement for TCR signals in lineage commitment is universal, accumulating evidence indicates that, besides varying cytokine environments, differences in the strength of TCR signaling can also have a tremendous impact on $CD4^+$ T cells' fate determination. This was initially discovered by Bottomly and colleagues and further confirmed by others: in general, weak TCR signals

are thought to bias T cells toward the Th2 lineage while strong TCR signals facilitate the formation of the Th1 subset[120-122]. Recently, it was shown that the differentiation of Th17 cells could also be promoted by weak TCR activation[13]. However, the molecular mechanism governing this fate determination is largely unknown.

In addition to effector T helper cells, TCR signal strength influences the differentiation of $CD4^+Foxp3^+$ regulatory T cells (Tregs). Tregs are suppressor T cells that play a dominant role in the maintenance of peripheral tolerance and immune homeostasis[31]. These cells express the master transcription factor Foxp3, which is essential for their differentiation, maintenance and suppressive function[123-126]. Mutation of the *Foxp3* gene in humans and mice results in lymphoproliferative disease that leads to severe inflammation in multiple organs and tissues[127,128]. Based on their origin of development, Tregs have been categorized into two types: thymic natural Tregs (nTregs) generated after thymocyte selection, and peripheral inducible Tregs (iTregs) derived from $CD4^+CD25^-$ conventional naïve T cells[7]. nTregs and iTregs share several common mechanisms for their development and differentiation, such as their reliance on TCR, IL-2, and TGF-β signaling. TCR stimulation leads to the activation of various transcription factors including NFAT[129], AP1[129], CREB1[130], and NF-kB[131], which were shown to bind to the *foxp3* locus directly and regulate its transcription. Paradoxically, although TCR mediated signaling is absolutely required for Treg differentiation, several lines of

evidences suggested that strong TCR stimulation disfavors foxp3 induction during iTreg differentiation[132 133]. However, the molecular mechanism of this is still unclear.

In addition to the regulation of *foxp3* by well-documented transcription factors, recent studies showed that *foxp3* transcription is also regulated by epigenetic mechanisms[134,135]. It was shown that both the promoter and conserved non-coding sequence 1 (CNS1) of the *foxp3* gene are more accessible in Tregs than in conventional effector T cells, as indicated by increased local histone acetylation in Tregs. Besides histone modifications, *foxp3* expression is also directly regulated at the DNA level by CpG methylation. The CpG islands within the promoter region of *foxp3* were almost completely demethylated in nTregs, while those in conventional effector T cells showed partial methylation[130,136]. In *foxp3*'s CNS2 region, the difference in methylation is even more striking: it was fully demethylated in nTregs but completely methylated in effector T cells[130,137]. Interestingly, and consistent with their transient and unstable Foxp3 expression, iTregs had *foxp3* CpG islands that were only partially demethylated in the CNS2 region[130]. Experiments using inhibitors to block methylation showed that changes in CpG methylation motifs did affect transcription factor binding and *foxp3* expression in antigen-stimulated conventional T cells. However, it was not clear how this methylation is regulated during the iTreg differentiation process.

Here, we show that strong TCR signaling—elicited by high affinity ligand or by extended ligand exposure—inhibits *foxp3* expression in conventional T cells at the

epigenetic level. This is achieved by both PLCγ- and PI3K-dependent signaling downstream of TCR, which blocks the GSK3β-dependent proteasome-mediated degradation of DNMT1 protein; and, by dampening miR-148a, the miRNA that targets DNMT1 mRNA. DNMT1, together with DNMT3b, is then able to methylate and suppress the *foxp3* locus. Meanwhile, TGF-β directly antagonizes these TCR signals by promoting drastic downregulation of DNMT1 via activation of p38. Thus, DNMT1 represents a crucial node where TCR and TGFβ signals converge to control iTreg fate.

4.2 Results

4.2.1 iTreg differentiation is controlled by both strength and duration of TCR signalling through the PI3K-Akt-mTOR and PLC pathways

While dissecting the functions of the miRNAs within the miR-17-92 cluster, we identified miR-19b as an inhibitor of iTreg differentiation, and further mechanistic analysis indicated that this was mediated through inhibition of PTEN expression and the consequent prolonged PI3K activation upon TCR/CD28 signaling[54]. Abbreviated anti-CD3/CD28 stimulation facilitates *in vitro* iTreg differentiation[132]; and previous adoptive transfer studies have shown that low doses of antigen and lack of costimulation favor induction of iTregs *in vivo*[133]. Therefore, we hypothesized that iTreg lineage differentiation would be determined by the integrated strength of TCR signaling based on both pMHC ligand affinity and the duration of ligand availability. To parse out the impacts of ligand affinity and stimulation duration in regulating iTreg

differentiation, we utilized $CD4^+$ T cells from 5C.C7 TCR transgenic mice, in which every primary T cell carries a unique TCR[138] recognizing a range of biochemically and biophysically well-characterized natural and synthetic variants of the moth cytochrome C (88-103) peptide in the context of the MHC II molecule I-E^k [139]. To determine the role of ligand strength in regulating iTreg differentiation, we stimulated sorted $CD4^+CD25^-$ 5C.C7 T cells using syngeneic APCs loaded with either the strong agonist MCC, or a weak agonist 102S[140]. To interrogate how the duration of stimulation influences iTreg induction, I-E^k-specific antibodies were added at different time points after the onset of stimulation (e.g. 6hrs, 18hrs); this treatment blocks TCR engagement with pMHC within minutes[141]. Under these two regimes, and without addition of exogenous cytokines, we analyzed the percentages of $Foxp3^+$ $CD4^+$ T cells 72hrs after initial TCR stimulation (Figure 11A). Consistent with our hypothesis, a minimal percentage of T cells upregulated Foxp3 when stimulated for a prolonged period (72hrs), regardless of whether a strong or weak antigenic peptide was used. However, when cells were stimulated with the weak agonist 102S for a shorter period of time (6hrs or 18hrs), we observed a substantial frequency of iTreg conversion (Figure 11B&D). We further confirmed that this elevation of Foxp3 expression occurred at the transcript level (Figure 11C). In contrast, even with the shortest tested duration of stimulation, MCC was unable to induce Foxp3 expression (Figure 11B-D). These data indicate that although brief exposure to weak TCR signaling is required for Foxp3 induction, extensive signaling

generated from high affinity ligands and/or a longer duration of antigen exposure actually inhibits *foxp3* expression and iTreg differentiation. We further evaluated the impact of TCR signalling strength and duration in regulating iTreg differentiation with $CD4^+$ T cells from wild type C57BL/6 mice upon anti-CD3 and anti-CD28 antibodies stimulation. As expected, when sorted $CD4^+CD25^-$ T cells were stimulated for 72 hours, very few $Foxp3^+$ cells were generated. In contrast, when cells were activated for 18 hours and then maintained without TCR stimulation for additional 54 hours, a substantial fraction of cells differentiated into Tregs (Figure 11E). Furthermore, reducing the concentration of anti-CD3 antibody further enhanced Foxp3 induction and iTreg differentiation (Figure 11E). These data confirmed that both TCR signalling strength and duration contribute to the negative regulation of iTreg differentiation by extensive TCR stimulation.

Although we do not know precisely how TCR signal strength is translated into cell fate decisions, several previous studies indicate that the PI3K-Akt-mTOR axis downstream of TCR activation might be critical. Blocking of this pathway with LY294002 or rapamycin after 18hrs of TCR stimulation resulted in robust Foxp3 induction *in vitro*[132]. In addition, expression of a constitutively active form of Akt in T cells diminished Foxp3 expression in peripheral T cells both *in vitro* and *in vivo*, suggesting that the activation of the PI3K-Akt-mTOR axis could contribute to the negative regulation of iTreg differentiation by strong TCR signaling[142]. To determine key

signaling events preventing *foxp3* expression upon extensive antigen stimulation, we repeated our iTreg induction experiments in the presence of a series of small pharmaceutical inhibitors to block specific pathways downstream of TCR activation. We first chose the regime of extended weak TCR stimulus (72hr 102S), which normally results in very little iTreg induction. In this setting, consistent with previous findings that prolonged PI3K-Akt-mTOR activation inhibits iTreg differentiation, we detected a substantial increase in iTreg conversion when cells were treated with LY294002, a small inhibitor that blocks both PI3 kinase and mTOR activity (Figure 12A). We further dissected these two pathways by treating cells with PIK-75, which specifically inhibits the P110α and P110γ subunits of PI3K at the dose used, and with rapamycin, which inhibits mTOR specifically (Figure 12A). We noted that both inhibitors could significantly potentiate iTreg differentiation. Meanwhile, despite having a dramatic impact on T cell proliferation[143], inhibition of calcineurin-NFAT signaling, NFkB function, or ERK activation had a minimal effect on Foxp3 induction (Figure 12A). Interestingly, we found that U-73122, a specific inhibitor of the PLCγ-dependent hydrolysis of PIP_2 to IP_3, could also enhance iTreg conversion to a similar extent as PI3K-mTOR inhibition (Figure 12A).

We next investigated whether inhibition of the PI3K-Akt-mTOR or ZAP70-PLCγ pathway can induce iTregs when TCRs are engaged with strong agonist. When we inhibited the PI3K and PLC pathway with specific inhibitors at 18 hours after TCR

engagement, cells stimulated with MCC expressed significantly less Foxp3 than those stimulated with 102S (Figure 12B&C). On the other hand, blocking ERK activation did not have any effects on iTreg conversion (Figure 12B&C). These data indicated that a short period (18hrs) of strong PI3K and PLC activation with MCC peptide is sufficient to inhibit iTreg induction. Furthermore, it strongly suggested that both the PI3K-Akt-mTOR axis and the ZAP70-PLCγ pathway are specifically involved in the negative regulation of iTreg differentiation in response to extensive TCR signalling mediated by higher ligand affinity or prolonged duration.

4.2.2 TCR signaling regulates CpG methylation at the foxp3 locus

During iTreg differentiation, *foxp3* gene expression is driven by the activation of the transcription factors STAT5, Smad3, NFAT, AP1, CREB1 and NFkB[144]; the latter four of which are collectively potentiated by strong and sustained TCR signaling. Paradoxically, in the absence of TGF-β, TCR signaling of this magnitude instead suppresses the transcription of *foxp3*. This apparent conundrum suggested that, in parallel with transcription factor activation, extensive TCR signaling must target a distinct regulatory mechanism. DNA methylation controls the accessibility of general and gene-specific transcription factors toward the regulatory regions of genes, and this has been demonstrated to be one of the central mechanisms controlling *foxp3* transcription[134]. We hypothesized that, during iTreg differentiation, differences in

strength and duration of TCR signaling would result in differential DNA methylation within the *foxp3* regulatory regions.

To examine this, we evaluated the methylation status of the *foxp3* gene in different T cell populations from male 5C.C7 mice, including naïve T cells, T cells activated with 102S or MCC for 6hrs, and T cells activated with 102S peptide for 72hrs. As we sought modifications that could explain Foxp3 induction prior to iTreg commitment, we analysed the whole population (within which the highest ratio of differentiated iTregs is less than 20%), rather than purified iTreg cells under these various conditions. In agreement with previous reports[130,136], we found that in naïve $CD4^+$ T cells, CpG islands residing in *foxp3's* promoter region were largely unmethylated (Figure 13A). While a short and weak stimulation did not alter the overall methylation pattern of the promoter, stronger stimulation in terms of duration and ligand affinity significantly elevated *foxp3* promoter methylation (Figure 13A), and this methylation pattern mirrored the final expression level of Foxp3 protein (Figure 11B). In addition, the CpG islands within *foxp3*'s CNS2 region were completely methylated in naïve T cells and T cells that had experienced various TCR stimulations (Figure 13B). It was not surprising to observe that the methylation status in CNS2 was largely unchanged in conventional $CD4^+$ T cells: It has been shown that even in fully-differentiated iTregs induced by TGF-β and IL-2 treatment, the CpG islands within CNS2 still remains largely methylated[130]. Furthermore, while the genetic modification demonstrates that CNS2 is

rather essential for the maintenance of Foxp3 expression in mature nTregs [75], our data validate that CNS2 is likely dispensable for Foxp3 induction during iTreg induction. To further functionally determine whether extensive TCR stimulation blocks *foxp3* expression through DNA methylation, we stimulated 5C.C7 T cells with 102S for 72hrs, while also treating samples at 18hrs post stimulation with 5-azacytidine, a cytosine nucleoside analogue that inhibits DNA methylation. In agreement with our methylation data, 5-azacytidine treatment abrogated the inhibition of Foxp3 expression by prolonged TCR signaling (Figure 13C). These data indicate that extensive TCR stimulation suppresses iTreg differentiation by enhancing CpG methylation in the *foxp3* gene's regulatory regions.

4.2.3 TCR signaling augments levels of DNMT proteins and their bindings to the foxp3 locus

We next examined how TCR signaling controls DNA methylation within the *foxp3* locus. As one of the major DNA methyltransferases in mammalian cells, DNMT1 was recently linked to the regulation of Foxp3 expression in T cells[145]. In addition to its well-known function in maintaining DNA methylation during cell proliferation, DNMT1 has also been shown to be associated with DNMT3 to induce *de novo* methylation in CpG islands[146] and silence genes in human cells[147]. Since we observed a substantial change in DNA methylation in *foxp3*'s regulatory regions, we hypothesized that extensive TCR signaling modulates *foxp3* gene methylation by controlling the level of DNMTs. Under various stimulatory conditions that we employed for iTreg induction,

mRNA levels of DNMT1 (Figure 14A) and DNMT3b (Figure 14B) largely remained steady. However, at the protein level, DNMT1 was slightly elevated with a short duration of 102S stimulation, and was dramatically increased when this stimulation was prolonged (Figure 14C). Similarly, DNMT3b protein was also significantly elevated with as short as 6 hours of moderate TCR stimulation (Figure 14D). Consistent with our hypothesis that DNMT1 mediates iTreg differentiation through interpretation of TCR signalling strength and duration, similar magnitudes of DNMT1 elevation were caused by prolonged stimulus with a weak agonist (102S), as by a shorter stimulation with a strong agonist (MCC) (Figure 14E&F). To examine whether DNMT1 and Foxp3 expression are inversely correlated under the permissive condition for iTreg conversion, we directly compared DNMT1 levels between $Foxp3^+$ and $Foxp3^-$ populations in $CD4^+$ T cells with the same TCR priming. We employed a BAC transgenic mice expressing the GFP-Cre fusion protein under the control of the *foxp3* promoter, in which GFP expression faithfully reflects endogenous Foxp3 expression[95]. We then stimulated sorted $CD4^+GFP^-$ conventional T cells from these mice with the permissive condition optimized in Figure 11E. GFP^- ($Foxp3^-$) and converted GFP^+ ($Foxp3^+$) $CD4^+$ T cells were then sorted to determine DNMT1 expression. In agreement with a critical role of DNMT1 in negatively controlling Foxp3 expression, we detected significant lower DNMT1 levels in GFP^+ cells as compared to the GFP^- population (Figure 14G).

We next examined whether the overall accumulation of DNMT1 and DNMT3b protein by strong TCR signaling leads to enhanced enrichment of these two enzymes at the *foxp3* locus, which could account for the increased CpG methylation status in the promoter of the *foxp3* gene. As shown by our immunocytochemistry experiments, DNMT1 protein resides in small punctate structures within naïve $CD4^+$ T cells' nuclei (Figure 15A). In agreement with our western blot results, the total signal intensity of DNMT1 staining rose sharply upon stimulation in a TCR- signal-strength-dependent manner. Moreover, in contrast to a few concentrated DNMT1 punctae observed in naïve cells (TCR-0h) or cells given a short and weak priming (102S-6h), T cells with strong TCR signaling (102S-72h, MCC-6h/72h) had significantly increased nuclear DNMT1 staining not only with respect to the intensity of each individual puncta, but also the number of punctae (Figure 15A). We predicted that this increased quantity and broadened distribution would impact the occupancy of DNMT1 on the *foxp3* gene's regulatory regions. The locus-specific recruitment of DNMT1 and DNMT3b was quantified by chromatin immunoprecipitation (ChIP). Consistent with the overall demethylated status of promoter CpG islands in unstimulated and weakly stimulated $CD4^+$ T cells, we did not detect any specific DNMT1 or DNMT3b binding to the *foxp3* promoter in these two populations (Figure 15B&E). In contrast, cells that were suboptimally stimulated—either with weak agonist for a long duration or with strong agonist for a short duration—showed significantly enhanced binding of DNMT1 and

DNMT3b to *foxp3*'s CpG islands (Figure 15B&E). Interestingly, strong TCR signaling also enhanced DNMT1 occupancy at the CNS2 region, but not DNMT3b occupancy (Figure 15C&F). Importantly, as implied by the local accumulation of DNMT1 at punctae within the nucleus, we could demonstrate a degree of specificity in the local recruitment of DNMT1 to the *foxp3* locus. In agreement with the fact that strong stimulation of 5C.C7 T cells favours their Th1 lineage differentiation, no significant DNMT1 binding was detected within the CNS-6 region of the *ifng* gene after MCC stimulation (Figure 15D), which was methylated in naïve cells but completely demethylated and accessible to support IFNγ production in Th1 cells[148]. This biochemical evidence, combined with the associated epigenetic and functional outcomes, indicates that strong TCR signaling blocks the accessibility of the *foxp3* locus through the elevation of DNMT1 and DNMT3b protein levels, delivery of these two enzymes to *foxp3*'s regulatory region, and the resultant enhanced local methylation.

4.2.4 TCR signaling stabilizes DNMT1 protein through inhibition of Gsk3β activity and protection from proteasome-mediated degradation

Based on the data presented above, we hypothesized that there must be a signaling node that is capable of receiving signals from both PI3K and PLCγ pathways downstream of TCR, and then integrating these signals to post-translationally modify the level of DNMT1 protein. Within the TCR signaling network, a good candidate for such a modulator is glycogen synthase kinase 3 beta (Gsk3β). Gsk3β is a constitutively active serine/threonine protein kinase in resting cells[149]. Upon receptor signaling, its

activity can be silenced by phosphorylation mediated through PI3K-Akt[150] and/or PLCγ-PKCθ signaling[151]. Interestingly, in some human tumor cell lines, suppression of Gsk3β activity upon PI3K activation has been implicated as the cause for stabilized DNMT1 protein levels: PI3K prohibits Gsk3β-mediated phosphorylation of DNMT1 and thus protects it from ubiquitin-mediated proteasomal degradation[152]. We examined whether this DNMT1 stabilization mechanism is exploited by TCR signaling. T cells were stimulated with 102S peptide antigen for 18hrs, and then treated with a specific proteasome inhibitor, MG-132 or SB-216763, a specific inhibitor of Gsk3β activity[152]. When these cells were analyzed at the 72hr endpoint, both inhibitor treatments partially but significantly enhanced the level of DNMT1 protein in response to weak TCR signaling (Figure 16A). Reciprocally, whereas blocking TCR engagement, PI3K activation, or PLC activity at the 18hr point led to a substantial Foxp3 induction, the addition of Gsk3β inhibitor could partially diminish this effect (Figure 16B). Overall, these data suggest that extensive TCR signaling stabilizes DNMT1 protein by inhibiting Gsk3β-mediated phosphorylation and proteasomal degradation of DNMT1.

4.2.5 TCR signaling elevates DNMT1 protein levels by dampening its miRNA modulator, miR-148a

The fact that MG-132 and Gsk3b inhibitor could only partially rescue the level of DNMT1 protein led us to speculate that there is another layer of control, possibly at the level of DNMT1 translation. miRNAs are small non-coding RNAs that regulate gene expression posttranscriptionally, via a combination of mRNA degradation and/or

translational repression, depending on the particular miRNA[153]. Since DNMT1 transcript levels were not altered in our T cells, we explored the possibility that TCR signaling could release miRNA-mediated translational inhibition of DNMT1 expression. Two members of the miR-148 family, miR-148a[154] and miR-152[155], were previously suggested to be direct modulators of DNMT1 expression. Upon TCR engagement, expression levels of all three miRNAs within this family, miR-148a, miR-148b, and miR-152 were suppressed (Figure 16C). When ectopically expressed using a retroviral tool during T cell activation, all three failed to suppress DNMT1 mRNA levels (Figure 16D). However, one of the three—miR-148a—significantly suppressed DNMT1 expression at the protein level (Figure 16E). Furthermore, $CD4^+$ T cells that forcibly overexpressed miR-148a enhanced their Foxp3 induction significantly (Figure 16F). This suggested that dampening of miR-148a expression is a complimentary pathway that contributes to TCR-mediated epigenetic regulation of the *foxp3* gene.

4.2.6 TGF-β antagonizes TCR signaling by targeting DNMT1 for degradation via p38 activation

In addition to TCR signal strength, TGF-β signaling also strongly modulates iTreg induction. Although 72 hours of 102S stimulation normally leads to very few iTregs, TGF-β can exert a dominant effect which increases the proportion of iTregs substantially (Figure 17A). It is known that TGF-β acts through its receptor complex to trigger the activation of Smad3 protein, which then translocates to the nucleus and promotes *foxp3* transcription[74]. However, this classical pathway cannot explain how

TGF-β overcomes methylation-mediated transcriptional silencing within the *foxp3* locus under the circumstance of strong TCR signaling. We thus investigated the direct impact of TGF-β on epigenetic regulation of the *foxp3* gene. When strong signals from both the TCR and TGFβ receptors were induced simultaneously, the TCR-mediated accumulation of DNMT1 protein was abolished (Figure 17A&B). The dampening of DNMT1 protein levels was also not related to TGF-β's inhibitory effects on T cell proliferation: a reduction of DNMT1 was observed in each successive generation when TGF-β was present (Figure 17B). The regulation of DNMT1 by TGF-β mainly occurred at the protein level, as the DNMT1 mRNA level was not affected by TGF-β treatment (Figure 17C). As could be expected from the reduced protein level of DNMT1, TGF-β treatment also resulted in reduced CpG methylation within the promoter (Figure 17D) region of *foxp3*.

We also examined whether TGF-β signaling can effectively antagonize strong agonist-induced DNMT1 accumulation and iTreg differentiation. $CD4^+$ T cells stimulated with MCC alone for 72 hours have more DNMT1 protein accumulated than those stimulated with 102S for 72 hours (Figure 18A). Similarly, in contrast to a relatively strong impact of TGF-β signaling on DNMT1 accumulation in 102S-stimulated cells, TGF-β could only moderately downregulate the DNMT1 protein in cells stimulated with MCC (Figure 18A). In agreement with this, when same concentrations of TGF-β were supplemented, MCC induced significantly less $Foxp3^+$ cells (Figure 18B).

This suggested that excessive TCR signalling can antagonize TGF-β effects on iTreg differentiation.

In addition to Smad-mediated transcriptional regulation, TGF-β can also initiate alternative signalling via the Ras-ERK, TAK-MKK4-JNK, and TAK-MKK3-6-p38 pathways[156]. During TCR stimulation of naïve T cells, ERK activation is inhibited by TGF-β treatment[157], and this curtailed ERK signaling failed to increase *foxp3* expression (Figure 12A). We thus investigated the potential roles of the other two MAPK pathways in potentially linking TGFβ receptors to DNMT1 using well-established specific inhibitors. Whereas treatment with a specific JNK inhibitor had no effect, treatment with a p38 inhibitor completely abolished TGF-β-induced DNMT1 downregulation, as shown by both the frequency of $DNMT1^+$ cells and the intensity of DNMT1 staining at the single-cell level (Figure 17E). Consistent with these increased DNMT1 protein levels, blockade of the p38 pathway also resulted in a significant reduction of Foxp3 induction by TGF-β (Figure 17F). These data suggest that TGF-β signaling antagonizes the effect of TCR signaling on DNMT1 stabilization and *foxp3* gene methylation through the activation of p38.

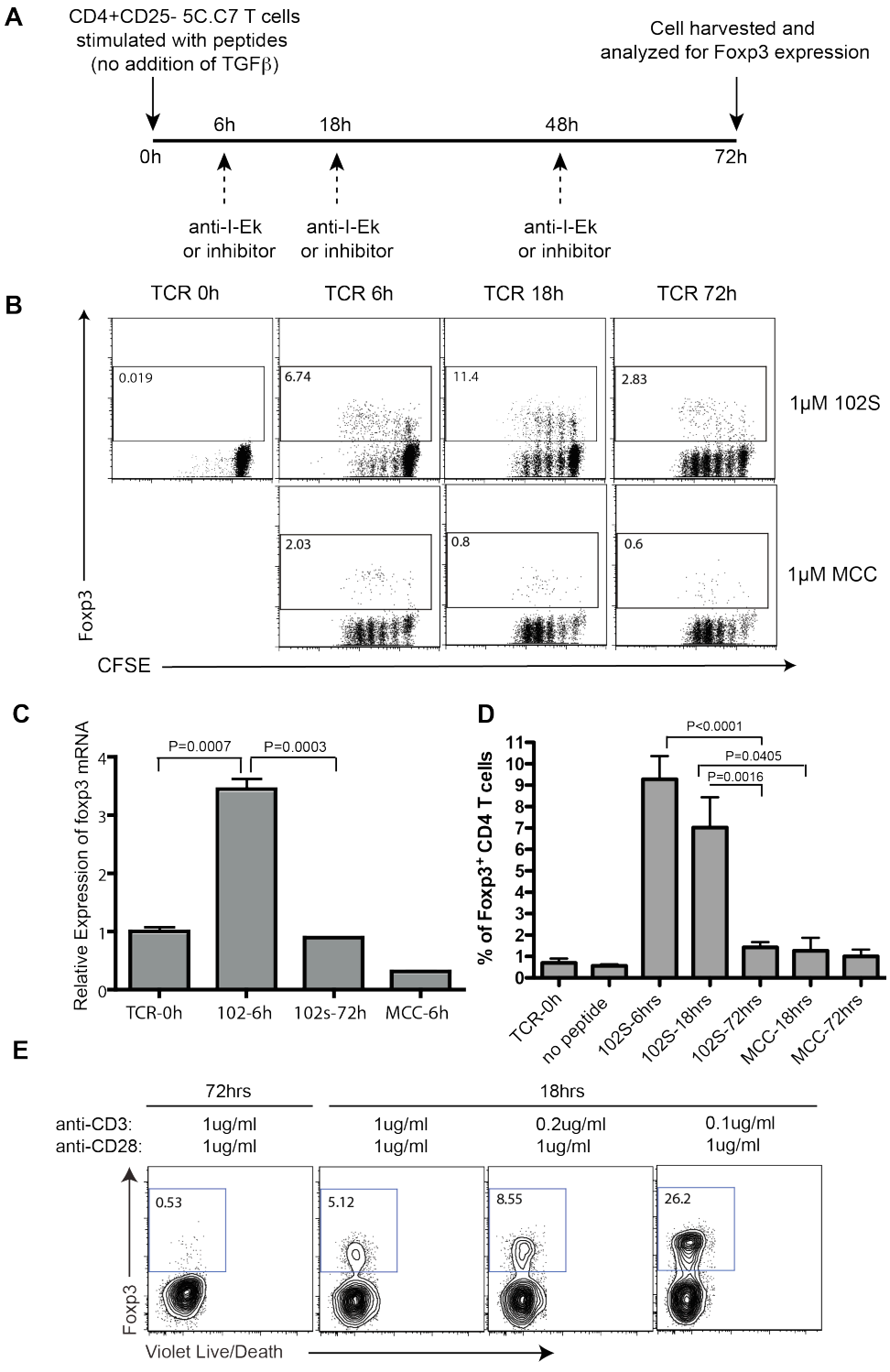

Figure 11: Suboptimal TCR activation in terms of both strength and duration favors iTreg differentiation.

(A) Schematic view of the workflow for analyzing the role of TCR strength and duration in iTreg differentiation. Briefly, sorted $CD4^+CD25^-$ T cells from the lymph nodes of 5C.C7 TCR transgenic mice were labeled with CFSE, cultured with syngeneic T cell-depleted splenocytes without peptide in the presence of 10 ng/ml recombinant IL-7, or stimulated by syngeneic T cell-depleted splenocytes loaded with a strong agonist peptide MCC (1 μM) or a weak agonist 102S (1 μM). Anti-I-E^k antibody or small molecule inhibitors that block specific pathways were added at the indicated time points. The percentages of $CD4^+Foxp3^+$ T cells were analyzed by intracellular staining and flow cytometry at 72 h. (B&D) Percentages of iTregs generated with the indicated TCR stimulatory strength and duration are shown. (B) Representative FACS plot. (D) Statistical analysis. Data show the means ± SEM from three independent experiments. (C) At the end of culture, $CD4^+$ T cells were FACS-sorted, and total RNA was extracted for quantitative PCR analysis. Data show the means ± SEM from three independent experiments. (E) Sorted $CD4^+CD25^-$ T cells from the lymph nodes of C57BL/6 mice were labeled with CFSE and then stimulated with various concentrations of plate-bound anti-CD3 and anti- CD28 antibody for 18 h. After this, the cells were either further stimulated with anti-CD3 and anti-CD28 for 54 h (TCR 72 h total) or maintained without TCR stimulation for 54 h (TCR 18 h). The induction of Foxp3 was then examined by intracellular staining. Data represent three independent experiments.

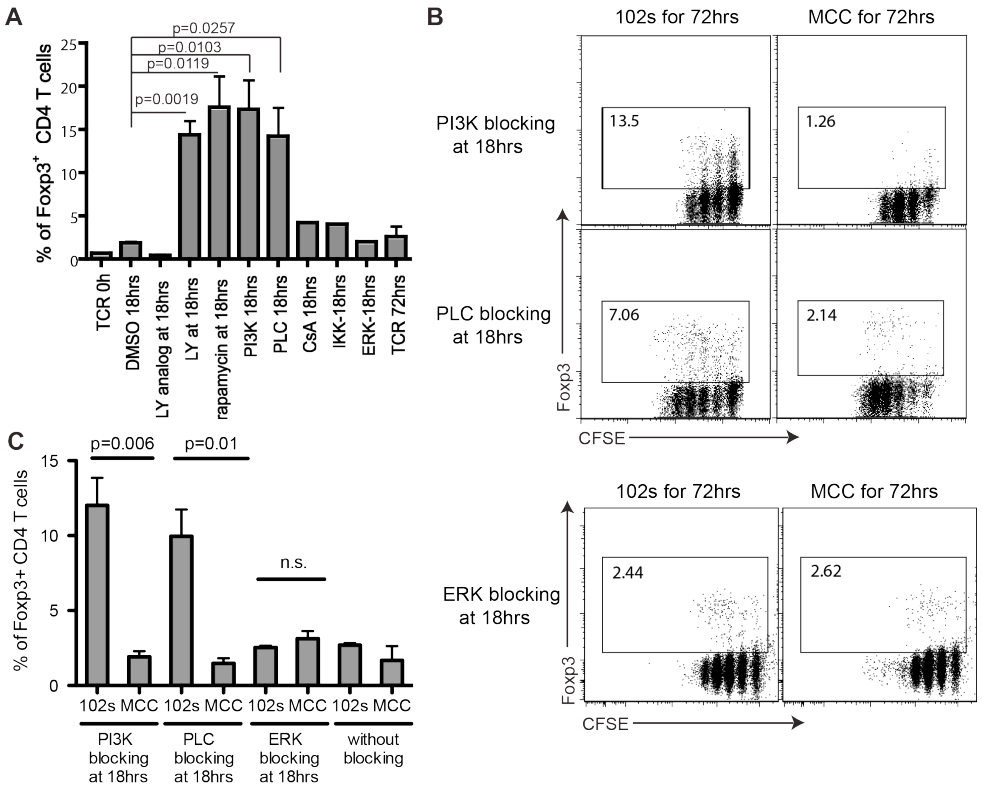

Figure 12: PI3K-Akt-mTOR and PLC pathways downstream of TCR signaling negatively regulate iTreg differentiation.

(A) Sorted $CD4^+$ $CD25^-$ T cells from 5C.C7 transgenic mice were stimulated with 1 μM 102S for 72 h as described in Fig. 1A. LY 294002 (10 μM), rapamycin (25 nM), cyclosporin A (CsA), 1 μg/ml), IκB kinase inhibitor III (IKK, BMS-345541, 1 μM), ERK (ERK inhibitor II, FR180204, 1 μM), PI3K (PIK-75, 100 nM), or PLC (U-73122, 1 μM) were added at the indicated time points to block specific pathways downstream of TCR signaling. The percentages of $CD4^+Foxp3^+$ T cells were analyzed by flow cytometry at 72h after TCR activation. The bar graph shows the means ± SEM from three independent experiments. (B&C) Sorted $CD4^+CD25^-$ T cells from 5C.C7 transgenic mice were stimulated with 1 μM 102S or MCC for 72 h. Inhibitors that specifically block the PI3K,

PLC, or ERK pathways were added at 18 h after TCR stimulation. The percentages of $CD4^+Foxp3^+$ T cells were analyzed by flow cytometry at 72 h after TCR activation. (B) Representative FACS plots. (C) The bar graph shows the means ± SEM from three independent experiments.

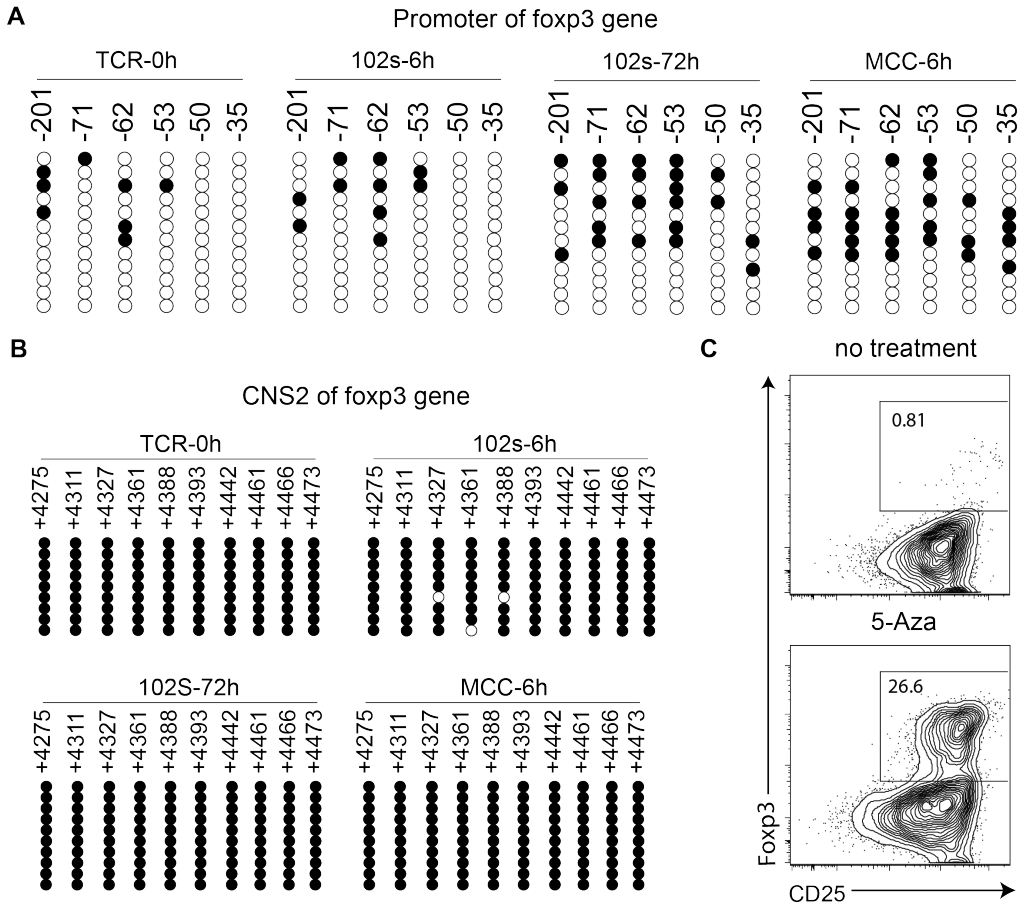

Figure 13: Strong TCR signaling enhances CpG methylation within the *foxp3* locus.

(A&B) $CD4^+$ $CD25^-$ T cells from male 5C.C7 transgenic mice were stimulated as described in Fig. 11A. The methylation status of CpG islands within the *foxp3* promoter (A) or *foxp3* CNS2 (B) from these cells was determined by bisulfite sequencing analysis. Each row represents one DNA strand. The number on top indicates the position of CpGs relative to the transcription start site of the *foxp3* gene. Open circles, unmethylated CpGs; filled circles, methylated CpGs. Data represent three independent experiments. (C) 5C.C7 T cells were activated with 102S for 72 h while also being treated with 5-

azacytidine (5-Aza) at 18 h post-stimulation. The percentages of $CD4^+Foxp3^+$ T cells were analyzed by flow cytometry at 72 h after TCR activation. Data represent three independent experiments.

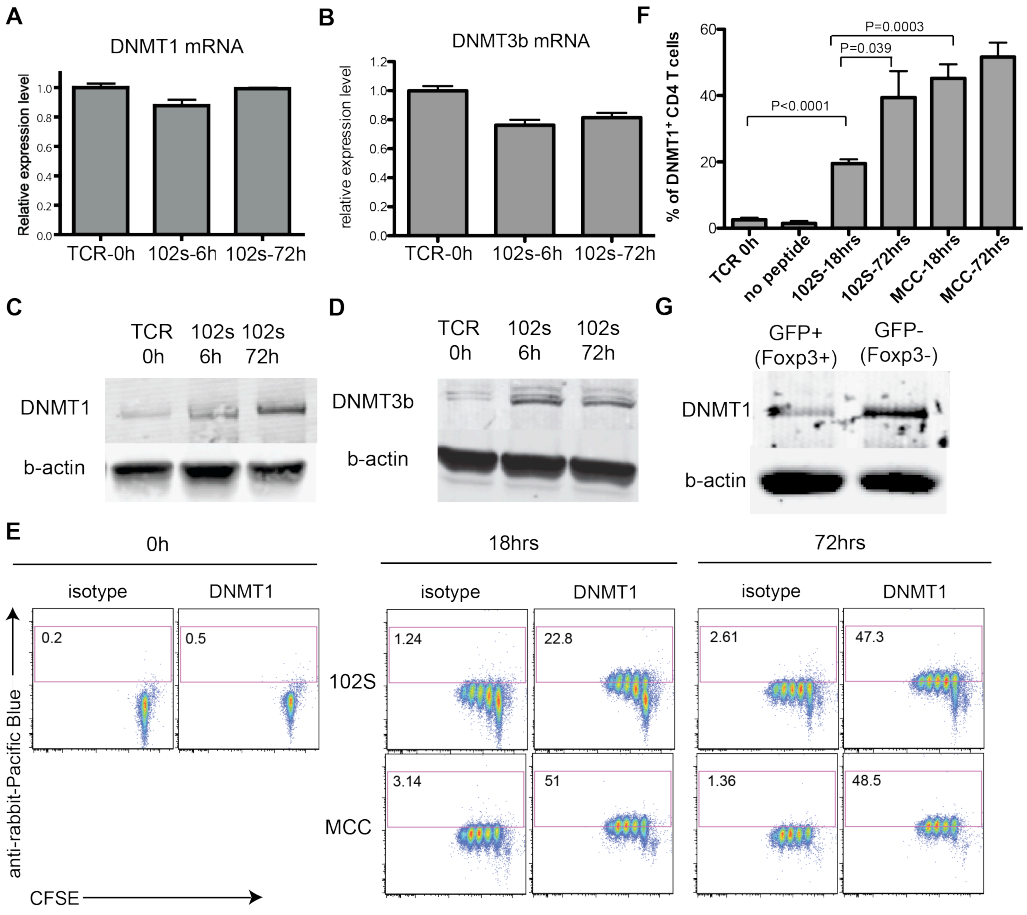

Figure 14: DNMT1 and DNMT3b are posttranscriptionally upregulated by TCR signaling in a strength- and duration-dependent manner.

(A&B) $CD4^+CD25^-$ T cells from 5C.C7 transgenic mice were left unstimulated (TCR-0h) or stimulated with 1 μM 102S for 6 h (TCR-6h) or 72 h (TCR-72h) and then sorted by FACS. Total RNA and protein were extracted, and relative expression of dnmt1 mRNA (A) and dnmt3b mRNA (B) and DNMT1 protein (C) DNMT3b protein (D) were determined by quantitative PCR and Western blot analysis. In A and B, data show the means ± SEM from three independent experiments. (E&F) $CD4^+$ $CD25^-$ T cells from 5C.C7 transgenic mice were labeled with CFSE and stimulated as described in Fig. 11A.

The expression of DNMT1 protein at the single cell level was determined by intracellular staining. (E) Representative FACS plots. (F) Statistical analysis. Data show the means ± SEM from three independent experiments. (G) Sorted $CD4^{+}GFP^{-}$ T cells from the lymph nodes of Foxp3-GFP-Cre mice were stimulated with 0.1 μg/ml plate-bound anti-CD3 and 1 μg/ml anti-CD28 antibody for 18 h and then maintained without further TCR stimulation for 54 h. GFP^{+} and GFP^{-} $CD4^{+}$ T cells were then sorted for examination of DNMT1 protein by Western blot.

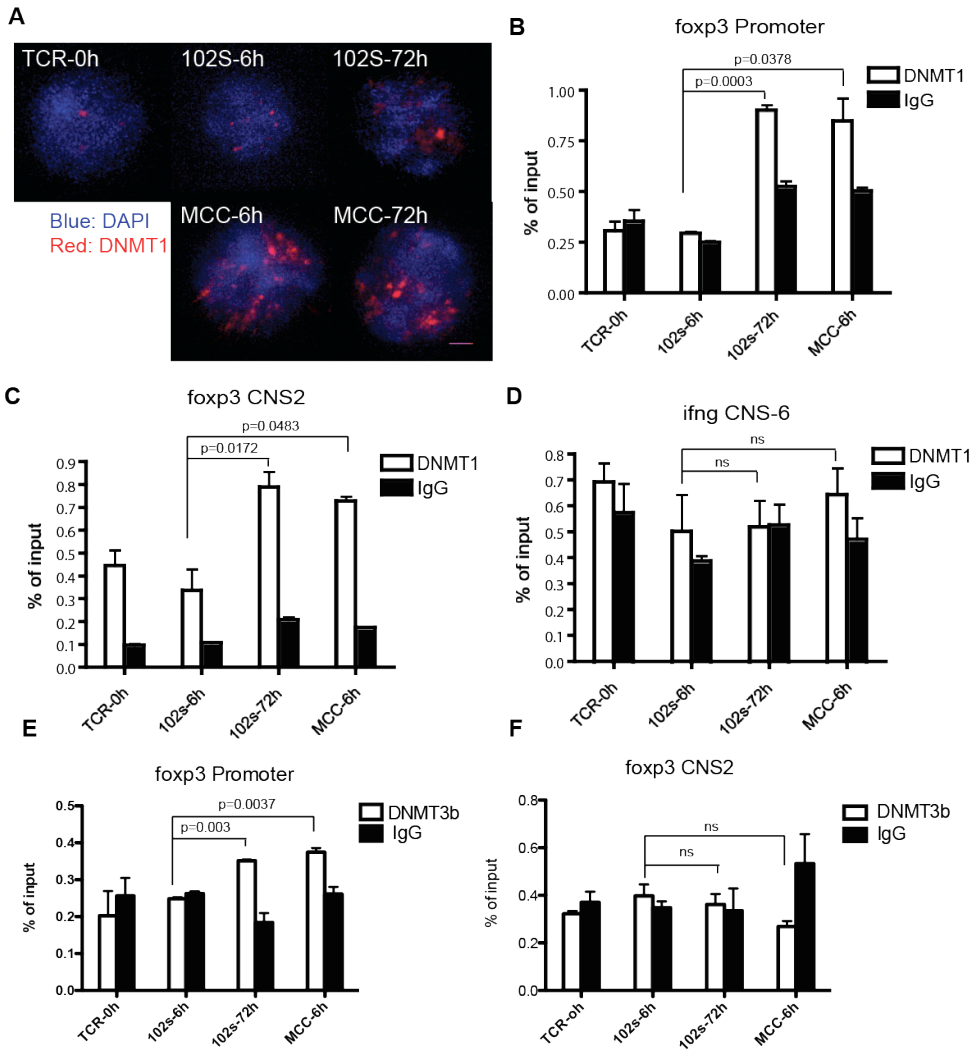

Figure 15: Strong TCR signaling causes enhanced enrichment of DNMT1 and DNMT3b at the *foxp3* locus.

(A) Representative images show the nuclear localization of DNMT1. $CD4^{+}CD25^{-}$ T cells from 5C.C7 transgenic mice were stimulated as described in Fig. 11A. The cells were then fixed with 4% paraformaldehyde on cover slips and stained for intracellular DNMT1. DAPI was used to label the nucleus. Data represent three independent experiments. (B–F) Chromatin immunoprecipitation analysis for the enrichment of

DNMT1 at *foxp3* promoter (B), *foxp3* CNS2 (C), and *Ifng* CNS-6 (D) or DNMT3b at *foxp3* promoter (E) and *foxp3* CNS2 (F) in 5C.C7 transgenic $CD4^{+}CD25^{-}$ T cells that were left unstimulated (TCR-0h) or stimulated as in A. The amount of DNA immunoprecipitated by the DNMT1or DNMT3b-specific antibody or a nonspecific control IgG antibody was quantified by quantitative PCR using primers specific for the indicated gene-regulatory regions and normalized to the input before immunoprecipitation. Data show the means ± SEM from three independent experiments. ns, not significant.

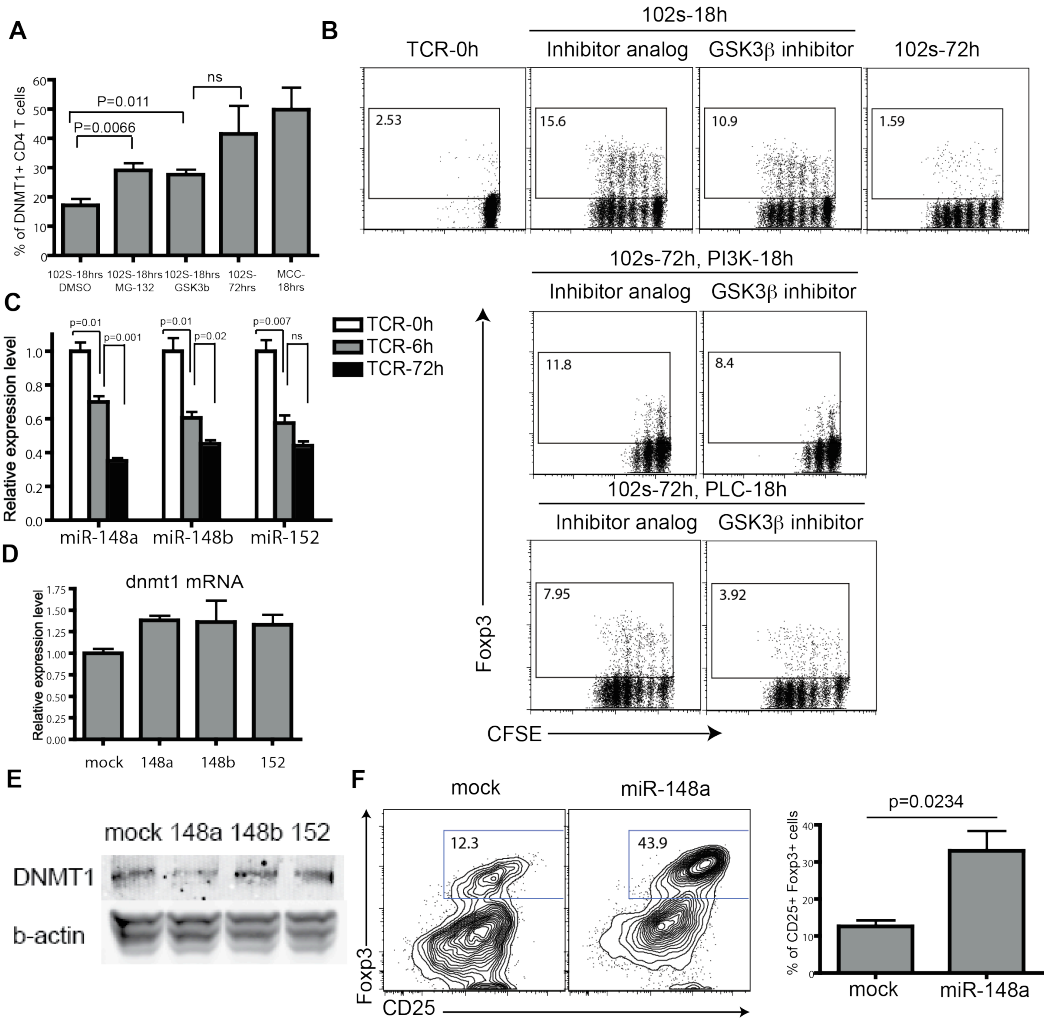

Figure 16: TCR signaling stabilizes DNMT1 by inhibiting GSK3-β-induced proteasomal degradation of DNMT1 and repressing miR-148a-mediated inhibition of DNMT1 translation.

(A) $CD4^{+}CD25^{-}$ T cells from 5C.C7 transgenic mice were stimulated with 1 μM 102S for 18 h and treated with 0.4 μM MG-132 or 1 μM GSK3- β inhibitor SB-216763 at 18h post-TCR stimulation. The expression of DNMT1 protein at 72 h was quantified by intracellular staining of DNMT1 followed by flow cytometry analysis. Cells that were activated with 1 μM 102S for 72 h or 1 μM MCC for 18 h without other treatment were

used as controls. Data show the means ± SEM from three independent experiments. (B) $CD4^+CD25^-$ T cells from 5C.C7 transgenic mice were labeled with CFSE and stimulated with 1 μM 102S for the indicated durations. 1 μM GSK3- β inhibitor or its non-functional analog were added at 18 h together with either 100 nM PIK-75 (PI3K-18h) or 1 μM U-73122 (PLC-18h). The percentages of $CD4^+Foxp3^+$ T cells were analyzed by flow cytometry at 72 h after TCR activation. Data represent three independent experiments. (C) 5C.C7 $CD4^+CD25^-$ T cells were stimulated with 1 μM 102S for the indicated durations. The $CD4^+$ T cells were then FACS-sorted, and total RNA was extracted. The relative expression of miR-148a, miR-148b, and miR-152 transcript was quantified by quantitative PCR analysis. Data show the means ± SEM from three independent experiments. (D) 5C.C7 $CD4^+CD25^-$ T cells were activated with 1 μM 102S and transduced with retrovirus that encodes GFP only (mock), miR-148a together with GFP (miR-148a), miR-148b together with GFP (miR-148b), and miR-152 together with GFP (miR-152). Three days after transduction, $CD4^+GFP^+$ T cells were sorted and extracted for total protein. DNMT1 protein level was quantified by Western blot analysis. Data represent three independent experiments. (E&F) 5C.C7 $CD4^+CD25^-$ T cells were primed and transduced with mock virus or miR-148a as described above and then cultured in the presence of 50 units/ml IL-2 and 2 ng/ml TGF-β for 4 days. The percentages of $CD25^+$ $Foxp3^+$ T cells were analyzed by flow cytometry. (E) Representative FACS plot. (F) Statistical analysis. Data show the means ± SEM from three independent experiments.

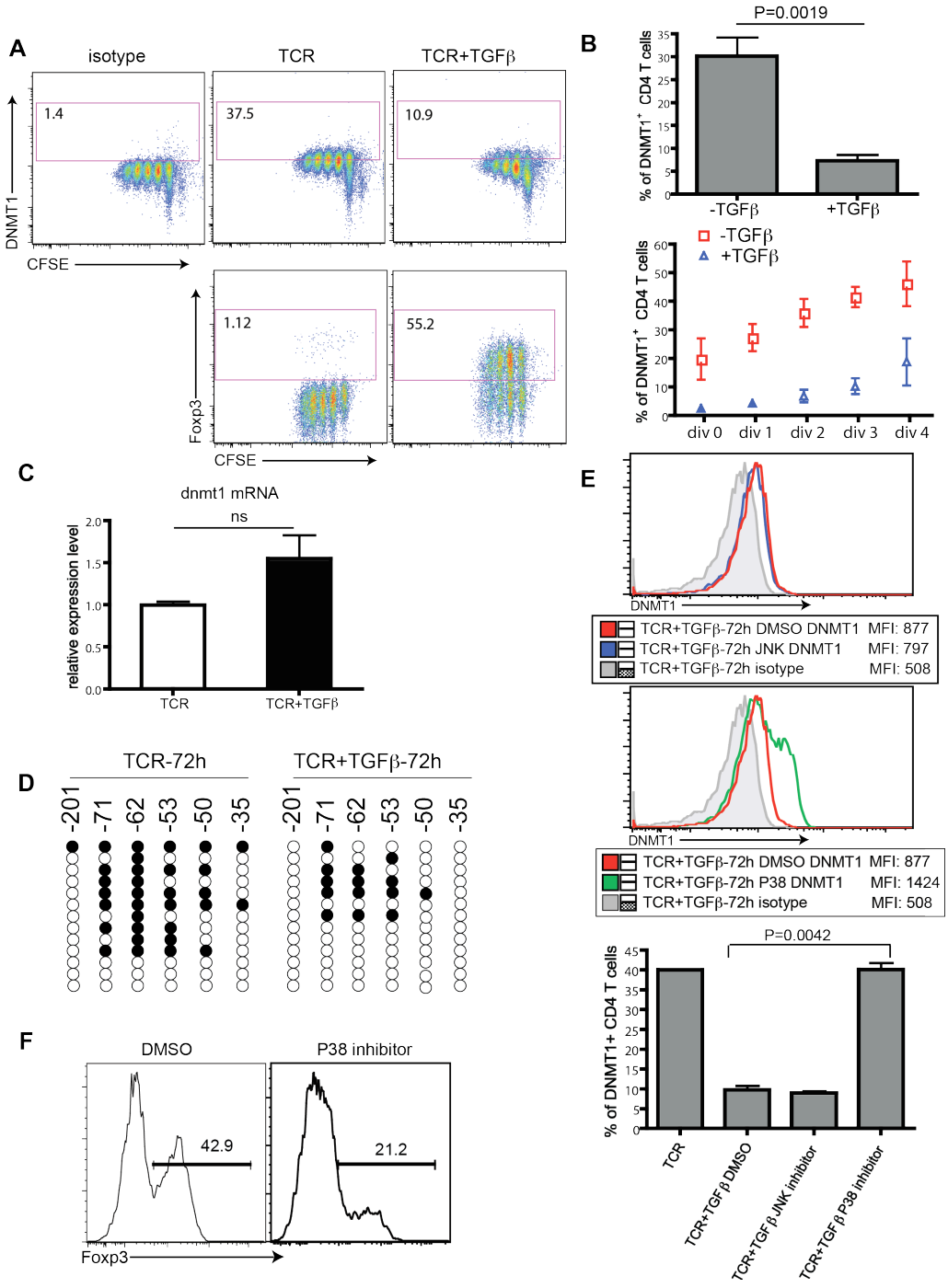

Figure 17: TGF-β signaling antagonizes TCR-signal-mediated DNMT1 stabilization via the p38 pathway.

(A-C) $CD4^+CD25^-$ T cells from 5C.C7 transgenic mice were labeled with CFSE and stimulated with 1 μM 102S in the absence (TCR) or presence of 5 ng/ml TGF-β (TCR+TGFβ) for 72 h. The expression of DNMT1 (both protein and mRNA level) and Foxp3 at the single cell level was quantified by intracellular staining. (A) Representative FACS plots. (B) Statistical analysis. Data show the means ± SEM from three independent experiments. (C) mRNA level of dnmt1. (D) The methylation status of CpG islands in these cell *foxp3* promoters was determined by bisulfite sequencing analysis. Data represent three independent experiments. (E) $CD4^+CD25^-$ T cells from 5C.C7 transgenic mice were stimulated with 1 μM 102S and 5 ng/ml TGF-β in the presence of 1 μM JNK inhibitor II (SP600125) or 10 μM p38 MAP kinase inhibitor III (ML3403) for 72 h. The expression of DNMT1 was determined by intracellular staining. MFI, mean fluorescence intensity. Top, representative FACS plot. Bottom, statistical analysis. Data show the means ± SEM from three independent experiments. (F) 5C.C7 transgenic $CD4^+CD25^-$ T cells were stimulated with 1 μM 102S and 5 ng/ml TGF-β in the presence of 10 μM p38 MAP kinase inhibitor III (ML3403) or DMSO for 72 h. The percentages of $CD4^+Foxp3^+$ T cells were analyzed by flow cytometry. Top, representative FACS plot. Bottom, Statistical analysis. Data show the means ± SEM from four independent experiments.

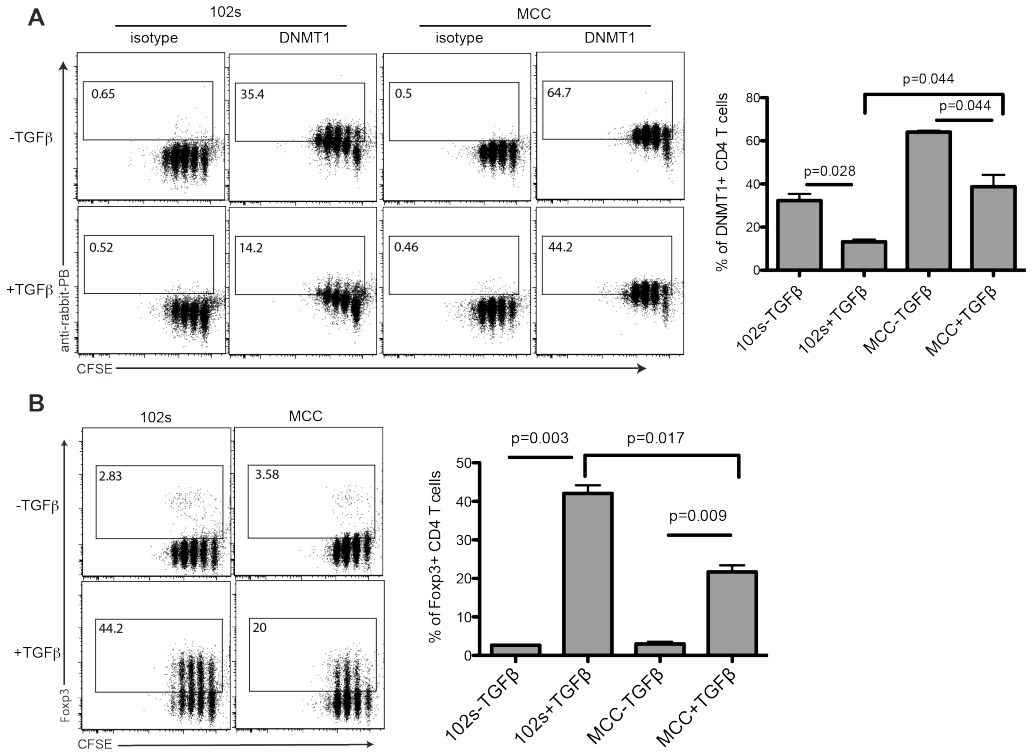

Figure 18: DNMT1 level and iTreg differentiation is tightly controlled by the balance between TCR signaling strength/duration and TGF-β signaling.

(A&B) $CD4^{+}CD25^{-}$ T cells from 5C.C7 transgenic mice were labeled with CFSE, and stimulated with 1μM 102S or 1μM MCC in the absence (-TGF-β) or presence of 5ng/ml TGF-β (+TGF-β) for 72hrs. The expression of DNMT1 (A) and Foxp3 (B) at the single cell level was quantified by intracellular staining. Left: Representative FACS plots. Right: Statistical analysis. Data show means ± SEM from three independent experiments.

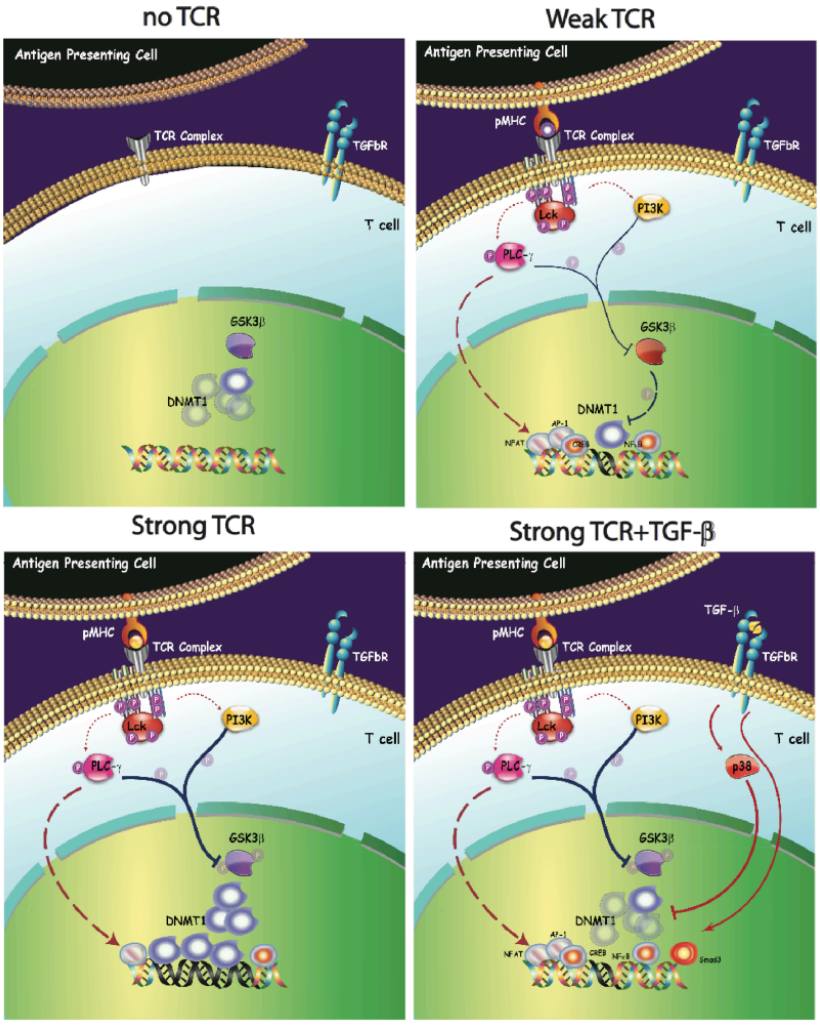

Figure 19: Model for the epigenetic regulation of iTreg differentiation by TCR and TGFβ signaling.

In naïve CD4⁺ conventional T cells, the promoter of *foxp3* gene was mostly demethylated and the cells are poised for Foxp3 induction. Weak TCR stimulation induced only modest DNMT1 accumulation so the *foxp3* promoter still mostly maintains demethylated. At the same time, the transcription factors (NFAT, AP-1) are activated and bind to the accessible *foxp3* promoter to promote *foxp3* transcription. However,

when $CD4^+$ T cells are stimulated with antigens with higher affinity or for longer durations, the level of DNMT1 and its enrichment to *foxp3* locus are significantly elevated, which leads to substantial DNA methylation in the CpG island of *foxp3* promoter and inhibits *foxp3* transcription. During this process the augmentation of DNMT1 is regulated through at least two posttranscriptional mechanisms; that is, strong TCR signal inactivates GSK3β to rescue DNMT1 protein from proteasomal degradation, and strong TCR signal suppresses miR-148a to derepress DNMT1 mRNA translation. Meanwhile, TGF-β directly antagonizes TCR-induced DNA methylation of *foxp3* locus by promoting drastic downregulation of DNMT1 via activation of p38. At the same time, TGF-β also directly promotes *foxp3* transcription through activation of Smad3.

4.3 Discussion

Since it was first appreciated that Tregs could be induced from naïve T cell precursors[158], the combinatorial roles of TCR signaling and TGF-β receptor signaling have been well established as important determinants of *foxp3* transcriptional activation[74,129-131]. Here we have identified multiple pathways by which signaling through TCR and TGFbR converge to control the protein level of DNMT1, an epigenetic modifier that we and others[145] have shown to strongly influence *foxp3* locus accessibility and iTreg differentiation (Figure 19). Our data suggest that DNMT1-mediated methylation in *foxp3* locus is likely aided by DNMT3b. Upon short TCR stimulation, prior to strong DNMT1 elevation, a significant accumulation of DNMT3b protein is observed (Figure 14C&D). However, this cellular accumulation does not translate into increased DNMT3b occupancy within the *foxp3* promoter region, which was only observed in cells receiving a prolonged stimulation (Figure 15E). This suggests that there are additional factors required for the recruitment of DNMT3b to the *foxp3* promoter. Previous studies showed that DNMT1 and DNMT3b co-localize and directly associate with each other through the N-terminal domain[146], which indicates that sufficient accumulation of DNMT1 triggered by a prolonged TCR stimulation may be required to recruit or anchor DNMT3b to the *foxp3* locus. Therefore, our model suggests DNMT1 serves as the key modulator controlling transcriptional accessibility to *foxp3*'s regulatory regions.

In its role as a signal integrator, we believe that DNMT1 represents the node where TCR-based self/non-self discrimination converges with environmentally-cued danger signals. TCR signals mitigate miR-148a-mediated DNMT1 translation inhibition, and also relieve GSK3β-mediated DNMT1 protein degradation via PI3K and PLC-γ signaling (Figure 16). Because TCRs with high avidity for self-antigens are preferentially deleted or converted to nTregs in the thymus, stronger TCR signaling can be interpreted via higher DNMT1 levels as an indication of foreignness, which then favors *foxp3* methylation. CD28 costimulation can provide an independent indication of foreignness, as its ligands are induced on APCs by signaling in response to microbial and viral products. CD28 signaling can then also feed in to regulation of DNMT1 by enhancing TCR-induced PI3K activity, inhibiting GSK3β, stabilizing DNMT1, and further favoring *foxp3* methylation. Meanwhile, naïve T cells maintain an only partially methylated *foxp3* promoter, presumably because the level of DNMT1 attained by tonic/homeostatic TCR signaling is below the threshold needed for *foxp3* methylation. Finally, healthy or tumor tissues can exert influence on T cell priming by secreting TGF-β, which can act via p38 to antagonize strong TCR signaling by diminishing DNMT1 protein, impeding *foxp3* methylation, and pushing the balance of immunity toward iTreg-mediated tolerance.

Whereas transcription factors such as NFAT can be activated within minutes, and less than one hour of TCR signaling is sufficient to drive T cells into the proliferative cycle[141], DNMT1 accumulates and methylates *foxp3* over the course of days. This

mechanistic and temporal segregation of epigenetic control from transcription factor-mediated control could allow T cells to gauge the duration of TCR signaling over long periods (which likely represents the persistence of antigen). Furthermore, by segregating the commitment to proliferation from the commitment to silence *foxp3*, T cells can make the decision for clonal expansion shortly upon antigen encounter, but can integrate signals over the following days before finalizing their iTreg vs. Th fate. This dichotomous commitment process may thus support the adaptive immune response's dual requirement for rapidity of response on the one hand, and accuracy of pathogenic discrimination on the other. In line with this possibility, it is noteworthy that human naïve T cells transiently express Foxp3 during priming, even when their eventual fate is an effector Th lineage[159,160]. In the DNMT1-centric view, this would represent the early activity of NFAT/NFkB/AP1 on a naïve T cell's partially-methylated *foxp3* promoter, which would only be completely repressed by DNMT1-mediated methylation after a much longer course of TCR signaling.

Overall, it is a well-appreciated concept that T cells interpret subtle differences between antigens and between antigens' contextual cues to enact their fate decision; and, that it is epigenetic modifications that enforce the heritage of differentiated T cells[70,161-163]. Our data illustrate a mechanism whereby TCR signaling and environmental cues can target the epigenetic machinery directly in order to instruct differentiating T cells. Unlike most cell types, in which differentiation and proliferation are in general mutually

exclusive, T cells acquire their identities in the midst of rapid proliferation. It would be difficult to imagine how T cells could employ transcription factor activation as a heritable mechanism: first, in the absence of ligands, the activation status of TCR[141] or transcription factors (e.g. NFAT[164]) can only be maintained within the range of minutes following ligand withdrawal, and so would be unlikely to preserve their activation state between mother and daughter cells; second, the newly divided daughter cell makes brief contact with APCs *in vivo*[165], which likely gives them different antigen experience than their mother cells. In contrast, direct TCR-driven epigenetic reprogramming can mark mother cells' antigen experiences in the genome during the commitment to cell division, which then keeps daughter T cells poised according to their mothers' lineage choice. These features are also not likely to be exclusive to the iTreg lineage choice. The Th2 and Th17 lineages are also antagonized by strong TCR signal strength, and *il-4* and *il-17* are both expressed in a methylation-sensitive manner[13,120-122]. Thus, upon TCR activation, it may be possible that DNMT1 or another epigenetic mechanism also controls master transcription factors or signature cytokines of Th2 and Th17 lineages in a manner analogous to *foxp3.*

5. MeCP2 enforces Foxp3 expression to determine nTregs' resilience to inflammation: A key epigenetic regulator controlling Foxp3 maintenance

The contents of this dissertation chapter have been slightly modified from the following manuscript that was current under review at *Immunity*.

Chaoran Li*, Shan Jiang*, Si-Qi Liu, Erik Lykken, Lin-Tao Zhao, Jose Sevilla, Bo Zhu and Qi-Jing Li. (* equal contribution). MeCP2 enforces Foxp3 expression to determine natural regulatory T cells' resilience to inflammation.

5.1 Introduction

Methyl-CpG binding protein 2 (MeCP2) is an X-chromosome linked nuclear protein[166] that binds methylated DNA[167,168], and has been reported to play bifunctional roles in regulating gene expression[169]. As the docking of MeCP2 can recruit Histone deacetylases (HDAC)[170] and DNA (cytosine-5)-methyltransferase 1 (DNMT1)[171] to methylated CpG elements, this protein has traditionally been considered to be a transcription repressor. However, recent genome-wide studies have revealed that MeCP2 can also bind avidly to unmethylated CpG DNA and facilitate the transcription of a large proportion of genes[169,172]. Specifically, MeCP2 was shown to associate directly with transcription activators such as cAMP responsive element binding protein 1 (CREB1) in promoters, where they synergistically promote gene expression[169]. Thus, the current consensus is that, depending on the genomic context, MeCP2 acts as either a transcriptional repressor or activator[173].

Previous studies have centered almost exclusively on MeCP2's role in the central nervous system. This is attributed to the fact that loss-of-function mutations in the *mecp2* locus is the etiological cause of 95% of typical Rett Syndrome (RTT)[174,175]. RTT is a devastating disorder that afflicts 1 in 10,000 females and whose symptoms are largely neurodevelopmental[176]. Based on the limited immunological studies on RTT patients, however, hints of immunological abnormalities have gradually emerged: polymorphisms within the human *mecp2* locus have recently been associated with an increased susceptibility to systemic lupus erythematosus (SLE)[177,178] and primary Sjögren's syndrome (pSS)[179], suggesting that *mecp2* gene mutations may also contribute to the pathogenesis of inflammatory diseases; and a cohort study also demonstrated significantly elevated levels of IgG against food proteins in the sera of RTT patients[180], which may reflect the possibility of gut inflammation or breakdown of the intestinal barrier; most intriguingly, the transplantation of wild type (WT) bone marrow successfully arrested RTT disease in MeCP2 null mice[181]. Nevertheless, apart from these correlative studies, MeCP2's causative role in immune regulation remains largely unexplored.

As potent suppressors of inflammation, $CD4^+$ $CD25^+$ regulatory T cells (Tregs) are an indispensable T cell subset responsible for peripheral tolerance and immune homeostasis[31]. Foxp3 is the master regulator of the Treg gene expression program, and consequently Foxp3 mutation in both humans and mice is sufficient to trigger the

development of severe lymphoproliferative autoimmune disorders[124,182-187]. Foxp3 is essential both for driving natural Treg (nTreg) development within the thymus, and for maintaining lineage identity and suppressive function of peripheral Tregs: deletion of Foxp3 specifically in post-thymic mature Tregs completely abolishes their ability to suppress the onset of effector T cell-mediated autoimmunity[188]. Extensive studies on the molecular mechanisms regulating Foxp3 expression[5] have revealed that many transcription factors, including NFAT[39,73], AP-1[73], Smad3[39], STAT5[36,189], NF-kB[131], Ets-1[190], GATA3[78], Foxo1/3[191] and CREB1[72], bind directly to the *foxp3* locus to promote its expression during Treg differentiation, and the Foxp3/Runx1/CBFb protein complex has recently been suggested to confer the heritable maintenance of Foxp3 expression through an autoregulatory loop[75,192].

In addition to these "trans" regulatory factors, the expression of Foxp3 is also tightly controlled at the epigenetic level[193]. Besides the promoter, three "cis"-regulatory regions including three Conserved Non-Coding sequences (CNS) within the *foxp3* locus are essential in regulating Foxp3's expression. Interestingly, genetic ablation of these individual elements revealed a division of labour in gene regulation[75]: for instance, CNS1, which contains the NFAT-Smad3 binding sites[39], is critical for the peripheral induction of Foxp3 expression in conventional T cells that drives inducible Treg differentiation; on the other hand, CNS2 is specifically required for the maintenance of Foxp3 expression in daughter cells during nTreg cell division. Of note, the CNS2

genomic region is composed of multiple highly conserved CpG islands[72], which suggests that the maintenance of Foxp3 expression is potentially enforced by CpG-associated epigenetic regulators. As MeCP2 is a CpG island-binding protein and known epigenetic regulator, we considered that MeCP2 might potentially play some role in orchestrating *foxp3* gene transcription.

In this study, using genetic approaches that delete MeCP2 specifically in Treg cells, we examined the role of MeCP2 in regulating Treg homeostasis. We find that, although MeCP2 is dispensable for the initial induction of Foxp3 expression during thymus-derived nTreg development and *in vitro*–induced Treg (iTreg) differentiation, it is essential for maintaining the stable expression of Foxp3 and the lineage identity of mature nTregs during inflammation.

5.2 Results

5.2.1 MeCP2 ablation does not affect iTreg differentiation or nTreg development

While dissecting the role of the miRNA cluster miR-17-92 in regulating T cells' effector response, we biochemically identified MeCP2 as a novel target of miR-19b (data not shown). miR-19b promotes $CD4^+$ T cell effector responses, in part through suppressing the differentiation of inducible regulatory T cells (iTregs)[54]. This led to our hypothesis that miR-19b blocks iTreg conversion by dampening the expression of MeCP2, a *foxp3* locus-associated protein (data not shown and Lal et al[194]). To determine

this functional linkage, we initially crossed mice carrying conditional *mecp2* alleles with mice expressing the Cre recombinase transgene under the control of the proximal Lck promoter. In this way, we attained T cell-specific deletion of the *mecp2* gene as early as the late DN2 stage. Contradictory to our initial hypothesis, when $CD4^{+}CD25^{-}$ conventional T cells from $MeCP2^{f/y}$ Lck-Cre mice or their wild type littermates were purified by FACS sorting and cultured under various iTreg skewing conditions, we found no significant differences in the generation of $Foxp3^{+}$ iTreg cells (Figure 20A-C). This indicated that, at least *in vitro*, it is unlikely that a functional linkage exists between miR-19b and MeCP2 during iTreg differentiation, and that MeCP2 is dispensable for the *de novo* expression of Foxp3 in conventional $CD4^{+}$ T cells. Furthermore, the thymic nTreg development was entirely intact in the $MeCP2^{f/y}$ Lck-Cre animals (Figure 20D&E).

5.2.2 Young adult mice with Treg-specific MeCP2 deletion develop spontaneous T cell activation

To examine the role of MeCP2 specifically in mature nTregs, we crossed mice carrying conditional *mecp2* alleles with BAC transgenic mice expressing Cre and GFP proteins under the control of the *foxp3* promoter[95]. This allows us to specifically ablate the *mecp2* gene after T cells establish their commitment into the Treg lineage (Figure 21A). The ablation of Mecp2 protein did not change the relative size of $CD25^{+}Foxp3^{+}$ population within the pool of $CD4^{+}$ T cells (Figure 21B). However, in mice as young as 8 to 10 weeks of age, we observed a significant increase in the total number of cells in the lymph nodes from $MeCP2^{f/y}$ Foxp3-GFP-Cre mice (Figure 21C). In addition, the

proportion of $CD4^+$ T cells adopting an activated phenotype ($CD44^{hi}$ $CD62L^{lo}$) in the spleen and lymph nodes of $MeCP2^{f/y}$ Foxp3-GFP-Cre mice was significantly increased (Figure 21D&E). We then examined the cytokine production of the $CD4^+Foxp3^-$ T cells in these mice: Treg-specific deletion of MeCP2 resulted in significantly elevated levels of IL-17 producing conventional $CD4^+$ T cells (Figure 21F&G). When these mice were aged for more than 6 months, while there were no immunopathologies of the kidney, liver or lung (data not shown), $MeCP2^{f/y}$ Foxp3-GFP-Cre mice frequently developed skin lesions near the neck area and further histological analysis unveiled extensive inflammatory infiltration (Figure 22). Collectively, these data suggest that MeCP2 expression in Tregs is required to enforce immune homeostasis *in vivo*.

5.2.3 MeCP2-deficient nTregs fail to suppress effector T cell-mediated colitis *in vivo*

Although immune activation in $MeCP2^{f/y}$ Foxp3-GFP-Cre mice is apparent, this inflammation is relatively mild compared to the severe lymphoproliferation in Treg depleted mice[195]. In agreement with this, $MeCP2^{f/y}$ Foxp3-GFP-Cre mice and their wild type littermate controls had comparable percentages of $CD25^+Foxp3^+$ $CD4^+$ T cells in the peripheral lymphoid organs as well as in the thymus (Figure 21B). However, loss of MeCP2-deficient Tregs over time might be obscured by the inflammation-induced compensatory expansion of Tregs[38,78], or the continuous Treg output from the thymus. To rule out these possibilities, we examined the functionality of MeCP2-deficient Tregs

using a classical T cell adoptive transfer model for the induction of systemic colitis in lymphopenic hosts.

We sorted Thy1.2^{+} CD25^{+}GFP^{+} Treg cells from MeCP2$^{f/y}$ Foxp3-GFP-Cre or MeCP2$^{x/y}$ Foxp3-GFP-Cre mice, mixed them with wild type Thy1.1^{+} naïve conventional CD4^{+} T cells, and transferred them into RAG2$^{-/-}$ recipients (Fig. 23A). For lineage tracing, Tregs (Thy1.2^{+}) and conventional CD4^{+} T cells (Thy1.1^{+}) were labelled with different congenic markers. As expected, WT Tregs were capable of mitigating the development of severe colitis in recipient mice, monitored by both weight changes and histological analysis. In contrast, mice receiving co-transfers of conventional T cells and MeCP2-deficient Tregs manifested more severe colitis symptoms characterized by dramatic weight loss (Fig. 23B), massive leukocyte infiltration, and severe mucosal tissue damage in the colon (Fig. 23C&D). Accompanying this inflammation, the numbers of total splenocytes (Fig. 23E) and, more specifically, Thy1.1^{+} effector T cells (Fig. 23F), were significantly elevated in recipients co-transferred with MeCP2-deficient Tregs. Furthermore, upon MeCP2 deletion, although the number of Thy1.2^{+} cells was comparable (Fig. 23H), we observed a significant reduction of the percentage of Foxp3^{+} Tregs in the Thy1.2^{+} population and dampened Foxp3 expression at the individual cell level (Fig. 23G). Consequently, the frequency of inflammatory cytokine-producing cells of conventional T cell origin (Thy1.1+) was significantly increased (Fig. 23I). Overall,

these data suggest that MeCP2 expression in Tregs critically supports their ability to suppress T effector cell-mediated inflammation *in vivo*.

5.2.4 MeCP2 deficient Tregs are competent in suppressing effector T cell activation during short-term culture

At least two potential mechanisms may account for the failure of MeCP2 deficient nTregs in suppressing inflammation: firstly, either independent of or in conjunction with Foxp3, MeCP2 acts as a master regulator controlling the expression of effector molecules that directly execute immune suppression; alternatively, MeCP2 may be essential in maintaining Foxp3 expression to enforce the nTreg lineage identity, specifically under inflammatory conditions. We first examined whether MeCP2 modulates effector molecule expression with a standard *in vitro* suppression assay. Thy1.2$^+$ MeCP2-deficient nTregs were co-cultured with Thy1.1$^+$ wild type conventional T cells at various ratios, and stimulated with soluble anti-CD3/CD28 in the presence of antigen presenting cells for a short-term (3 days) *in vitro* (Figure 24A). Under these conditions, the absence of MeCP2 did not affect the viability of Tregs (Figure 24B), expression of Foxp3 (Figure 24C), or ratio of conversion from regulatory to effector T cell (Figure 24D). Using effector T cells proliferation, as well as the IL-2 and IFN-γ cytokine production as functional readouts of Treg-mediated immune inhibition, we found no significant differences in the suppressive capacities of WT and MeCP2 deficient nTregs (Figure 24E&F). Yet, under this lineage-unbiased condition, we consistently observe a moderate, but reproducible, increase in IL-17 production from conventional T cells when

co-cultured with MeCP2-deficient Tregs (Figure 24G), which mirrored the enhanced IL-17 production by conventional T cells in intact MeCP2$^{f/y}$ Foxp3-Cre-GFP mice (Figure 21F&G).

At the end of these mixed cultures, we sorted the remaining viable Thy1.2^{+} Tregs to further analyze their expression of a panel of molecules known to be crucial for Tregs' suppressive function. This panel included the effector molecules[90] CD25, IL-10, TGFβ, perforin, granzyme B, CTLA4, LAG3, CD39, GITR, IL-35; as well as their upstream regulators Blimp1[196], IRF4[196] (for *Il10*) and Foxo transcription factors (for *ctla4*)[197]. Consistent with comparable functional outcomes, we found that at the transcriptional level, the suppressive machinery of MeCP2-deficient Tregs was largely intact (Figure 24H).

5.2.5 MeCP2 is critical for maintaining Foxp3 expression in nTregs during inflammation *in vitro*

We next examined the alternative hypothesis that MeCP2 is essential for the long-term maintenance of Foxp3 expression during inflammation. Yang et al. previously showed that *in vitro* treatment of nTregs with inflammatory cytokines, such as IL-6, causes a gradual loss of Foxp3 expression[42]. To determine whether MeCP2 ablation facilitated this process, we stimulated MeCP2-sufficient or -deficient nTregs with anti-CD3/28, IL-2, and IL-6. As a non-inflammatory control, these nTregs were also cultured with only anti-CD3/28 and IL-2. We found that without IL-6, both wild type and MeCP2-deficient Tregs could maintain Foxp3 expression. However, when IL-6 was added into

the culture, MeCP2 deficient nTregs demonstrated an accelerated loss of Foxp3 expression, both at the protein (Figure 25A) and mRNA level (Figure 25E): while no significant difference was evident on day 3, extending the cultures to five and seven days showed that the percentage of MeCP2-deficient Treg cells that maintained CD25 and Foxp3 expression was merely half of that seen in the WT cells (Figure 25A). We also monitored the survival and proliferation of Tregs to exclude the possibility that this decrease in percentage was caused by altered cell death or proliferation of MeCP2-deficient Tregs (Figure 25B&C). In addition, accompanying the accelerated loss of Foxp3 expression, IL-17 production from MeCP2-deficient Tregs was significantly elevated (Figure 25D). This elevated Treg-to-effector conversion supports our hypothesis that MeCP2 preserves the characteristics of Tregs in response to IL-6-mediated *foxp3* silencing *in vitro*.

Since Foxp3 is required to enforce the transcriptional program of Tregs[71], we also assessed whether the expression of Treg signature genes was disrupted by MeCP2 deficiency in this inflammatory setting. As expected, accompanying the significant reduction of *foxp3* transcripts in MeCP2-deficient Tregs, many Treg signature genes that regulate Treg function were downregulated (Figure 25E). In contrast, genes that have been suggested to act in parallel with Foxp3 to control Treg function, such as Foxo1 [198]and Foxo3, were either unchanged or even slightly elevated (Figure 25E).

Next, we expanded the panel of inflammatory stimulation to other lineage specific cytokines such as IL-12, IFN-γ (for Th1 responses) and IL-4 (for Th2 responses). In general, we observed that these cytokines were much weaker modifiers of Foxp3 expression (Figure 26). Nevertheless, although we did not detect overt differences in Foxp3 expression after 5 days of cytokine stimulations, we found that, on day 7, Th1 and Th2 cytokines also induced a more severe reduction of CD25 and Foxp3 expression in Tregs with MeCP2 ablation (Figure 26). These data suggested that, under a broad range of inflammatory conditions, MeCP2 in Treg cells may be universally involved in protecting Foxp3 expression *in vitro*.

5.2.6 MeCP2 is critical for maintaining Foxp3 expression in nTregs during inflammation *in vivo*

We took a similar adoptive transfer approach to examine the role of MeCP2 in sustaining Foxp3 expression *in vivo*. We sorted Thy1.2^{+} CD25^{+}GFP^{+} nTreg cells from MeCP2$^{f/y}$ Foxp3-GFP-Cre or MeCP2$^{x/y}$ Foxp3-GFP-Cre mice, and mixed them with Thy1.1^{+} CD4^{+}CD25^{-} Tcon cells at a 1:2 ratio before co-transfer into RAG2$^{-/-}$ mice (Figure 27A). A 1:2 ratio of nTreg:Tcon allowed us to recover enough Thy1.2^{+} T cells for reliable endpoint analysis after a long term transplantation. Three weeks after transfer, the mice were sacrificed and T cells of the Thy1.2^{+} nTreg origin were analyzed. In mice carrying WT nTreg, a majority of the Thy1.2^{+} population remained Foxp3^{+} (Figure 27B); in contrast, the MeCP2-deficient Tregs exhibited a dramatic loss in Foxp3 expression (Figure 27B). A significant portion of these ex-Tregs were converted into IL-17- and/or

IFN-γ-producing effector cells (Figure 27C&D). Coordinately, conventional T cells co-transferred with MeCP2-deficient Tregs also showed augmented proinflammatory cytokine production (Figure 27E).

Using two models of autoimmunity, we further examined the role of MeCP2 in sustaining Foxp3 expression during inflammation in intact MeCP2$^{f/f}$ or $^{f/y}$ Foxp3-GFP-Cre mice. Non-obese diabetic (NOD) mice are susceptible to developing autoimmune insulin-dependent diabetes mellitus, and, the pancreatic autoimmune lesion in these mice is associated with diminishment of local Tregs[199,200]. Taking a Speed Congenic approach, we crossed conditional MeCP2 allele and Foxp3-GFP-Cre BAC transgene to mice on the NOD background. In aged diabetic mice, the percentage of Tregs was comparable between WT and MeCP2$^{f/f}$ Foxp3-GFP-Cre NOD mice (Figure 27F). However at the single cell level, MeCP2-deficient NOD Tregs exhibited a moderate but consistent reduction in Foxp3 expression (Figure 27F). Coordinately, CD4$^+$ T cells from pancreatic draining lymph nodes and spleens of MeCP2$^{f/f}$ Foxp3-GFP-Cre NOD mice produced significantly elevated levels of IFN-γ (Figure 27G&H). We next examined the role of MeCP2 in Treg maintenance during experimental autoimmune encephalomyelitis (EAE), which is characterized by strong Th17 and Th1-mediated inflammation in the central nervous system. We found that upon disease induction, although the percentages of Tregs in the spinal cord were comparable between WT and MeCP2$^{f/y}$ Foxp3-GFP-Cre mice (KO) mice (data not shown), Foxp3 expression in individual

MeCP2-deficient Tregs was consistently reduced (Figure 27J). Coordinately, MeCP2$^{f/y}$ Foxp3-GFP-Cre mice exhibited accelerated disease onset, more severe symptoms (Figure 27I), as well as enhanced pro-inflammatory cytokine production (in particular, an increased IL-17^{+}IFN-γ^{+} population) from effector T cells in the spinal cords (Figure 27K). Taken together, these data suggest that MeCP2 is critical to maintain Foxp3 expression in Tregs during inflammation *in vivo*.

5.2.7 Restoring Foxp3 expression sufficiently rescues the competence of MeCP2-deficient Tregs to suppress inflammation *in vivo*

Recent studies demonstrated that, besides the expression of Foxp3, epigenetically, nTreg development also requires a Treg-specific CpG hypomethylation[201]. In our case, the incompetence of MeCP2-deficient Tregs in suppressing inflammation could also be influenced by certain undetected epigenetic modifications. To further determine causality between MeCP2, Foxp3, and immune protection, we transduced MeCP2-deficient Tregs with retrovirus that ectopically expresses Foxp3 transcripts, and then examined their ability to suppress systemic colitis in the aforementioned adoptive transfer model (Figure 28A). Five weeks after the initial transfer, we confirmed that the retroviral expression restored Foxp3 protein expression in MeCP2-deficient Tregs to that of wild type levels (Figure 28B). Coordinately, we observed a complete rescue of Treg identity at the population level (Figure 28C), and, more importantly, a complete rescue of their competence to suppress the colitis

development, as reflected by the maintained body weight (Figure 28D) and diminished colon pathology (Figure 28E&F). Taken together, these data indicated that the critical role of MeCP2 in immune protection is to maintain a stable Foxp3 expression.

5.2.8 During inflammation, defective Foxp3 maintenance in MeCP2-deficient Tregs in is not caused by accelerated proliferation or enhanced inflammatory cytokine signaling

Our data indicated that MeCP2 was important for bolstering *foxp3* expression specifically in response to inflammation-induced transcriptional silencing, but not for *de novo* transcription of *foxp3* per se. It was previously reported that *foxp3* silencing may be attributed to TCR-induced Treg proliferation[75]. To investigate the molecular mechanism by which MeCP2 sustains Foxp3 expression, we first examined whether the MeCP2-supported Foxp3 expression depends on T cell cycling. Using CFSE dilution to distinguish cell generations, we found that the loss of Foxp3 expression does occur with a higher incidence in Tregs that have undergone extensive cell divisions. However, this occurred in both wild type and MeCP2-deficient groups (Figure 29A&B). In this assay, we also excluded the possibility that the enhanced loss of Foxp3 expression in MeCP2-deficient Tregs was a result of accelerated Treg proliferation: the proliferative capacity between wild type and MeCP2-deficient Tregs were almost identical (Figure 29A); and in each generation, MeCP2-deficient Tregs displayed a more pronounced reduction in Foxp3 expression (Figure 29B). Furthermore, it has been recently shown that, during the development of acute murine graft-versus-host disease, STAT3 activation downstream

of IL-6 stimulation destabilizes Foxp3 expression in Tregs[202]. We examined whether the deletion of *mecp2* gene enhances IL-6 signalling. Again, in MeCP2-deficient Tregs, as reflected by Tyr705 phosphorylation, there were no obvious alterations in STAT3 activation in response to IL-6 stimulation (Figure 29C).

5.2.9 MeCP2 opposes *foxp3* gene silencing by recruiting CREB1 and enforcing local histone acetylation in the *foxp3* CNS2 region

Among the identified cis-elements known to be important for *foxp3* gene regulation, the promoter and CNS2 region contain CpG islands[72] that could potentially recruit MeCP2. Using chromatin immunoprecipitation (ChIP), we examined the interaction between MeCP2 and cis-elements under different conditions. In freshly isolated WT nTreg cells, CpG islands within the promoter and CNS2 regions of *foxp3* were almost completely unmethylated (Figure 30A&B). Somewhat surprisingly, these regions were still partially occupied by MeCP2 protein, suggesting that MeCP2 can bind to unmethylated DNA elements in both regions (Figure 31A). However, in the presence of TCR stimulation and inflammatory cytokines, although the DNA sequence within the *foxp3* promoter remained largely unmethylated, methylation was rapidly initiated across the entire CNS2 region (Figure 31B). Accordingly, MeCP2 protein was preferentially recruited to and accumulated within the CpG-methylated CNS2 region (Figure 31A).

To determine the functional importance of inflammation-induced MeCP2 recruitment to the *foxp3* locus, we first examined the status of DNA CpG methylation in freshly isolated MeCP2-deficient nTregs. The loss of MeCP2 resulted in a comparable, or

even a modest reduction, in DNA methylation at both the promoter and CNS2 region (Figure 30). Therefore, MeCP2 is not likely to be responsible for *foxp3* methylation, and, methylation itself cannot explain the protective effect of MeCP2 on foxp3 gene expression. To identify a possible positive gene regulatory function for MeCP2, we next scanned the status of histone H3 acetylation—a known mediator of chromatin accessibility—in all regulatory regions of the *foxp3* gene. Under noninflammatory conditions, the ablation of MeCP2 did not affect H3 acetylation in the promoter, CNS1 and CNS3 region, but reduced H3 acetylation in the CNS2 region by 43% (Figure 31C). When the MeCP2-deficient Tregs were stimulated with anti-CD3/28 and inflammatory cytokines, the H3 acetylation defect in the CNS2 region was even more drastic, reaching a mere 18% of wild type levels (Figure 31E, DMSO panel). Thus it seemed likely that MeCP2 recruitment to the CNS2 region might be important for sustaining chromatin accessibility via H3 histone acetylation, and that inflammation-induced CNS2 methylation might specifically recruit MeCP2 to counteract methylation-mediated chromatin silencing.

Consistent with our data from the MeCP2 ChIP, mice with a knock-in deletion of *foxp3's* CNS2 demonstrated that CNS2 is primarily responsible for the maintenance of Foxp3 transcription, in contrast to its initial induction[75]. Various transcription factors, including STAT5, NF-kB, Ets-1, GATA3, Foxo1/3, the Foxp3/Runx/CBFb complex and CREB1 have been identified to operate within this region[5]. Among these transcription

factors, CREB1 forms a histone acetyltransferase complex with CBP/p300, and is also known to partner with MeCP2 to synergistically activate the transcription of somatostatin (*Sst*) in neurons[169]. We therefore hypothesized that, in nTregs exposed to inflammatory stimuli, MeCP2-mediated protection of *foxp3* expression might also depend on CREB1. To this end, we examined the binding of CREB1 to *foxp3* regulatory elements under inflammatory stimuli in the presence or absence of MeCP2. CREB1 expression levels were similar between wild type and MeCP2-deficient Tregs (data not shown), and CREB1 bound avidly to the *foxp3* CNS2 in wild type Tregs; however, this binding was completely abolished in the absence of MeCP2 (Figure 31D). Consistent with a possible role for CREB1 in MeCP2-dependent histone accessibility, we observed that H3 acetylation within the CNS2 region was reduced by 5.6-fold in the MeCP2-ablated Tregs. Furthermore, when CREB1 activation was blocked with the PKA pathway-specific inhibitor H89[203], the MeCP2-dependent H3 acetylation of CNS2 was largely abrogated (Figure 31E). Taken together, these results suggest that at the *foxp3* locus, recruitment of the CREB1 transcription factor/acetyltransferase complex is MeCP2-dependent, and that epigenetic regulation enacted by MeCP2 in response to inflammation is mediated through CREB1.

Finally, to determine whether MeCP2-mediated epigenetic modulation at the CNS2 region functionally impacts *foxp3* gene transcription, luciferase reporter constructs containing either the *foxp3* promoter alone, or the *foxp3* promoter together with the

CNS2 region were transfected into Jurkat T cells as described previously[78]. MeCP2 siRNA was co-transfected to assess the role of MeCP2 in regulating CNS2 activity. Transfected Jurkat T cells were then treated with Phorbol 12,13-dibutyrate (PdBU) plus ionomycin to mimic TCR activation. In agreement with its previously reported enhancer activity, the presence of the CNS2 region significantly boosted TCR-induced luciferase reporter activity. When MeCP2 was silenced to 20% of its normal expression level (insert in Figure 31F), *foxp3* promoter activity was not affected, but we observed a significant reduction in CNS2-dependent transcription (Figure 31F). Therefore, we conclude that MeCP2-dependent chromatin remodeling specifically at the CNS2 region is an important contributor to *foxp3* expression, especially in the face of inflammatory signals that act to silence *foxp3*.

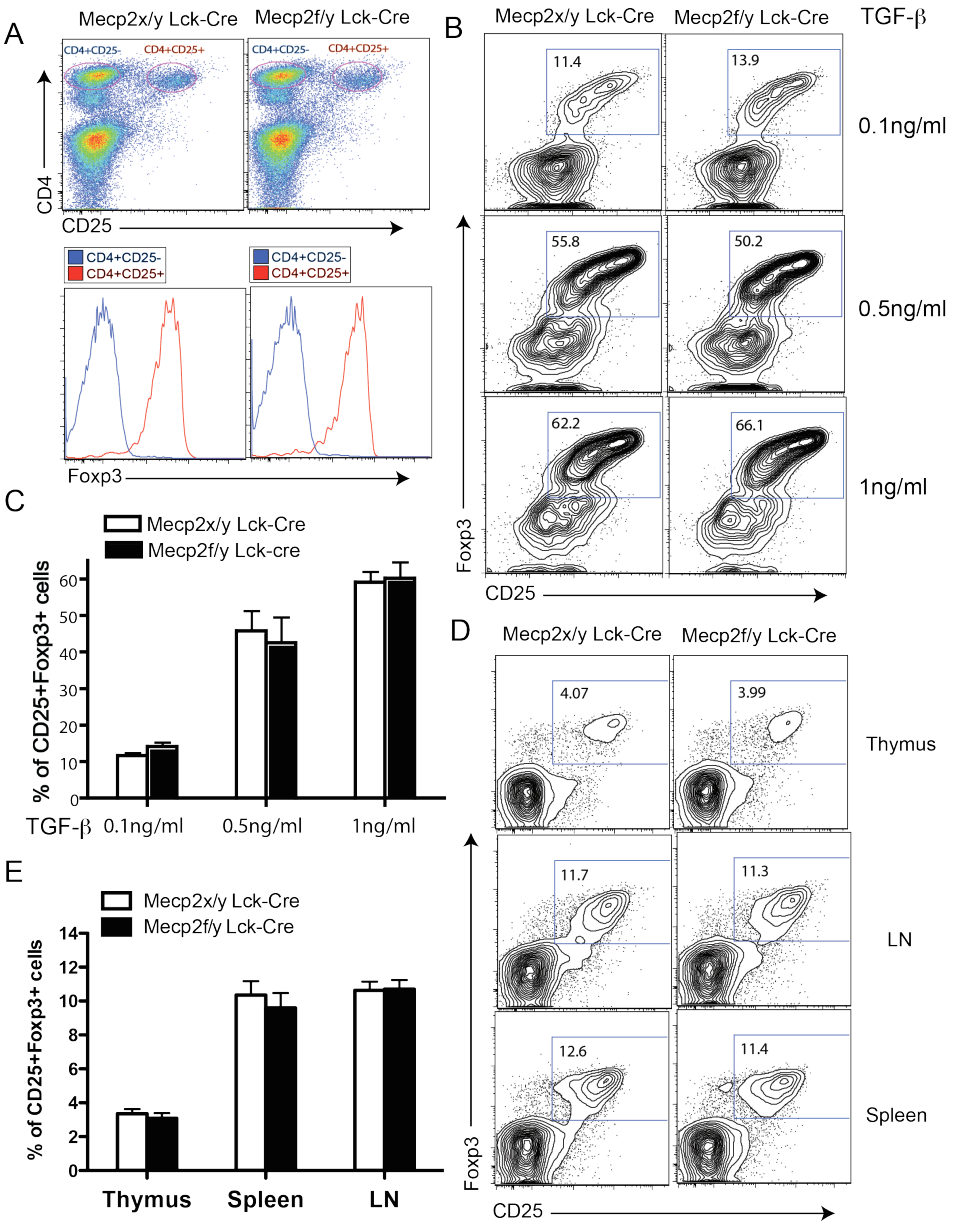

Figure 20: MeCP2 ablation does not affect iTreg differentiation and nTreg development.

(A-C) $CD4^{+}CD25^{-}$ conventional T cells were sorted from the lymph nodes and spleens of $MeCP2^{f/y}$ Lck-Cre mice or their wild type littermates and cultured under iTreg differentiation conditions for 5 days (1ug/ml anti-CD3 & anti-CD28, 0.1 -1.0 ng/ml

recombinant human TGFβ (Peprotech), 50U/ml recombinant mouse IL-2 (Peprotech), 10 μg/ml anti-IL-4 (11B11), 10 μg/ml anti-IFN-γ (XMG1.2), and 10 μg/ml anti-IL-6 (BD)). The percentage of Treg cells was measured by CD25 and Foxp3 staining. (A) Gating of $CD4^+CD25^-$ conventional T cells and $CD4^+CD25^+$ Tregs during sorting and their Foxp3 expression. (B) Representative FACS plots showing the percentage of differentiated iTregs as measured by CD25 and Foxp3 staining. (C) Summary of iTreg differentiation showing means ± SEM of three independent experiments. (D-E) Percentage of $CD25^+Foxp3^+$ Tregs in the thymi and peripheral lymphoid organs of $MeCP2^{f/y}$ Lck-Cre mice or their wild type littermates. Bar graph shows means± SEM of data from three mice per group.

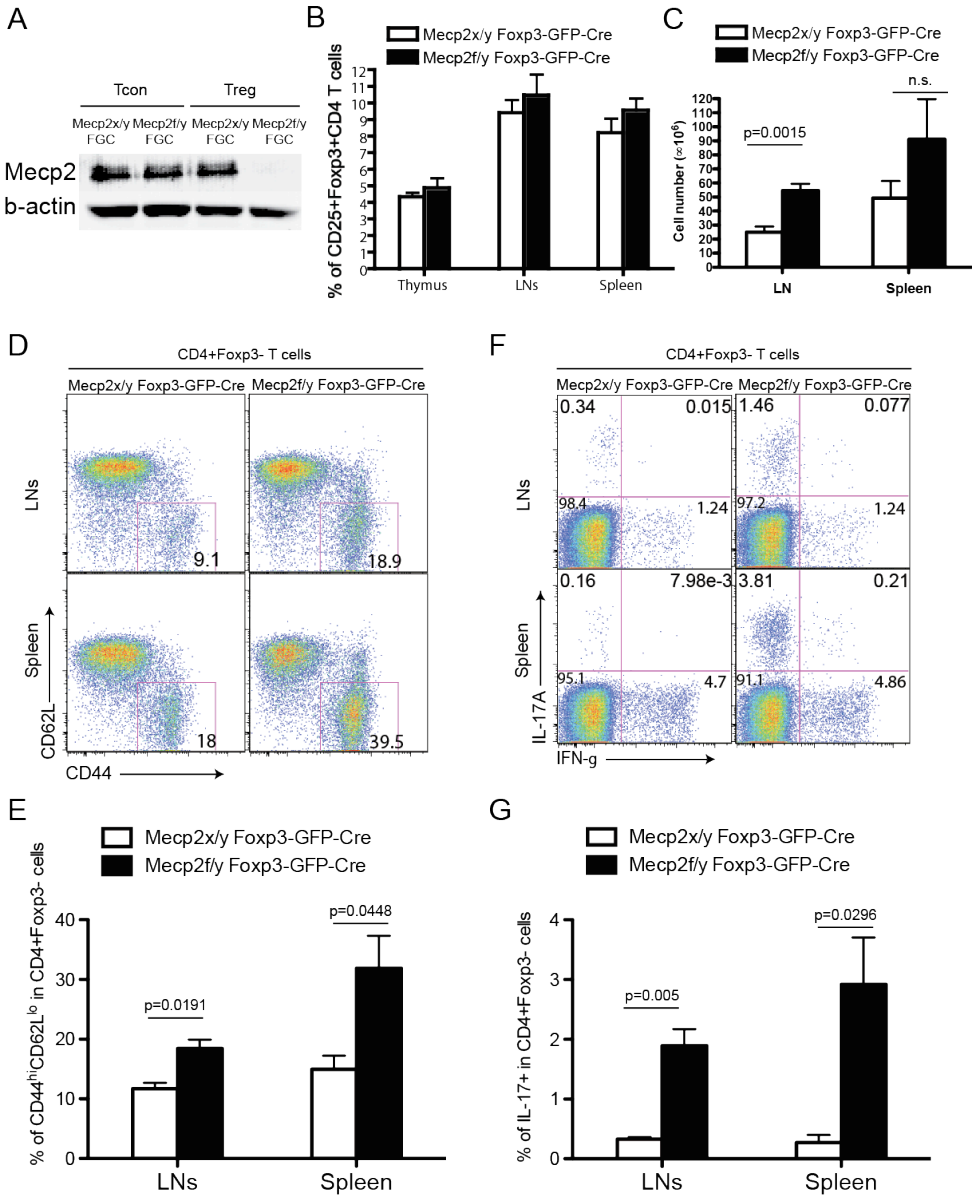

Figure 21: Mild immune activation in young adult MeCP2$^{f/y}$ Foxp3-GFP-Cre mice.

(A) MeCP2 expression was examined by western blot in sorted CD4^{+}CD25^{-}GFP^{-} Tcon and CD4^{+}CD25^{+}GFP^{+} Treg cells from the spleen and lymph nodes (LNs) of MeCP2$^{x/y}$ Foxp3-GFP-Cre (FGC) or MeCP2$^{f/y}$ Foxp3-GFP-Cre (FGC) mice. (B-G)

Lymphocytes from the thymus, LNs, and spleen of 8-10 week old MeCP2$^{f/y}$ Foxp3-GFP-Cre or littermate control mice were isolated for enumeration of cell numbers and flow cytometry analysis. Data shows means ± SEM (n=5). (B) Percentage of CD25^{+}Foxp3^{+} cells in CD4^{+} T cells. (C) Absolute cell numbers in the LNs and spleen. (D&E) Expression of CD44 and CD62L on the surface of CD4^{+}Foxp3^{-} T cells from LNs and spleens. (F&G) Lymphocytes isolated freshly *ex vivo* were stained for intracellular cytokines after 4 hours of stimulation with 0.9nM PdBU and 0.5μg/mL ionomycin in the presence of 5μg/mL brefeldin A and 2μM monensin.

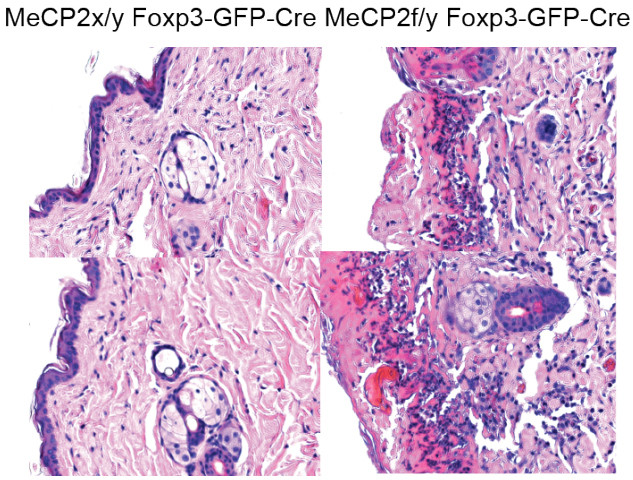

Figure 22: Aged MeCP2$^{f/y}$ Foxp3-GFP-Cre mice frequently develop skin lesions near the neck area.

Histological analysis of aged MeCP2$^{f/y}$ Foxp3-GFP-Cre mice. Skin from the neck area of 26-week old MeCP2$^{f/y}$ Foxp3-GFP-Cre mice or their wild type littermates was removed, fixed, and stained with hematoxylin and eosin. Images shown represent at least three different mice from each group.

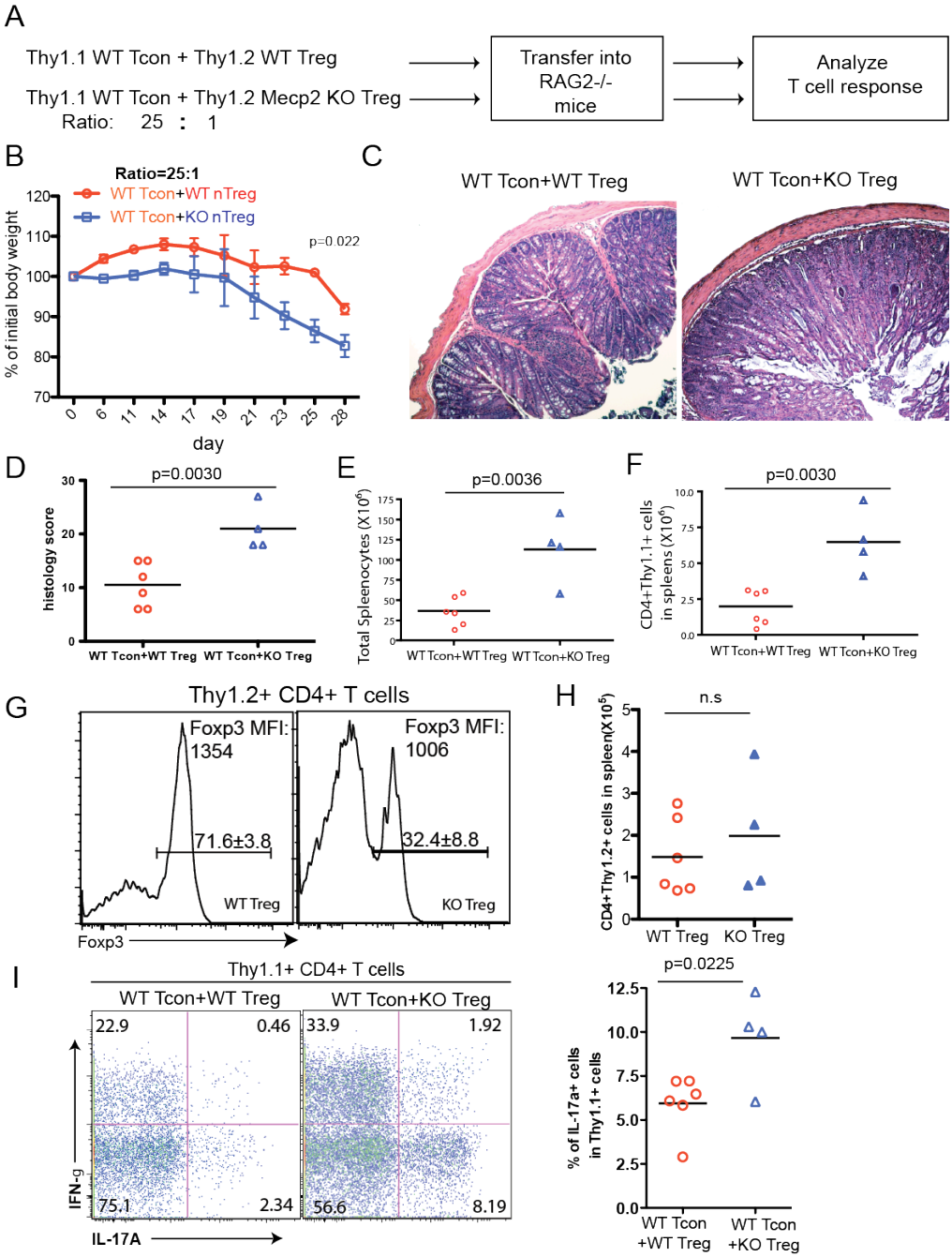

Figure 23: MeCP2-deficient Tregs are impaired in suppressing effector T cell mediated colitis.

(A-I) 5.0×10^5 $CD25^-$ $CD45RB^{hi}$ $CD4^+$ T cells from wild type $Thy1.1^+$ B6 mice (WT Tcon) were sorted and mixed with 2.0×10^4 $Thy1.2^+$ $CD4^+CD25^+$ GFP^+ Tregs from $MeCP2^{f/y}$

Foxp3-GFP-Cre (n=4) or MeCP2$^{x/y}$ Foxp3-GFP-Cre (n=6) littermate control mice, prior to co-transfer into RAG2$^{-/-}$ recipient mice. (A) Schematic representation of the workflow. (B) Weight changes of recipient mice after adoptive transfer were normalized to their initial body weights before transfer. Data shows means ± SEM. (C-D) Recipient mice were euthanized 4 weeks later. Colon tissues were isolated for histopathologic analysis. (C) Representative images of colon tissues with hematoxylin and eosin staining. (D) Summary of the histopathologic scores. (E) Absolute number of splenocytes. (F) Absolute number of CD4^{+}Thy1.1^{+} cells in spleens. (G) Percentage of Foxp3^{+} cells among Thy1.2^{+} cells and MFI of Foxp3 staining in Foxp3^{+} Tregs. (H) Absolute number of CD4^{+}Thy1.2^{+} cells in spleens. (I) Lymphocytes from spleens were stimulated by PdBU and ionomycin for 4 hours and stained for intracellular cytokines. Left: Representative FACS plot; Right: Summary from experimental groups.

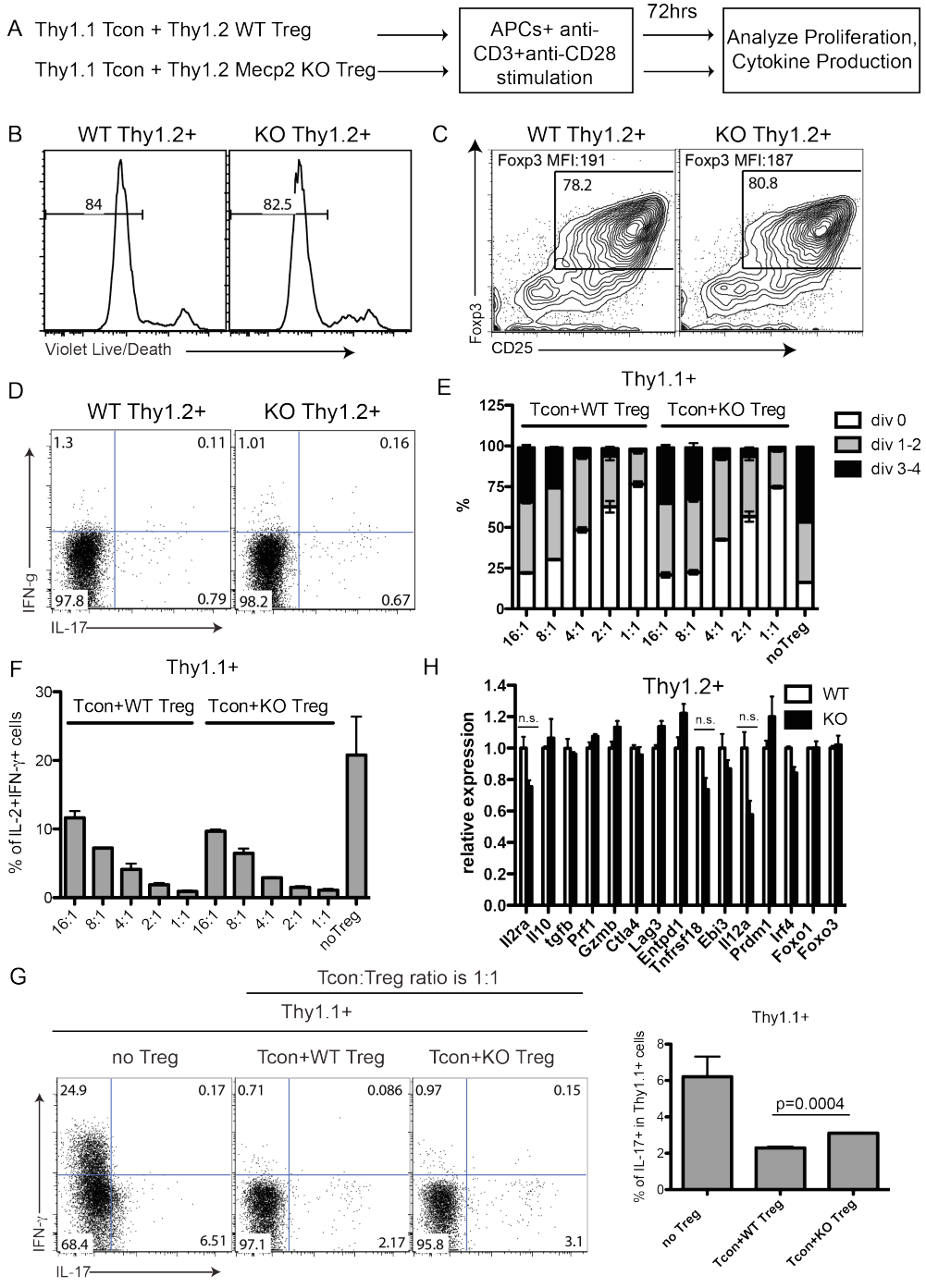

Figure 24: MeCP2-deficient Tregs are competent in suppressing effector T cell activation during short-term culture *in vitro*.

$CD4^+CD25^-$ conventional T cells from LNs and spleens of $Thy1.1^+$ B6 mice were FACS sorted, labeled with carboxyfluorescein succinimidyl ester (CFSE), mixed with $Thy1.2^+$ $CD4^+CD25^+$ Tregs from LNs and spleen of $MeCP2^{f/y}$ Lck-Cre or littermate control mice at the indicated ratios, and stimulated with 0.5ug/mL anti-CD3 and 0.5ug/mL anti-CD28 in the presence of T cell depleted splenocytes (as APCs) from B6 mice for 72 hours. (A) Schematic representation of the workflow. (B-D) The survival (B), Foxp3 maintenance (C), and cytokine production (D) from wild type or MeCP2-deficient Tregs ($Thy1.2^+$) as shown by LIVE/DEAD Fixable Violet Dead Cell Staining and intracellular staining, respectively. Data shown represents three independent experiments. (E-G) The suppression of effector T cell ($Thy1.1^+$) proliferation (E) and cytokine production (F&G) by MeCP2-sufficient or -deficient Tregs ($Thy1.2^+$) as shown by CFSE dilution and intracellular staining. Bar graphs show Means ± SEM of three independent experiments. (H) Viable wild type and MeCP2-deficient $Thy1.2^+$ Treg cells from the 4:1 Tcon:Treg culture were sorted and expression of genes that are critical for Treg suppressive function was determined by qPCR. Data shows means ± SEM of two independent experiments.

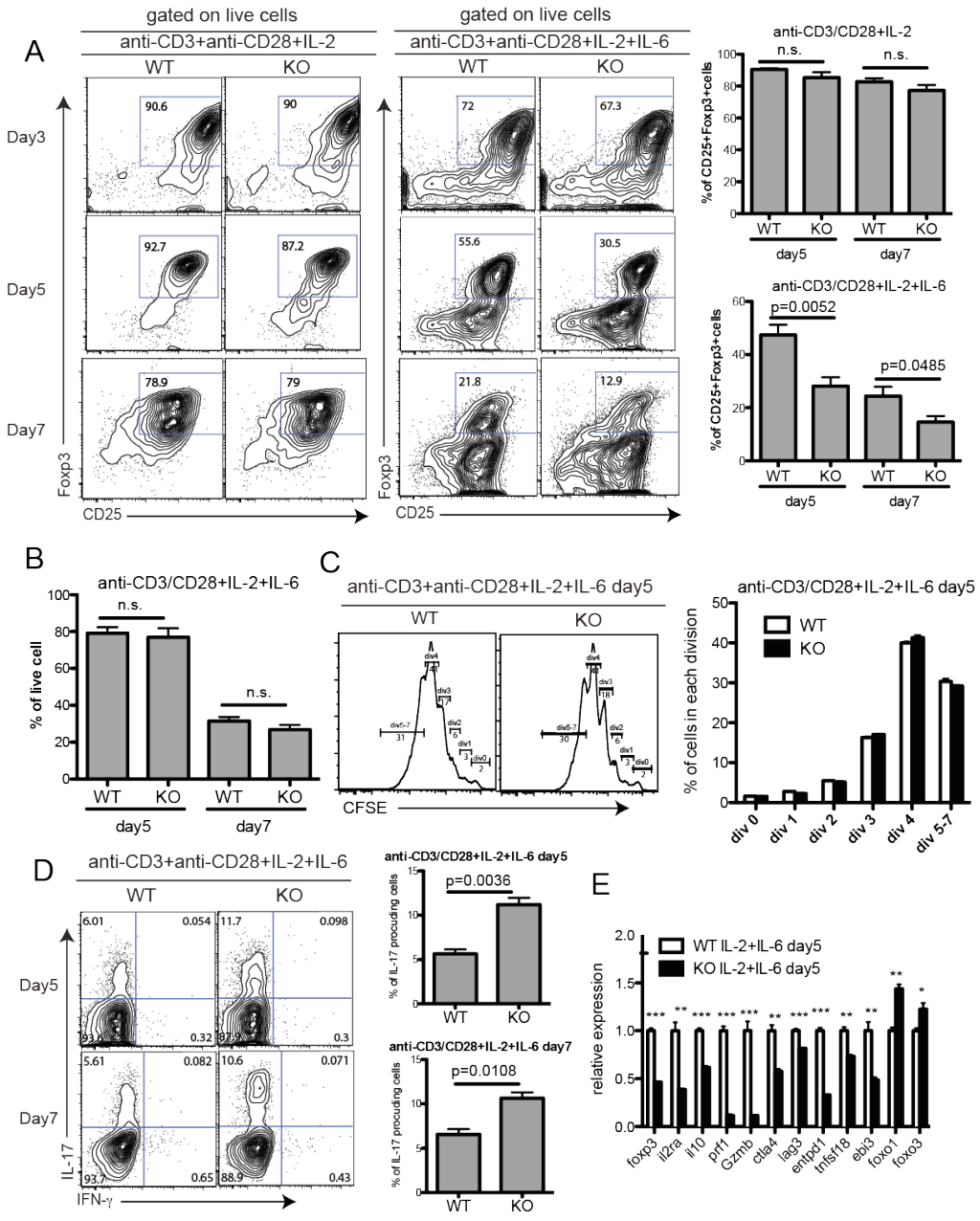

Figure 25: MeCP2 is required for the maintenance of Foxp3 expression in Tregs during inflammatory cytokine stimulation *in vitro*.

$CD4^+CD25^+$ Tregs from LNs and spleens of $MeCP2^{f/y}$ Lck-Cre or their wild type littermate control mice were sorted, labelled with CFSE, and stimulated with 1ug/mL

plate bound anti-CD3 and 1ug/mL plate bound anti-CD28 in the presence of 50U/mL IL-2 with or without 50ng/mL IL-6 for 3-7 days (n=5). (A) The percentages of viable cells retaining CD25 and Foxp3 expression at indicated time points were measured by flow cytometry. (B) The percentages of viable cells at the indicated time points were determined by LIVE/DEAD Fixable Violet Dead Cell Staining. (C) The proliferation of viable cells at the indicated time points were determined by CFSE dilution. (D) Cytokine production from viable wild type or MeCP2-deficient ex-Tregs was analysed by intracellular staining following 4 hours of PdBU and ionomycin stimulation. (E) Viable wild type and MeCP2-deficient Treg cells after 5 days of culture were sorted and expression of Treg signature genes was determined by qPCR. Data shows means ± SEM (n=3). *, $p<0.05$; **, $p<0.01$; ***, $p<0.001$.

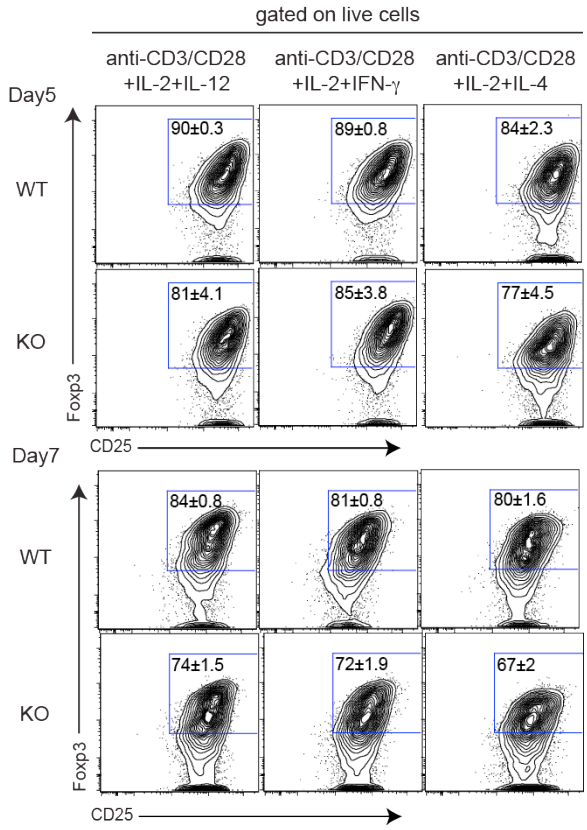

Figure 26: The maintenance of Foxp3 expression in MeCP2-deficient Tregs was moderately impaired following stimulation by several inflammatory cytokines.

$CD4^+CD25^+$ Tregs from LNs and spleens of $MeCP2^{fl/fl}$ Lck-Cre or their wild type littermate control mice were sorted and stimulated with 1ug/mL plate bound anti-CD3 and 1ug/mL plate bound anti-CD28 in the presence of 50U/mL IL-2 in conjugation with 20ng/mL IL-12 or 20ng/mL IFN-γ, or 20ng/mL IL-4 for 7 days (n=3). The percentages of viable cells retaining CD25 and Foxp3 expression at indicated time points were measured by flow cytometry.

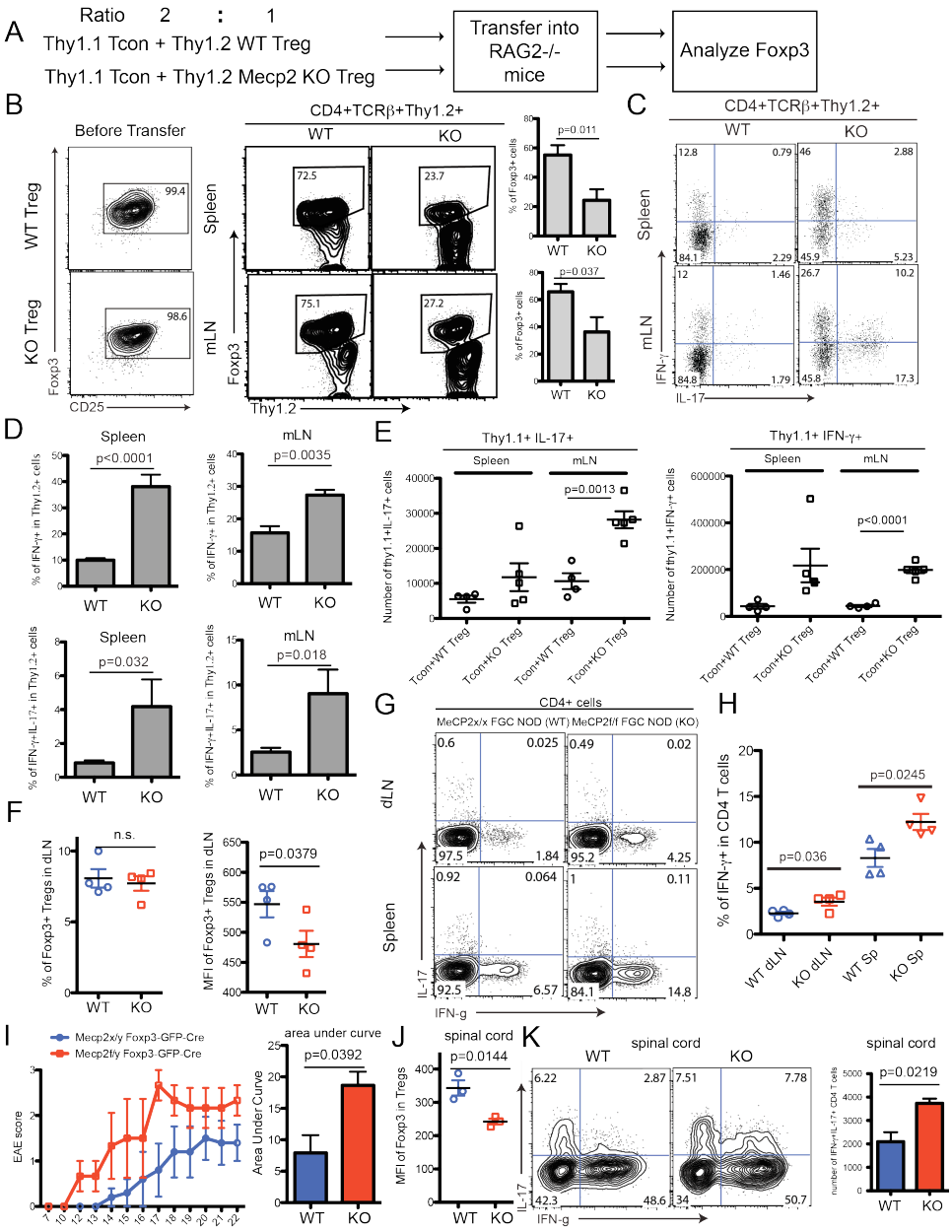

Figure 27: MeCP2 is critical for maintaining Foxp3 expression in nTregs during inflammation *in vivo*.

(A-E) 2.0×10^5 CD4$^+$CD25$^-$ T cells from Thy1.1$^+$ WT B6 mice were sorted and mixed with 1.0×10^5 Thy1.2$^+$ CD4$^+$CD25$^+$ GFP$^+$ Tregs from MeCP2$^{f/y}$ Foxp3-GFP-Cre (KO) or MeCP2$^{x/y}$ Foxp3-GFP-Cre (WT) littermate control mice, and the mixture was co-

transferred into RAG2$^{-/-}$ mice. Recipient mice were euthanized 3 weeks after transfer for flow cytometry analysis. Bar graphs in B&D show Means ± SEM of six mice. (A) Schematic view of the workflow. (B) Percentage of Thy1.2^{+}CD4^{+} T cells before transfer and those that maintain Foxp3 expression in the mesenteric lymph nodes (mLNs) and spleens of recipient mice (n=6). (C&D) Cytokine production from Thy1.2^{+} cells in the mLNs and spleens of recipient mice as determined by intracellular staining (n=6). (E) Absolute number of Thy1.1^{+} effector T cells that produce IL-17 and IFN-g in the mLNs and spleens of recipient mice (WT: n=4; KO: n=5). (F-H) MeCP2$^{f/f}$ alleles were transferred to pure NOD inbred background by speed congenic approach. With T cells from pancreatic draining lymph nodes (dLN) and spleens of 30-week-old WT NOD or MeCP2$^{f/f}$FoxP3-GFP-Cre (KO) littermate mice, the percentage of Foxp3^{+} Tregs and expression level of Foxp3 in Foxp3^{+} Tregs (F) and IFN-γ and IL-17 production (G&H) by CD4^{+} T cells were examined by intracellular staining *ex vivo* (n=4). (I-K) EAE was induced in MeCP2$^{f/y}$ Foxp3-GFP-Cre (KO) or MeCP2$^{x/y}$ Foxp3-GFP-Cre (WT) littermate control mice by immunization with MOG peptide emulsified in CFA, and mice were sacrificed at day 22 for cell analysis. (I) Clinical scores over time (Left) and area under curve (Right). (J) MFI of Foxp3 expression in Tregs from the spinal cord of WT or KO mice. (K) Percentage and number of CD4^{+}Foxp3^{-} cells that produce proinflammatory cytokines in spinal cords of WT and KO mice.

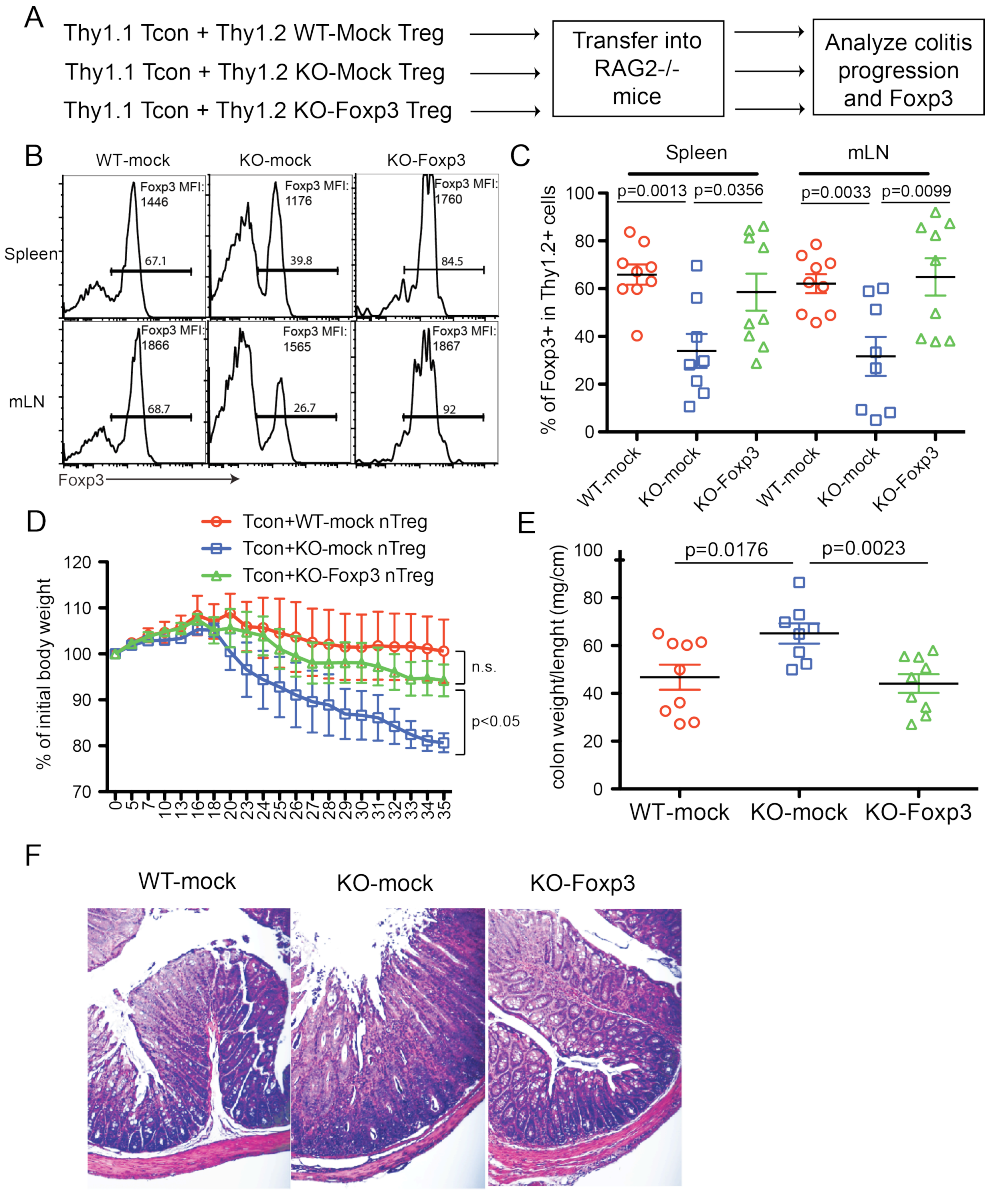

Figure 28: Ectopic expression of Foxp3 restores the capacity of MeCP2-deficient Tregs to suppress effector T cell-mediated colitis *in vivo*.

Thy1.2^{+} CD4^{+}CD25^{+} Tregs from LNs and spleen of MeCP2$^{f/y}$ Lck-Cre or their wild type littermate control mice were sorted and stimulated with 1ug/mL anti-CD3 and anti-CD28 in the presence of 50U/mL IL-2. 18 hours later, cells were transduced with

retrovirus that encodes the foxp3 coding sequence together with GFP (Foxp3) or GFP alone (mock). Two days later, 5.0×10^4 $Thy1.2^+GFP^+$ Tregs were sorted and mixed with 5.0×10^5 naïve conventional T cells ($CD25^-$ $CD45RB^{hi}$ $CD4^+$) from wild type $Thy1.1^+$ B6 donors, and then transferred into $RAG2^{-/-}$ mice. Colon pathology and phenotype of transferred cells were analyzed 5 weeks after adoptive transfer. (A) Schematic view of the workflow. (B&C) Percentage of recovered $Foxp3^+$ cells from the $Thy1.2^+$ origin and MFI of Foxp3 expression in $Foxp3^+$ Tregs. (B) Representative FACS plots. (C) Summary of results from various experimental groups. Each symbol represents one single recipient mouse. (D) Weight changes during the colitis progression. The weight of recipients at different time points was normalized to initial body weight of individual mouse before transfer. Data shows means ± SEM. (E-F) Colon immunopathology of recipient mice was indicated by the ratio of colon weight vs. length (E) and illustrated by H&E staining (F).

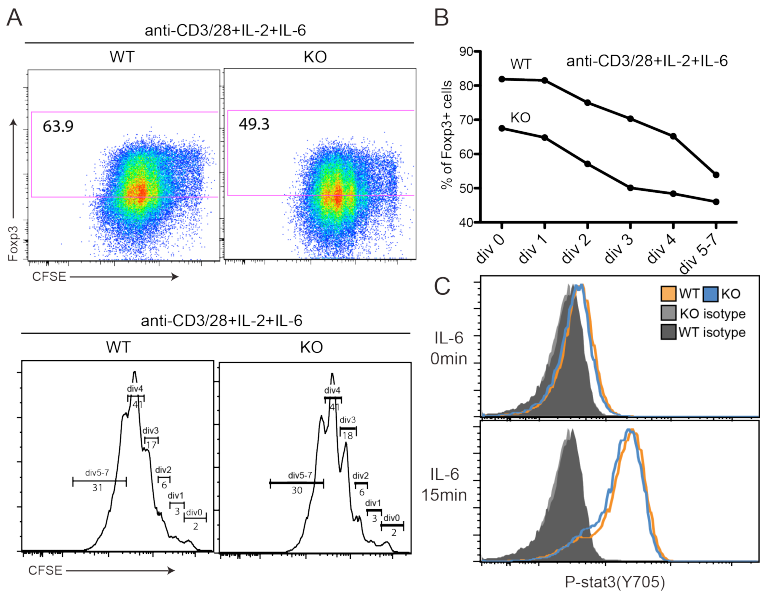

Figure 29: The defect of MeCP2-deficient Tregs to maintain Foxp3 during inflammation is not caused by accelerated proliferation or enhanced inflammatory cytokine signaling.

(A-B) $CD4^+CD25^+$ Tregs from LNs and spleens of $MeCP2^{fl/fl}$ Lck-Cre or their wild type littermate control mice were sorted, labelled with CFSE, and stimulated with 1ug/mL plate bound anti-CD3 and 1ug/mL plate bound anti-CD28 in the presence of 50U/mL IL-2 and 50ng/mL IL-6 for 4 days. The proliferation (A) and the percentages of viable cells retaining Foxp3 expression within each generation of cell cycle (B) were measured by flow cytometry. (C) $CD4^+CD25^+$ Tregs from LNs and spleens of $MeCP2^{fl/fl}$ Lck-Cre or their wild type littermate control mice were sorted and stimulated with 50ng/mL IL-6 for 15 minutes. The phosphorylation of STAT3 downstream of IL-6 receptor signalling was measured by intracellular staining and flow cytometry. Data represents three independent experiments.

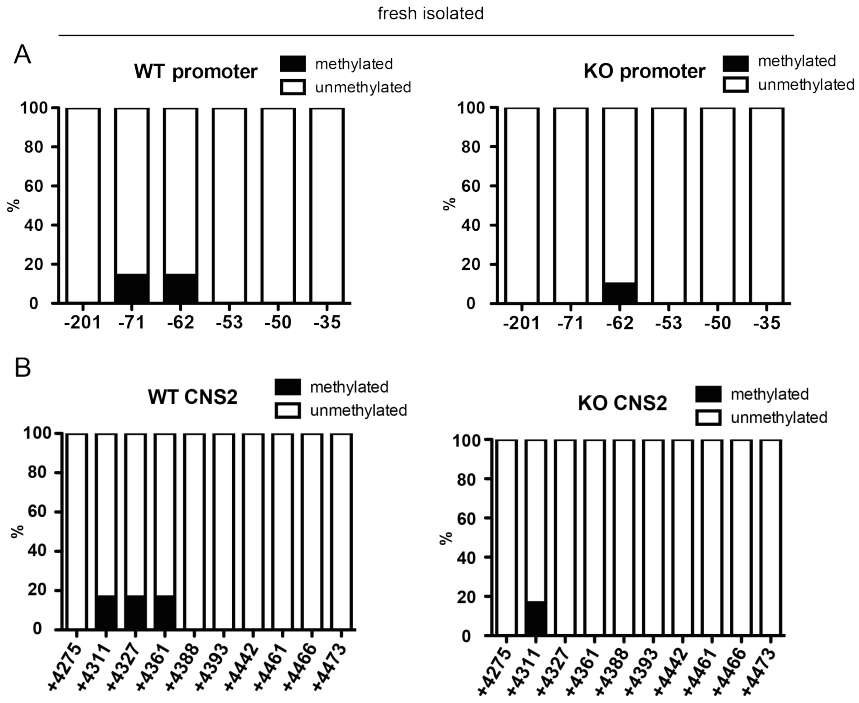

Figure 30: Mecp2-deficient nTregs have normal CpG methylation patterns in the promoter and CNS2 of the *foxp3* locus.

$CD4^+CD25^+GFP^+$ nTregs were sorted from the lymph nodes and spleens of $Mecp2^{x/y}$ Foxp3-GFP-Cre (WT) or $Mecp2^{f/y}$ (KO) mice, and the methylation status in the promoter (A) and CNS2 (B) of *foxp3* locus was analyzed by bisulfite sequencing. Numbers on the x-axes indicate the position of CpGs relative to the transcription start site of the *foxp3* gene. Bar graphs show the data quantified from sequencing of at least ten clones for each sample. Data shown represents three independent experiments.

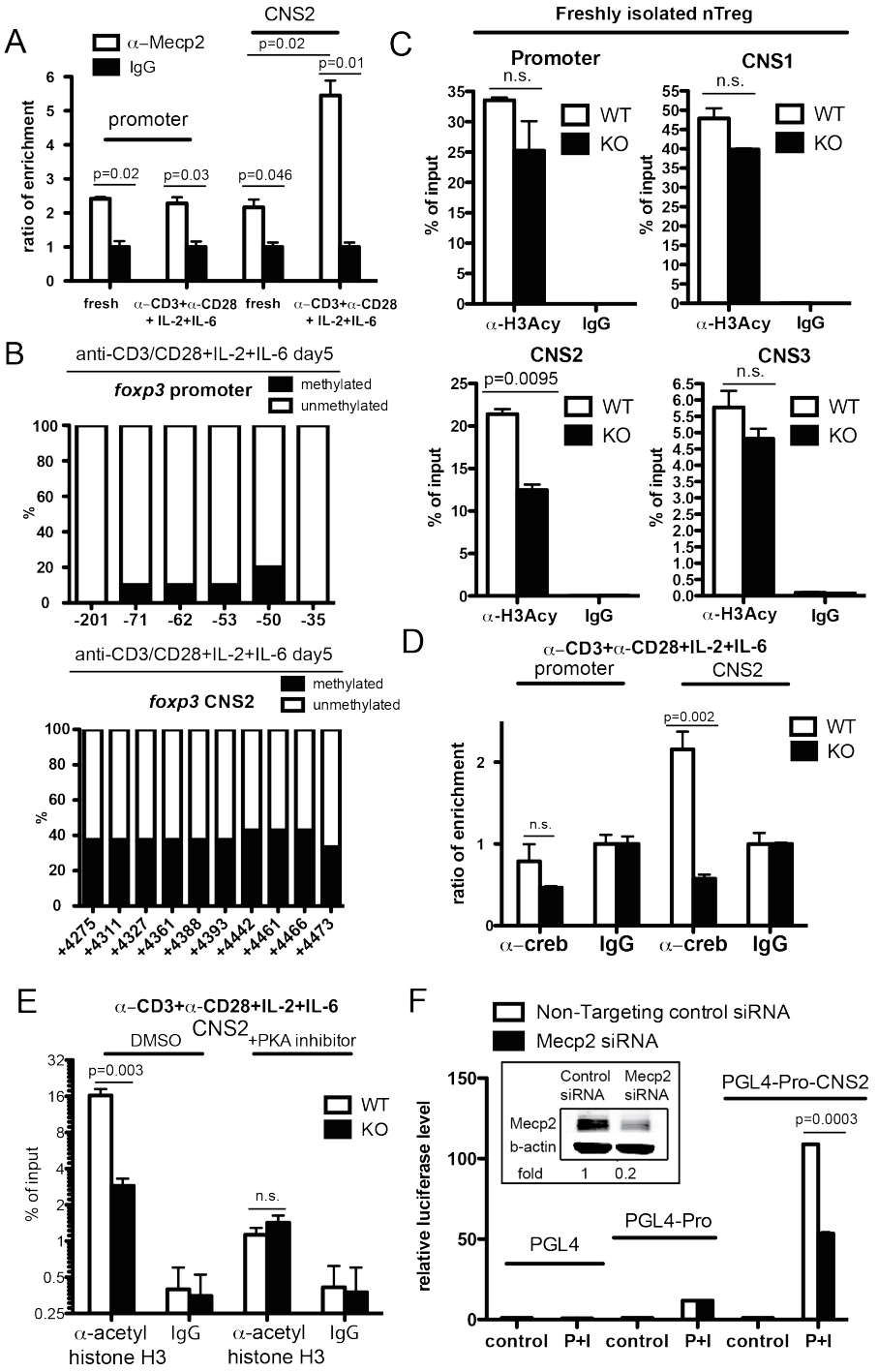

Figure 31: MeCP2 occupies the *foxp3* CNS2 region and regulates its chromatin accessibility through recruitment of CREB1.

(A) Freshly isolated Tregs from LNs and spleens of wild type B6 mice or Tregs that were stimulated with anti-CD3/CD28, 50U/mL IL-2 and 50ng/mL IL-6 for 5 days were subject to ChIP analysis for MeCP2 enrichment at the *foxp3* promoter and CNS2 region. Results show the enrichment ratios of immunoprecipitations using rabbit anti-MeCP2 versus nonspecific rabbit IgG. The bar graph shows Means ± SEM of three independent experiments. (B) $CD4^+CD25^+GFP^+$ nTregs were sorted from lymph nodes and spleen of $Mecp2^{x/y}$ Foxp3-GFP-Cre (WT) and stimulated with anti-CD3/CD28, 50U/mL IL-2 and 50ng/mL IL-6 for 5 days. The methylation status in the promoter and CNS2 of *foxp3* locus was analyzed by bisulfite sequencing. Numbers on the x-axes indicate the position of CpGs relative to the transcription start site of the *foxp3* gene. Bar graphs show the data quantified from sequencing at least ten clones for each sample. Data shown represents three independent experiments. (C) Freshly isolated $CD4^+$ $CD25^+GFP^+$ Tregs sorted from lymph nodes and spleens of $MeCP2^{f/y}$ Foxp3-GFP-Cre mice (KO) or $MeCP2^{x/y}$ Foxp3-GFP-Cre mice (WT) were analyzed for histone H3 acetylation at various cis-elements within the *foxp3* locus by ChIP (n=3). Means ± SEM are shown. (D) ChIP analysis for the enrichment of CREB1 at the *foxp3* promoter and CNS2 region in WT or KO Tregs that were stimulated with anti-CD3/CD28, IL-2 and IL-6 for 5 days. Results show the enrichment ratios of immunoprecipitation using rabbit anti-CREB1 versus nonspecific rabbit IgG. The bar graph shows Means ± SEM of three independent experiments. (E) Histone H3 acetylation of CNS2 in WT or KO Tregs that

were stimulated with anti-CD3/CD28, IL-2 and IL-6 for 5 days in the presence or absence of 5μM PKA pathway inhibitor H89 (Calbiochem) (n=3). Means ± SEM are shown. (F) Luciferase reporter assays. Reporter constructs of PGL4, PGL4 linked with Foxp3 promoter (PGL4-Pro), or PGL4 linked with Foxp3 promoter and CNS2 (PGL4-Pro-CNS2) were transfected into Jurkat T cells together with non-targeting control siRNA or siRNA against MeCP2. 48hrs later, cells were either untreated or treated with PdBU and ionomycin for 16-24 hours, and lysed for analysis of luciferase activity (n=3). Insert: the efficiency of siRNA treatment was examined by western blot 48hrs after transfection. Data shows Means ± SEM.

5.3 Discussion

Tregs' pivotal role in immune tolerance demands that they possess a dedicated molecular mechanism to maintain stable Foxp3 expression when challenged by an inflammatory environment. In this study, we show that MeCP2 is a crucial player in the epigenetic machinery that determines Tregs resilience in the face of inflammation. Interestingly, the function of MeCP2 is dedicated specifically to the maintenance as opposed to the induction of Foxp3. In the absence of immune activation, MeCP2 is dispensable for Foxp3 expression, both during nTreg and iTreg lineage commitment (Figure 20). In contrast, upon inflammation, MeCP2 is crucial for Foxp3 maintenance and Treg-enforced immune homeostasis. Mechanistically, the distinguishing feature is that Mecp2 binds to methylated DNA with enhanced affinity. TCR activation and inflammatory cytokine signaling subject the *foxp3* locus to gene silencing by promoting DNA methylation in its CNS2 region (Figure 31B), and whereas this modification is known to occlude transcription factor binding[75,77], We show that it also reciprocally recruits MeCP2 to associate specifically with CNS2 and thereby rescues *foxp3* transcription via local histone H3 acetylation. Specifically, the docking of MeCP2 achieves this by recruiting CREB1 (Figure 31D) and potentially the CREB1 binding partner, CBP/p300[204] histone acetyltransferase to CNS2. Previous studies using mass spectrometry have demonstrated that the direct interaction between CREB1 and MeCP2 synergistically promotes the expression of a wide range of genes in the hypothalamus[169].

In nTregs, we detected simultaneous and MeCP2-dependent binding of these two proteins to the CNS2 region (Figure 31A&D). This interaction between CREB1 and MeCP2 may be direct or indirect: it may also be possible that MeCP2 associates with other coactivators to maintain a locally accessible chromatin structure, thereby indirectly facilitating the binding of CREB1 in the absence of physical interaction. In either case, the result is that MeCP2 provides an important epigenetic safeguard that confers Tregs with resistance to inflammation-induced *foxp3* silencing.

Due to its association with Rett Syndrome, prior studies on MeCP2 have been centered almost exclusively on the central nervous system. Patients with Rett Syndrome show no overt abnormalities in the first 6 months of life, but they subsequently develop a profound neurodevelopmental disorder characterized by devastating periods of regression, which result in permanent cognitive impairment. Although immune attack against the central nervous system was suspected to be the etiological factor of Rett Syndrome in the early 90s, in-depth pathological analysis failed to provide any evidence for autoimmunity. Using a mouse model of Treg-specific MeCP2 gene ablation, we have identified spontaneous $CD4^+$ T cell activation in young adult mice, a secondary effect of defective Treg-mediated immune-suppression. Interestingly, this inflammatory phenotype vanished when *mecp2* was deleted in all T cells using CD4-Cre or Lck-Cre to drive gene depletion. This was a strong indication that the loss of MeCP2 in other T cell subsets might compensate for Treg dysfunction and prevent the onset of overt

autoimmunity. Indeed, we have examined the function of MeCP2 in effector T cell lineages and found that MeCP2-deficient effector $CD4^+$ T cells are severely impaired in their production of inflammatory Th1 and Th17 cytokines (See Chapter 6). Nonetheless, it is clear that T cell immunity is not normal in these animals: further analysis of the role of MeCP2 in other immune lineages will help to elucidate the regulatory nature of this protein in the immune system, and possibly in the neural system as well.

6. MeCP2 reinforces STAT3 signaling and effector T cell differentiation by controlling miR-124-mediated suppression of SOCS5: An important epigenetic regulator of Th1 and Th17 differentiation

The contents of this dissertation chapter have been slightly modified from the following manuscript that was current under revision at *Science Signaling*.

Shan Jiang*, Chaoran Li*, Gabrielle McRae, Erik Lykken, Jose Sevilla, Siqi Liu, Ying Wan & Qi-Jing Li. (* equal contribution and listed in an alphabetic order). MeCP2 reinforces STAT3 signaling and effector T cell differentiation by controlling miR-124-mediated suppression of SOCS5.

6.1 Introduction

Methyl-CpG binding protein 2 (MeCP2) was initially identified as a nuclear protein binding to cytosine-methylated DNA within dinucleotide CpG elements[167,168]. In early studies, MeCP2 was described as a transcription silencer, because it appeared to maintain dinucleotide methylation of target genes and to recruit the corepressor Sin3A and histone deacetylases (HDACs)[170,205]. However, recent biochemical and genomics data suggest that, rather than strictly a silencer, MeCP2 acts as a multifunctional regulator of gene transcription[173,206] and is actively involved in RNA splicing [207], chromatin remodeling[208,209], and transcriptional activation[169,172].

MeCP2 is especially relevant in biomedicine due to its role in Rett syndrome (RTT)[174,210], a progressive neurodevelopmental disorder that manifests in young girls at a

ratio of 1:10,000[211,212]. Heterozygous loss-of-function mutations in the *mecp2* gene underlie the etiology for more than 95% of typical RTT patients[174,175] , yet the resultant molecular pathology remains largely elusive[173]. The neurodegeneration phenotype of RTT is the result of loss-of-MeCP2 specifically in neuronal cells [213,214], and is unlikely to rely on immune cell dysfunction[215,216]. However, MeCP2 expression is not limited to the brain, and more recent data has implicated it in the regulation of immunological disorders. Specifically, polymorphisms of *mecp2* in humans have been linked to increased susceptibility to autoimmune diseases such as Systemic lupus erythematosus (SLE)[177,178] and primary Sjogren's syndrome (pSS)[179]; moreover, MeCP2 has been found in association with CpG elements within the regulatory regions of the *foxp3* gene[194], although the functional consequence of this association is yet to be examined.

Thus, although RTT does not appear to be phenotypically linked to immune cell dysregulation, we postulated that MeCP2's role in neuronal cells and in T cells might nonetheless be mechanistically linked by some common molecular pathways. We therefore generated T-cell-specific MeCP2-ablated mice, in order to investigate the potential role of MeCP2 in T cell function and immune regulation. Mechanistically, our investigation identified miRNA miR-124 as a direct downstream effector of MeCP2-mediated epigenetic regulation. Functionally, the MeCP2-miR-124-SOCS5 axis is indispensable for inflammatory cytokine-induced STAT3 activation in $CD4^+$ T cells, and, consequently, Th17 differentiation.

6.2 Results

6.2.1 MeCP2 is critical for the commitment of naive $CD4^+$ T cells to the Th17 lineage

Previously, we identified MeCP2 as an important "safe guard" that governs Tregs' resistance to inflammation-induced destabilization (See Chapter 5). Mice with a specific deletion of MeCP2 in Tregs developed spontaneous inflammation as young as 8 weeks. Interestingly, when CD4-Cre transgenes were employed to induce MeCP2 deletion in both natural Tregs (nTregs) and conventional T cells (Tcon), we failed to observe any obvious disruption of immune homeostasis (Figure 32). This suggests that the loss of MeCP2 in other T cell subsets might compensate for Treg dysfunction and prevent the onset of overt autoimmunity. To examine the intrinsic autoinflammatory potential of conventional $CD4^+$ T cells (Tcon), sorted $CD4^+CD25^-CD45Rb^{high}$ naïve Tcon cells from MeCP2-deficient or WT mice, in combination with WT regulatory T (Treg) cells, were transferred into lymphopenic $Rag2^{-/-}$ recipients at a 25:1 ratio to induce autoimmune colitis. Mice that received WT Tcon cells developed severe experimental colitis evidenced by the continuous loss in body weight; surprisingly, instead of promoting inflammation, the transfer of MeCP2-deficient Tcon conferred recipient mice with disease resistance (Figure 33B). Further histopathology analysis of the colon illustrated a striking difference in inflammatory leukocyte infiltration and the integrity of mucosal tissue architecture (Figure 33C). In this transfer model, the aberrant

generation of Th17 cells against host microbiota has been demonstrated to be the major cause of intestinal inflammation[217]. Accordingly, in the mesenteric lymph nodes of mice bearing MeCP2-deficient Tcon cells, the proportion of IL-17a producing $CD4^+$ T cells was significantly reduced (Figure 33D).

In response to specific immunization conditions, Tcon cells proliferate, contract and differentiate into various T helper cell lineages to orchestrate proper immune responses related to host defense and tolerance[8]. Defects in any of these steps could account for the reduced autoinflammatory Th17 population observed with MeCP2 deletion. To further dissect the intrinsic defect of MeCP2-deficient Tcon cells during inflammation, we backcrossed CD4-Cre^+*mecp2*$^{f/f}$ or *mecp2*$^{f/y}$ mice with strains carrying the LLO118 TCR transgene[218], which recognizes the dominant Listeria monocytogenes antigen (a.a.190-205 of the Listeriolysin O protein) in the context of the I-A^b MHC class II molecule . Upon *in vitro* stimulation with $LLO_{190\text{-}205}$ peptide-loaded APCs, $CD4^+$ Tcon cells proliferated, and then contracted, comparably in the presence or absence of MeCP2 protein (Figure 33G&H). However, when we cultured these cells under Th17-polarizing conditions *in vitro*, MeCP2-deficient Tcon cells exhibited severe defects in IL-17a production (Figure 33E). Consistent with this, the mRNA levels of *il-17a*, *il-17f*, and the master transcription factor for the Th17 lineage, *rorc*, were significantly suppressed in MeCP2-deficient Th17 cells (Figure 33F).

6.2.2 MeCP2 is required for the commitment of naive CD4$^+$ T cells to the Th1 lineage

IFN-γ producing Th1 cells represent another critical lineage mediating the onset and progression of autoimmune diseases[219,220]. We examined whether MeCP2 plays any role in Th1 lineage differentiation. When naïve T cells were cultured *in vitro* under Th1-polarizing conditions, the production of IFN-γ in MeCP2-deficicent CD4+ T cells was significantly suppressed (Figure 34A). To validate this phenotype *in vivo*, we sorted and transferred WT or MeCP2-deficient LLO118 T cells into TCR$\alpha^{-/-}$ recipients, and immunized recipient mice subcutaneously with $LLO_{190\text{-}205}$ peptide. The effector T cells generated *in vivo* were rechallenged with the same antigen to assess their lineage commitment. As observed *in vitro*, MeCP2-deficient CD4$^+$ T cells were significantly impaired in Th1 differentiation (Figure 34B). To exclude the possibility that this phenotype is limited to the LLO118 TCR, we directly challenged WT or CD4-Cre$^+$*mecp2*$^{f/y}$ mice with KLH protein through the footpad to induce delayed-type hypersensitivity (DTH), a classical Th1-dominated response. Defects in Th1 responses were apparent in mice with T-cell-specific deletion of MeCP2, as characterized by limited footpad swelling (Figure 34C), reduced inflammatory infiltration (Figure 34D), and reduced numbers of Th1 cells in the draining lymph node (Figure 34E). Collectively, our data indicate that MeCP2 is an indispensable factor that drives the differentiation of Th1 and Th17 cells *in vitro* and *in vivo*.

6.2.3 MeCP2 is indispensable for activation of STAT3 and STAT1 in $CD4^+$ T cells

To develop distinct and stable effector T cell lineages from naïve precursors, $CD4^+$ T cells respond to signals from APCs and the cytokine environment by activating lineage-specific transcription factors, which then fundamentally remodel local chromatin structures surrounding master cytokine genes in order to cement their lineage choices[3,8]. Since MeCP2 primarily functions at the epigenetic level, we first examined whether the loss of MeCP2 directly impaired the accessibility of the *il17* and *ifng* loci. With chromatin immunoprecipitation (ChIP) assays, we examined histone acetylation and methylation status (H3Acy, H3K4me2, H3K4me3 and H3K27me3) across critical regulatory regions of the *il17* and *ifng* genes in MeCP2-deleted T cells. Despite minor differences within some regions, no unidirectional changes in the accessibility of these master cytokine genes could be identified (Figure 35). Because the lineage choice of naïve $CD4^+$ T cells is primarily determined by their response to different environmental cytokines, we next considered whether MeCP2 ablation impacted cytokine signaling. Cytokines activate various transcription factors within the family of signal transducer and activator (STAT) proteins[8]: in particular, the Th17 lineage is specified by STAT3 activation[221-223]. In both naïve and antigen-primed CD4+ T cells, the deletion of MeCP2 did not alter the expression or induction of STAT3 protein; however, it did dampen IL-6-induced phosphorylation of STAT3 (Tyr 705), the hallmark of STAT3 activation (Figure 36A). Similarly, upon IFN-γ stimulation, MeCP2 deficiency also significantly inhibited

STAT1 activation (Figure 36B), a signaling intermediate crucial for Th1 differentiation. Collectively, these data indicate that the loss of MeCP2 results in the inhibition of multiple STAT protein signaling pathways.

6.2.4 SOCS5 accumulation in MeCP2-deficient CD4$^+$ T cells

Upon cytokine stimulation, STAT3 signaling is tightly controlled by JAK kinase activation and various negative feedback mechanisms, including those mediated by the suppressor of cytokine signaling (SOCS) family proteins[224]. Using qPCR, we profiled the expression of 70 genes related to STAT signaling (Figure 37A) in naïve and Th1- or Th17-polarized T cells. These tests failed to identify any significant differences between WT and MeCP2-deleted T cells at the mRNA level (Figure 37B and data not shown). However, at the protein level, we consistently observed a dramatic increase of SOCS5 protein in naïve MeCP2-deficient CD4$^+$ T cells (Figure 37C&D); Upon prolonged antigen and IL-6 stimulation, the loss of MeCP2 also resulted in an elevated accumulation of SOCS5 protein (Figure 37E), which spanned the duration of Th17 lineage specification.

6.2.5 SOCS5 negatively regulates STAT3 activation and naïve CD4$^+$ T cell commitment to the Th17 lineage

Unlike SOCS1 and SOCS3, studies on the function of SOCS5 in lymphocytes remain limited[225,226], and its impact on Th17 differentiation is unknown. However, SOCS5 has been identified as a potent STAT3 inhibitor in M1 macrophages[227]. Using retroviral transduction, we ectopically expressed SOCS5 in primary LLO118 T cells to mimic the effect of MeCP2 deletion. With a relatively modest augmentation of SOCS5

expression (Figure 38A), T cell responses to IL-6 stimulation *in vitro* were impaired (Figure 38B). To assess the role of SOCS5 *in vivo*, we competitively transferred equal numbers of GFP-expressing mock Thy1.1^{+} and SOCS5-overexpressing Thy1.2^{+} LLO118 T cells into TCR$\alpha^{-/-}$ recipients, and activated these T cells by subcutaneous $LLO_{190\text{-}205}$ antigen challenge. After 5 days of *in vivo* conditioning, we assessed the Th17 differentiation of these T cells. Like their MeCP2-deficient counterparts, SOCS5-expressing T cells showed a significant defect in Th17 differentiation at both the population level and on a per-cell basis (Figure 38C&D). To further determine whether this defect was absolute or was the result of competitive disadvantage, we transferred each of these two T cell populations into separate recipients and challenged them with the same immunization protocol. In this setting, *ex vivo* examination (Figure 38E) and *in vitro* antigen rechallenge (Figure 38F) revealed even more pronounced defects in the Th17 differentiation potential of SOCS5-expressing LLO T cells. Similarly, enforced SOCS5 expression also resulted in defective STAT1 activation (Figure 38G) and Th1 differentiation (Figure 38H-J). Taken together, we propose that in MeCP2 deficient T cells, the impaired STAT signaling and constraints on T cell differentiation are primarily a result of aberrant SOCS5 accumulation.

6.2.6 MeCP2 positively regulates the transcription of pri-mmu-miR-124-1 in CD4$^+$ T cells

What underlies the accumulation of SOCS5 in MeCP2 deficient T cells? One possibility is that MeCP2 functions as a transcriptional repressor of SOCS5 expression. However, the impact of MeCP2 loss on SOCS5 expression (Figure 39C, Left panel) is not statistically significant at the mRNA level. Therefore, we speculated that MeCP2 regulates SOCS5 expression in T cells indirectly at the posttranscriptional level.

miRNAs are one of the principle molecular machineries responsible for posttranscriptional regulation[46]. Although the majority of miRNA-mediated repression involves at least moderate mRNA destabilization, 11-16% of the regulation is attributed solely to translational inhibition[228]. Based on the divergent levels of mRNA and protein, we speculated that miRNAs may be key modulators for SOCS5 protein expression. Using qPCR, we analyzed the expression profiles of ~400 miRNAs from WT and MeCP2-deficient cells. Due to MeCP2's role in neural cells, we narrowed our analysis by focusing on miRNAs that downregulated in both MeCP2-deficient mouse CD4$^+$ T cells and primary human astrocytes (Figure 39A). We found five miRNAs that were downregulated in both cell types; among these candidates, miR-124 was computationally predicted to target *socs5* mRNA at a highly conserved site (Figure 39A).

miR-124 is one of the most abundant miRNAs expressed in the vertebrate central nervous system[229]. Loss of miR-124 is known to cause severe defects in neuronal maturation and survival[230]. In addition, recent clinical study suggested that the

expression of miR-124 can be dynamically modulated in human T cells from sepsis patients, and, its upregulation limited the anti-inflammatory effects of steroid treatment[231]. To assess absolute abundance of miR-124 in $CD4^+$ T cells, we quantitated the copy number of miR-124. With this assay, we estimated miR-124 to be in the range of $4X10^7$ copies/mg total RNA in naïve $CD4^+$ T cells (Figure 39B). This cellular concentration is similar to that of miR-19b, a miRNA executing comprehensive regulatory functions over T cells effector responses[54]. With the loss of MeCP2, the expression of miR-124 was consistently suppressed in naïve $CD4^+$ T cells (Figure 39C, right panel).

Mature miR-124 can be generated from three distinct precursor transcripts that are coded within three highly conserved genomic loci (pri-miR-124-1 on chr.14, pri-miR-124-2 on chr.3, pri-miR-124-3 on chr.2.). As previously demonstrated in the nervous system[230], the pri-miR-124-1 locus is also the dominant precursor of mature miR-124 expression in T cells: transcriptional levels of pri-miR-124-2 and pri-miR-124-3 are below the detection limit in our quantitative PCR assays. Based on information collected from the ENCODE project, the proximate regulatory regions for pri-miR-124-1 transcription locates within the -4.7kb to +3.5kb region surrounding its transcription initiation site. Our ChIP assays showed that in naïve T cells, MeCP2 readily associates with multiple CpG islands within the -2.8kb to +2.4kb region (Figure 39D). Using H3K4 dimethylation as an epigenetic marker, we also examined the genomic accessibility and transcriptional

capacity of these regions. In wild type $CD4^+$ T cells, the -2.8kb and -1.6kb regions, which were associated with enriched MeCP2 binding, constituted regions with higher accessibility. Most importantly, loss of MeCP2 protein reduced the accessibility across this locus (Figure 39E). Furthermore, with *mecp2* deletion, the reduced chromatin accessibility resulted in dampened pri-miR-124-1 transcription in naïve $CD4^+$ T cells (Figure 39F). These data suggested a direct role for MeCP2 in promoting pri-miR-124-1 transcription.

6.2.7 miR-124 inhibits the translation of socs5 in $CD4^+$ T cells

To determine whether miR-124 represents the missing link that bridges MeCP2 deficiency with SOCS5 accumulation, we first used a luciferase-based reporter assay to verify that the predicted targeting site in the SOCS5 3'UTR (Figure 40A) was specifically targeted for suppression by miR-124 (Figure 40B). Furthermore, when miR-124 was ectopically introduced into antigen-primed LLO118 T cells, it dampened the expression of SOCS5 protein (Figure 40C) without any significant impact on SOCS5 mRNA (Figure 40D), mirroring the pattern of expression seen in T cells with *mecp2* ablation. In primed WT T cells, during IL-6-induced signaling, the forced miR-124 expression dramatically delayed dephosphorylation of STAT3 (Figure 40E), reinforcing the idea that the primary target(s) of miR-124 are negative regulatory elements of STAT3 signaling. Finally, we used a retroviral vector to restore miR-124 levels in MeCP2-deficient T cells back to WT levels. The restoration of miR-124 partially rescued STAT3 activation in T cells harboring

MeCP2 mutation (Figure 40F). Phenotypically, the exogenous miR-124 significantly augmented Th17 differentiation, in both WT and MeCP2-deficient LLO118 T cells. Statistically, the restoration of miR-124 in MeCP2-deficient T cells fully rescued IL-17 production at both the population level and on a per-cell basis (Figure 40G&H). Thus, miR-124-mediated SOCS5 targeting could account for the impaired Th17 differentiation observed in MeCP2-deficient T cells.

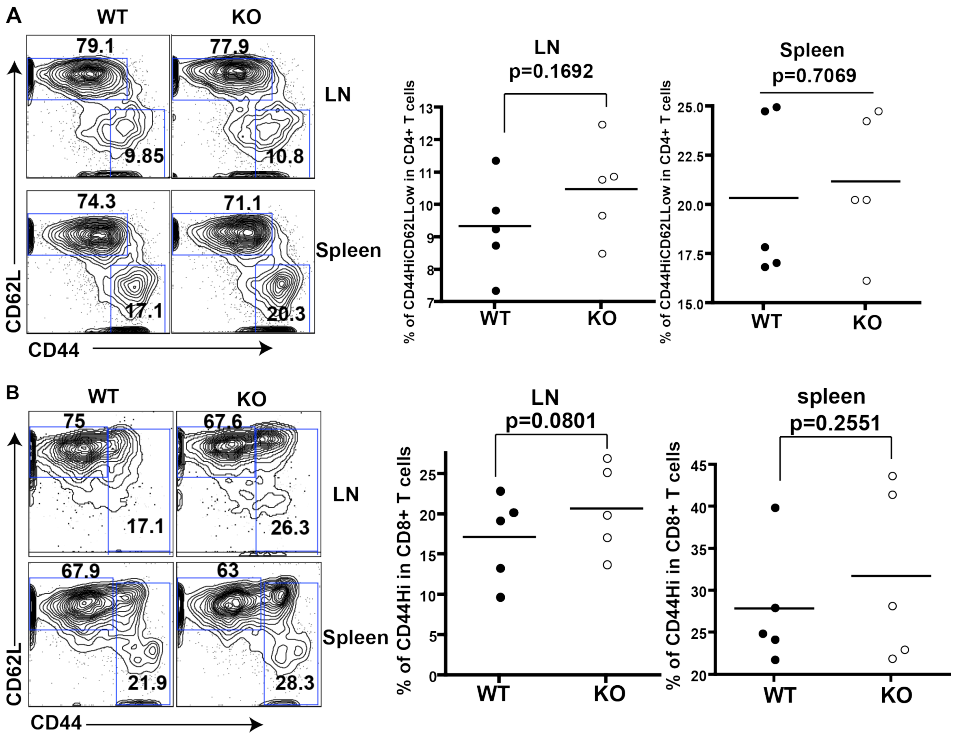

Figure 32: No spontaneous T cell activation in *mecp2*-KO mice.

(A&B) Percentages of effector cells in (A) $CD4^+$ T cells and (B) $CD8^+$ T cells from the LN and spleen of young adult WT and KO littermates (n=5, ages: 6-8 weeks).

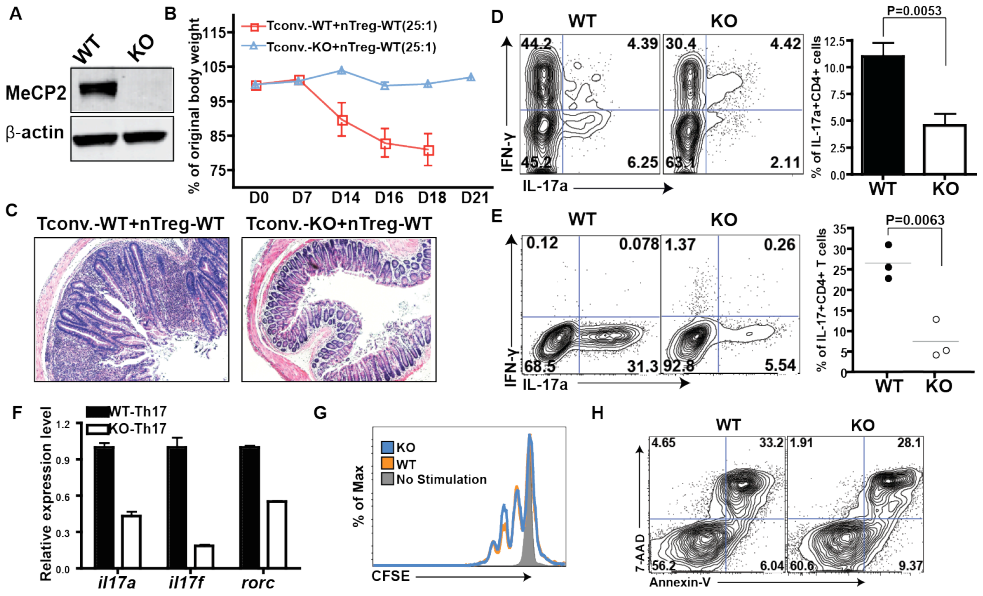

Figure 33: MeCP2 is indispensible for the commitment of naive CD4⁺ T cells into the Th17 lineage.

(A) Naïve CD4⁺CD25⁻ T cells from CD4-Cre⁺*mecp2*$^{x/x}$ or CD4-Cre⁺*mecp2*$^{x/y}$ (WT) and CD4-Cre⁺*mecp2*$^{f/f}$ or CD4-Cre⁺*mecp2*$^{f/y}$ (KO) littermates were sorted by flow cytometry. The expression of MeCP2 protein in these cells was detected by Western blot (WB). (B-D) CD4 ⁺CD25⁻CD45Rb^{high} naïve T cells from WT or KO mice were mixed with WT nTreg at a 25:1 ratio and injected intraperitoneally (i.p.) into *Rag2*$^{-/-}$ recipient mice to induce IBD. (B) Changes in body weights of *Rag2*$^{-/-}$ recipient mice are presented as percentages of their original weights. Data reflecting group averages from one experiment (error bars, s.e.m.; n=5), representative of four independent experiments is shown. (C) Histological sections of colon tissues with H&E staining. (D) The percentage of IL-17a producing CD4⁺TCRβ⁺ cells in mesenteric LN (n_{WT}=4; n_{KO}=8). Results represent four independent experiments. (E&F) Lymphocytes from LLO118 TCR transgenic WT

and KO littermates were cultured *in vitro* under Th17 skewing conditions for 4 days. (E) The percentage of IL-17a producing $CD4^+$ T cells (left), as quantified from three independent experiments (right). (F) $CD4^+$ T cells were sorted and the relative amounts of *il-17a*, *il-17f* and *rorc* mRNA was measured by qPCR. Data was normalized to a reference gene, SDHA, and shown relative to the WT. (G&H) Lymphocytes from LLO118 TCR transgenic WT or KO mice were labeled with CFSE, and stimulated with $LLO_{190\text{-}205}$ peptide for 3 days. The proliferation (G) and cell death (H) of $CD4^+$ T cells were determined by CFSE dilution and annexin V/7AAD staining, respectively.

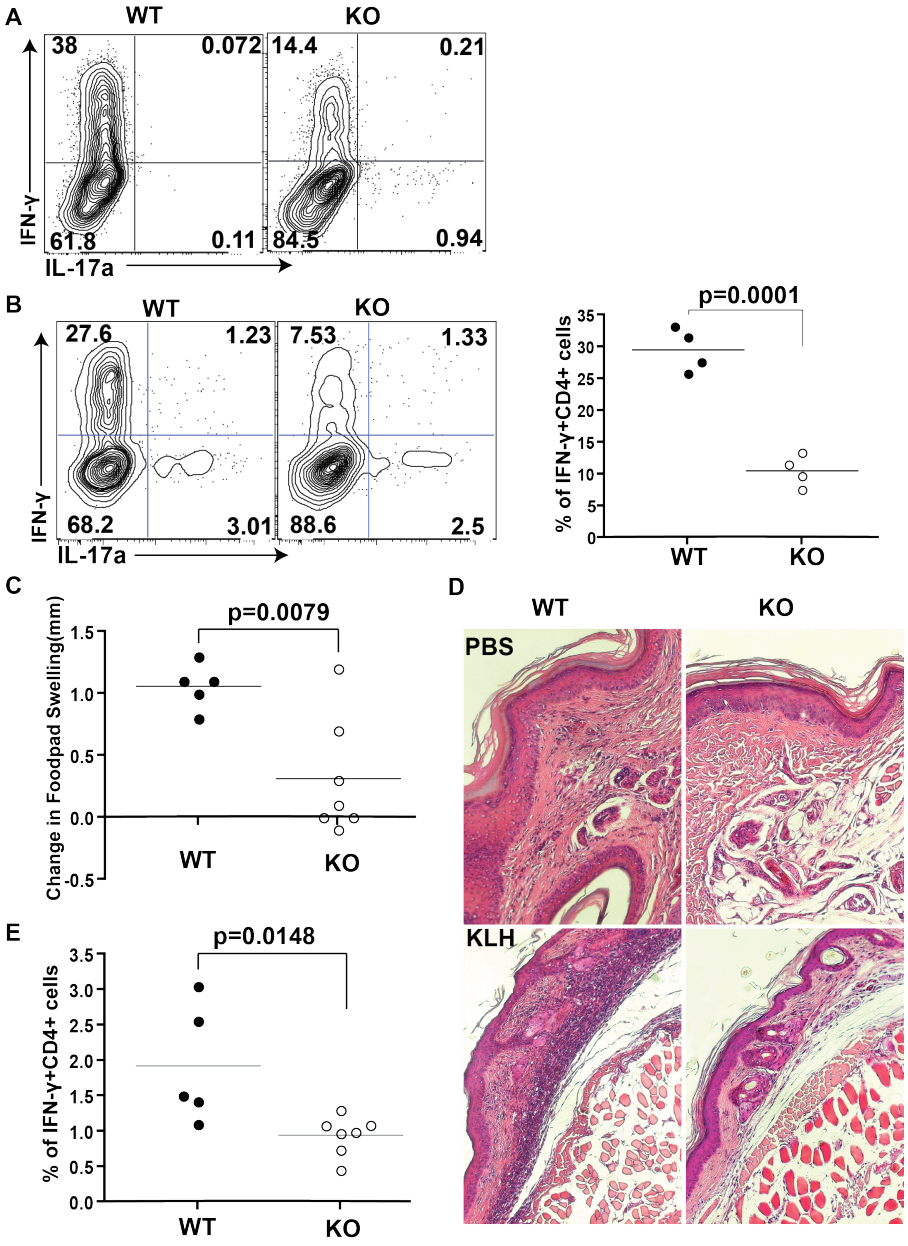

Figure 34: MeCP2 is indispensible for IFNγ production by Th1 cells.

(A) Lymphocytes from LLO118 TCR transgenic WT and KO littermates were activated with $LLO_{190\text{-}205}$ peptide under Th1-skewing conditions *in vitro* for 4 days. The percentage of IFNγ -producing $CD4^+$ T cells was detected by intracellular staining. Data

shown is representative of three independent experiments. (B) Naïve $CD4^+CD25^-$ T cells from LLO118 TCR transgenic WT or KO mice were transferred into *TCRα*-/- recipient mice (n=4) primed *in vivo* by subcutaneous immunization with $LLO_{190-205}$ peptide emulsified in CFA. Five days after immunization, splenocytes of recipient mice were challenged *in vitro* with $LLO_{190-205}$ peptide (5uM) for 48 hours and IFNγ production in $CD4^+$ T cells were detected by intracellular staining. (C-E) DTH response of WT and KO littermates induced by KLH immunization, as measured by (C) footpad swelling, (D) histology of footpad tissues by H&E staining and (E) the percentage of IFNγ-producing $CD4^+$ T cells in the popliteal LN.

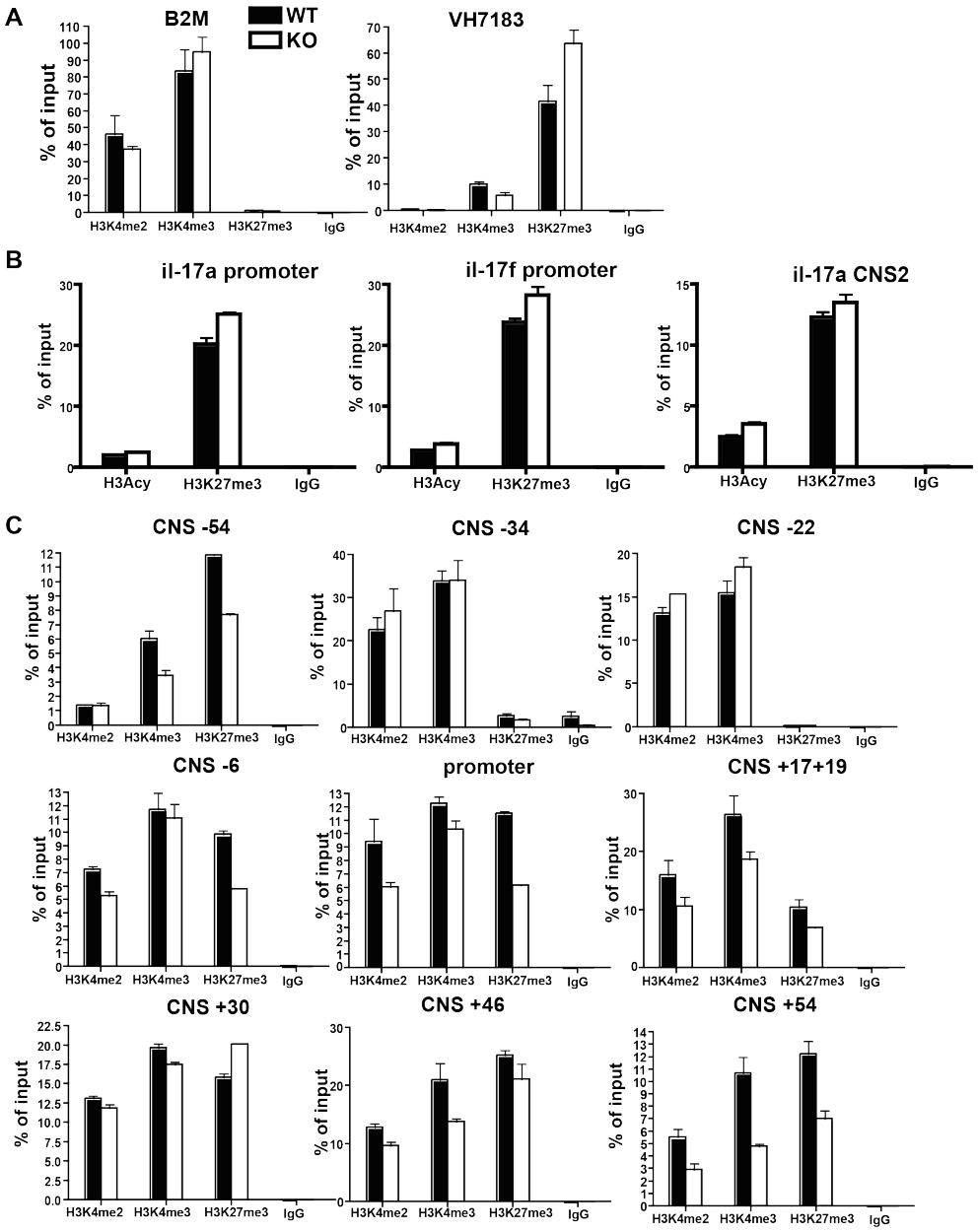

Figure 35: Normal chromatin accessibility of the *il17* and *ifng* loci in MeCP2-deficient naïve CD4$^+$CD25$^-$ T cells.

(A-C) Histone modifications of different cis-elements within the (B) *il17* and (C) *ifng* loci in naïve CD4$^+$CD25$^-$ were measured by chromatin immunoprecipitation analysis. The histone modifications of *β2m* and *vh7183* loci of CD4$^+$ T cells shown in (A)

serve as positive and negative controls, respectively. The bar graph shows Means ± SEM of triplicates done in one experiment. Data shown is representative of three independent experiments.

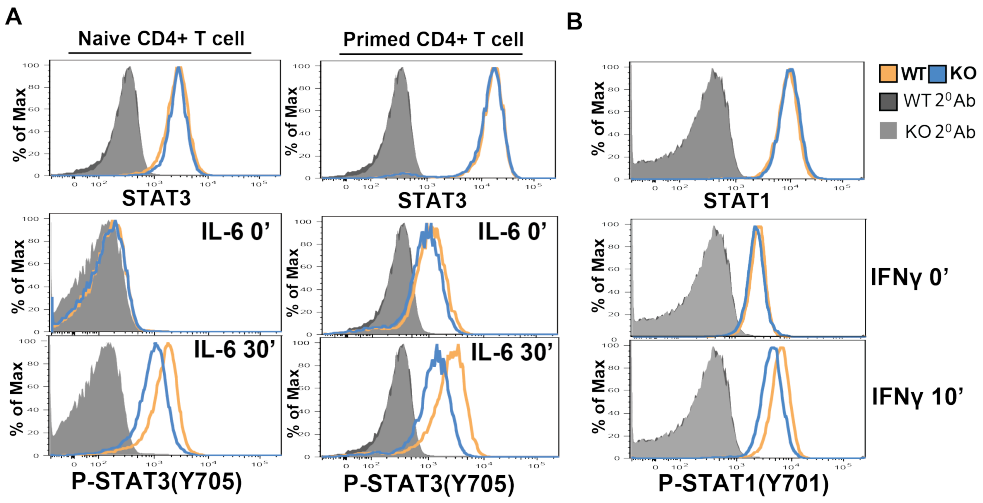

Figure 36: MeCP2 is necessary for activating the STAT3 and STAT1 signaling pathways in CD4⁺ T cells.

(A) $CD4^+CD25^-$ T cells sorted from WT and *mecp2*-KO littermates were stimulated with IL-6 (50ng/mL) for 30 minutes, and the amounts of total and phosphorylated STAT3 (Tyr705) were determined by intracellular staining and flow cytometry. Naïve $CD4^+$ T cells (left); primed $CD4^+$ T cells with anti-CD3 and anti-CD28 stimulation for 48 hours (right). Data shown is representative of four independent experiments. (B) $CD4^+CD25^-$ T cells sorted from the WT and KO littermates were stimulated with IFNγ (10ng/mL) for 10 minutes. Total STAT1 and phospho-STAT1 (Tyr701) were then detected by intracellular staining. Data shown is representative of three independent experiments.

A

List of genes whose mRNA amounts were measured by the q-PCR.

JAK and STAT Proteins:	JAK1, JAK2, JAK3, TYK2, STAT1, STAT2, STAT3, STAT4, STAT5A, STAT5B, STAT6.
Receptors that Bind and Activate JAK Proteins:	SH2B2 (APS), FAS (TNFRSF6), IL2RA, IL2RG, IL6ST, PTPRC (CD45), IL6RA, TCF8, ITGA4, CEBPD, RUNX1, RUNX3, CD6, BTG2, IRF2.
SH3 / SH2 Adaptor Protein Activity:	SH2B2 (APS), SIT1, SLA2.
Transcription Factors or Regulators that Interact with STAT Proteins:	IRF1, SLA2, CEBPB, GATA3, NR3C1.
Genes Induced by STAT Proteins:	IRF1, BCL2L1, CDKN1A (P21), FAS (TNFRSF6), SOCS1, IL2RA, GATA3.
Negative Regulators of the JAK/ STAT pathway:	PIAS1, PIAS2, PIAS3, PIAS4, PTPN1, PTPRC (CD45), SOCS1, SOCS2i, SOCS2ii, SOCS3, SOCS4, SOCS5, SOCS7.
Others:	SHP1, SHP2, PTPN2, PTPN22, PTPN13, PTEN,CDC42, RHOA, RAC-1, IL7RA, IL15RA, MCL1, FOXO1, FOXP3, RORC, TBET, IRF4, IRF5, IRF7, IRF9, BCL2, BAX, BAK, UBE3A.

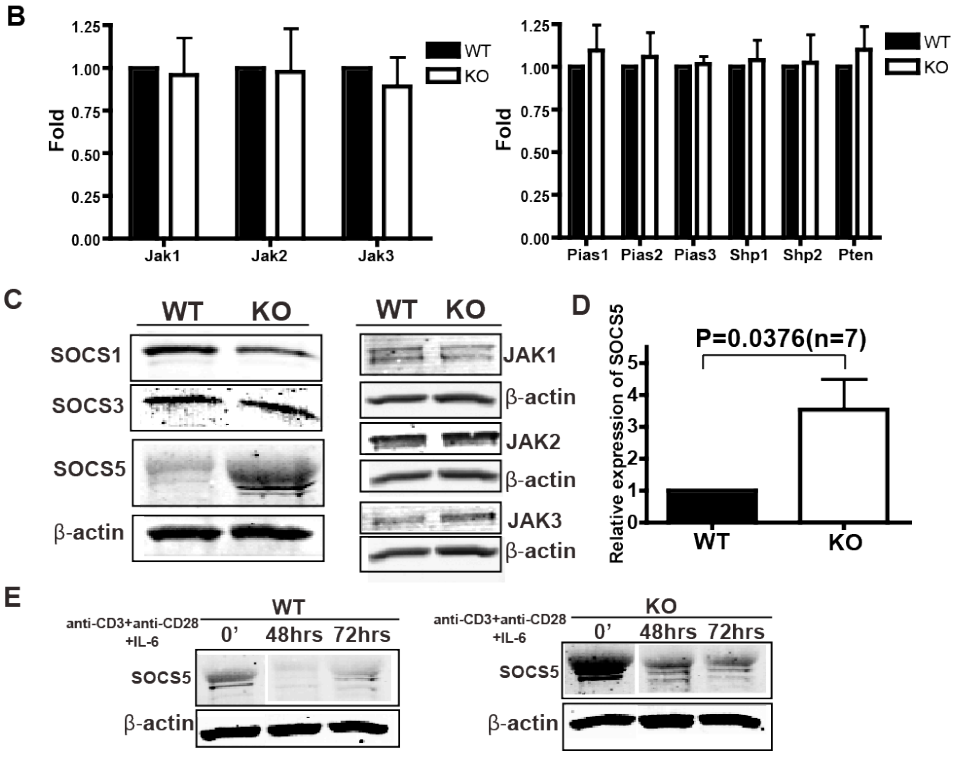

Figure 37: SOCS5 accumulation in *mecp2*-deficient CD4$^+$ T cells.

(A) List of genes whose mRNA amount were measured by qPCR. (B) The mRNA level of several positive and negative regulators of the JAK-STAT pathway. (C&D) The amount of SOCS and JAK protein in naive CD4$^+$CD25$^-$ cells. (D) Quantification of SOCS5

protein expression in $CD4^+CD25^-$ cells from seven independent experiments. Data was normalized to β-actin and shown relative to the WT. (E) $CD4^+CD25^-$ T cells primed with anti-CD3, anti-CD28 and IL-6 (50ng/mL) for different durations were assessed for SOCS5 expression by western blot.

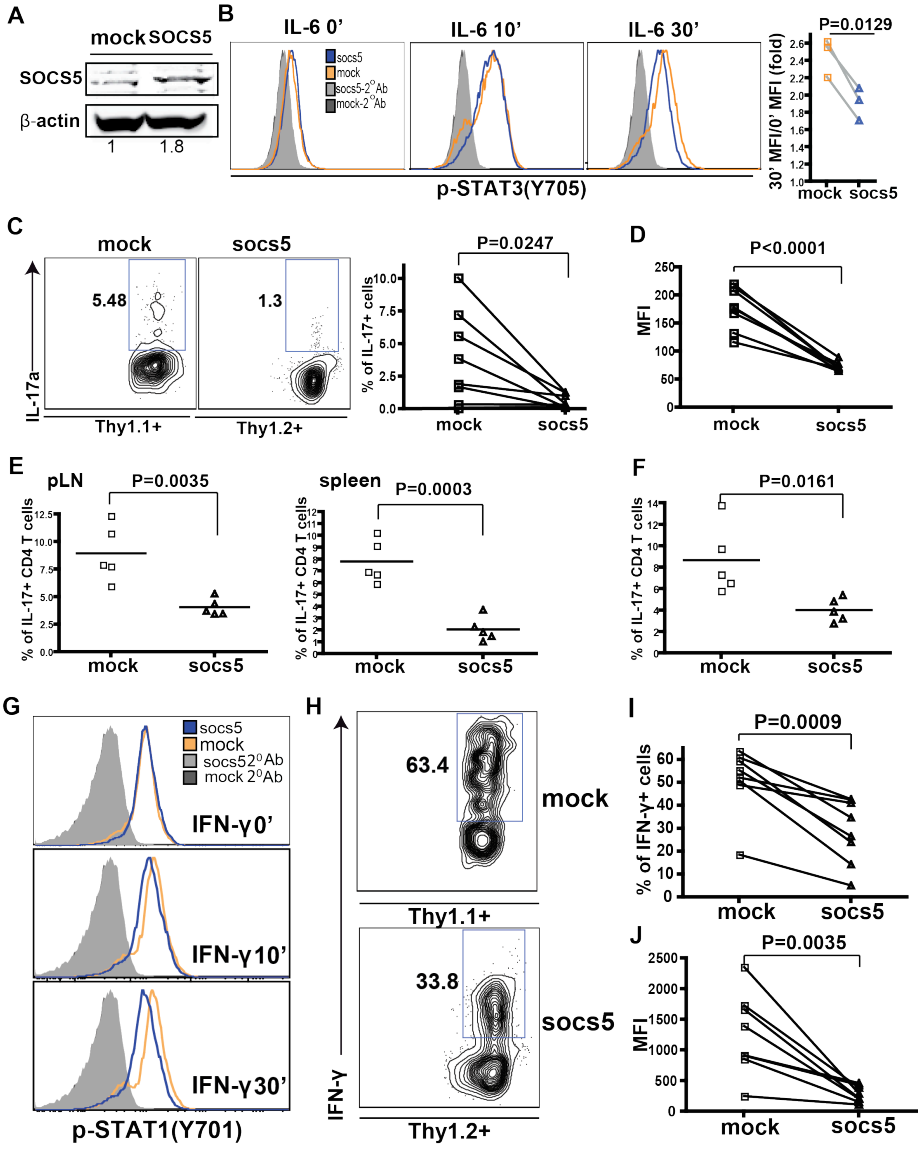

Figure 38: SOCS5 negatively regulates STAT3 activation and naïve CD4⁺ T cell commitment to the Th17 lineage.

(A&B) Lymphocytes from LLO118 TCR transgenic mice were retrovirally transduced with either an empty GFP vector (mock), or a mouse *socs5* overexpression vector (SOCS5), and sorted for $CD4^{+}GFP^{+}$ cells 72 hours after infection. (A) The expression of SOCS5 protein in these cells was detected by WB. (B) The cells were

treated with IL-6 (50ng/mL) for 10 or 30 minutes, and phospho-STAT3 (Tyr705) was detected by intracellular staining and flow cytometry. The plot (at far right) summarized results from three independent experiments. For each group of samples, the mean fluorescence intensity of pStat3 signal at the 30 mins time point was normalized by its pre-activation level (time zero). (C&D) Lymphocytes from LLO118 TCR transgenic mice with different Thy-markers were retrovirally transduced with either the mock ($Thy1.1^+$), or SOCS5 overexpression ($Thy1.2^+$) vector. Following intravenous competitive transfers of mock and SOCS5 ($CD4^+GFP^+$) cells (n=8; 1:1 ratio), $TCR\alpha^{-/-}$ recipient mice were immunized subcutaneously with $LLO_{190\text{-}205}$ peptide emulsified in CFA. Five days after immunization, splenocytes from recipient mice were rechallenged with $LLO_{190\text{-}205}$ peptide and cultured under Th17 skewing condition *in vitro*. 48 hours later, IL-17a producing $CD4^+$ T cells were enumerated by intracellular staining. (C) Percentage of IL-17a producing $CD4^+$ T cells. (D) MFI of IL-17a staining. (E&F) Mock and SOCS5 cells from LLO118 TCR transgenic mice were separately transferred into two groups of *TCRα-/-* recipient mice intravenously (n=5) and immunized as in (C&D). Seven days after immunization, recipient mice were rechallenged by footpad injections of $LLO_{190\text{-}205}$ peptide. (E) 48 hours after rechallenge, the percentages of IL-17a producing $CD4^+$ cells in the peripheral LN and spleen were measured *ex vivo* by intracellular staining. (F) Splenocytes from recipient mice were challenged with $LLO_{190\text{-}205}$ peptide for 48 hours *in vitro,* and IL-17a producing $CD4^+$ T cells were measured by intracellular staining.

A

Name of miRNA	Fold change (KO/WT)	p-value (paired *t –test*)
mmu-miR-124	**0.443**	**0.004**
mmu-miR-29c	0.599	0.007
mmu-miR-409-5p	0.838	0.017
mmu-miR-106b	0.272	0.030
mmu-miR-680	0.229	0.033

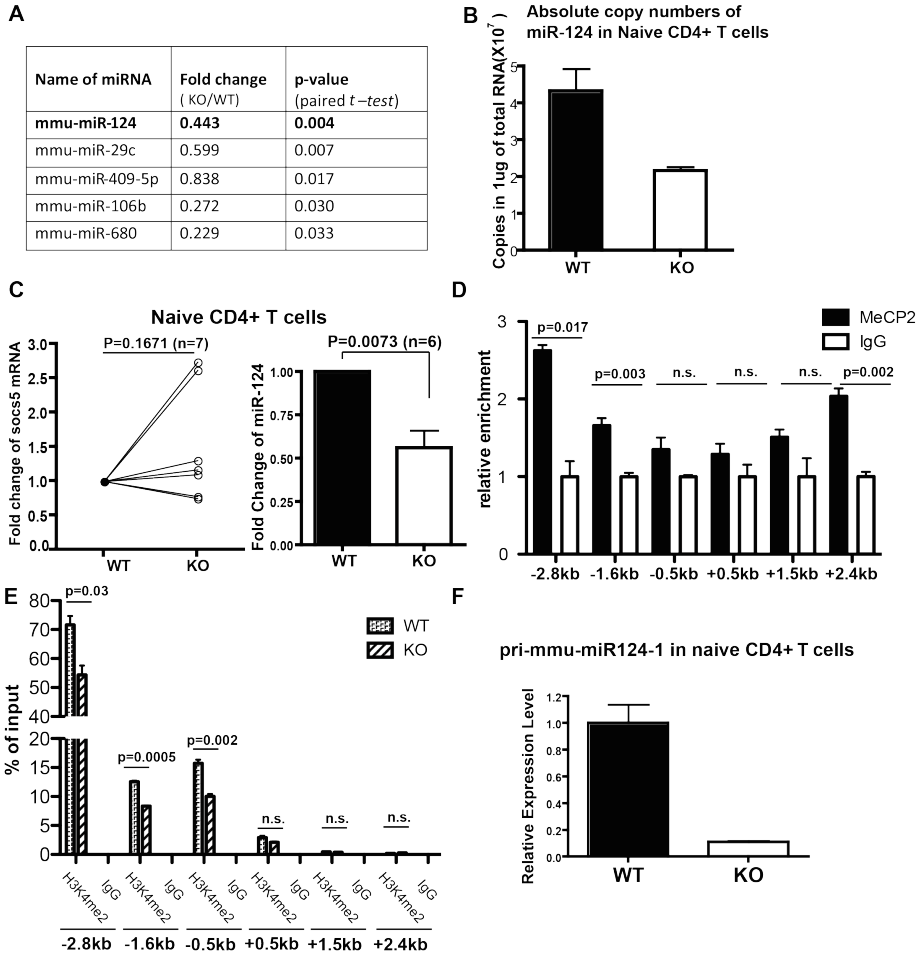

Figure 39: MeCP2 positively regulates the transcription of pri-mmu-miR-124-1 in CD4⁺ T cells.

(A) List of miRNAs significantly down-regulated in CD4⁺ T cells and primary human astrocytes upon deletion of MeCP2 ($p<0.05$). (B&C) Total RNA from naïve $CD4^+CD25^-$ cells was extracted and the amount of *socs5* mRNA (B&C) and miR-124 (right panel of C) was detected by q-PCR. (D) ChIP analysis for the enrichment of MeCP2 at the pri-mmu-miR124-1 gene locus in naïve $CD4^+CD25^-$ T cells. Data shown is representative of two independent experiments. (E) ChIP analysis for Lysine 4

dimethylation of histone H3 within the regulatory region of the *pri-mmu-miR124-1* gene locus in naïve $CD4^+$ T cells. Data shown is representative of two independent experiments. (F) The relative amount of pri-mmu-miR-124-1 transcript in naïve T cells was detected by qPCR. Data shown is representative of three independent experiments.

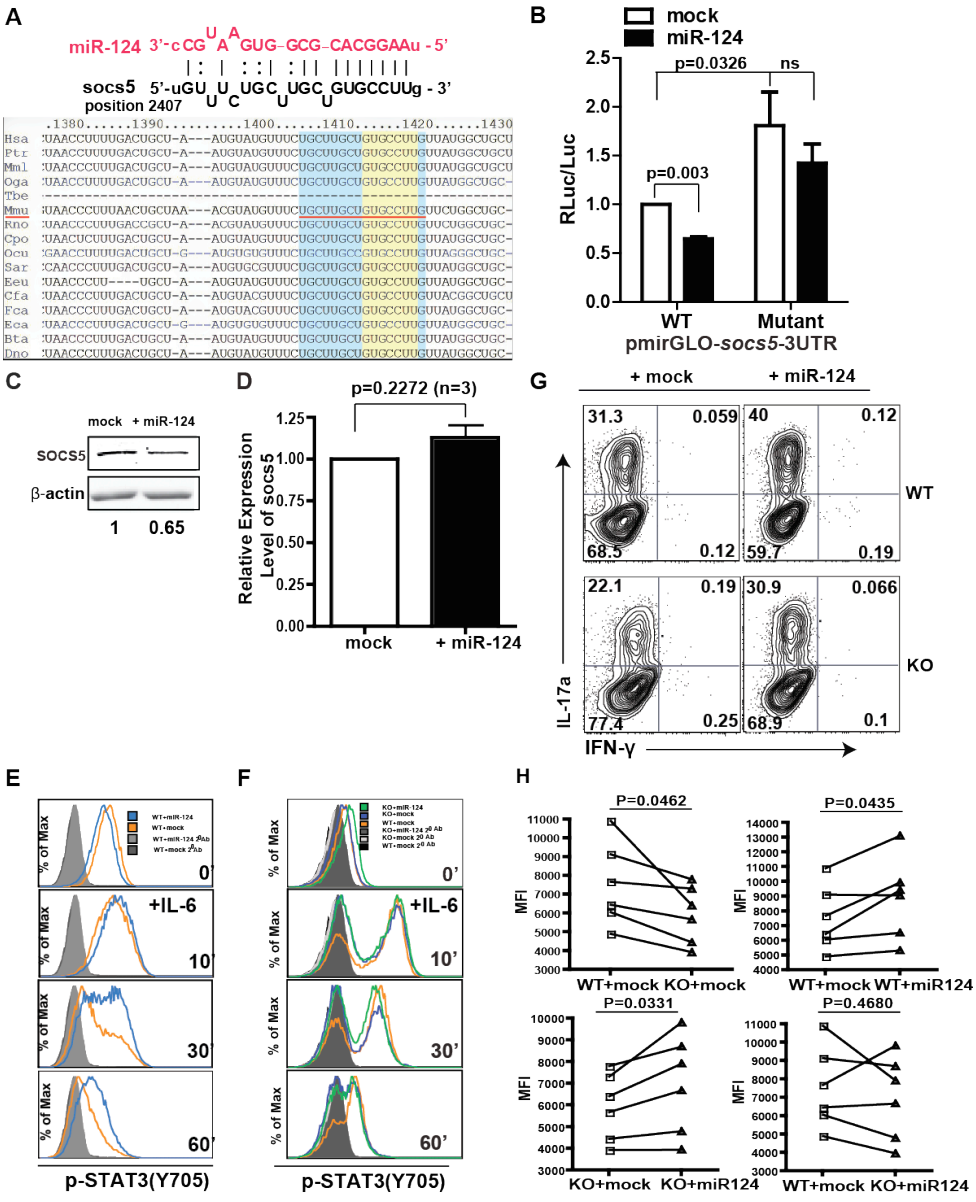

Figure 40: miR-124 inhibits the translation of *socs5* in CD4⁺ T cells.

(A) Schematic representation of the putative miR-124 binding site within the *socs5* 3′UTR. The sequences of *socs5* 3′UTR containing putative miR-124 binding sites from different species are shown in the table. (B) The entire 3′UTR of murine *socs5* (WT) or 3′UTR carrying miR-124 seed region-binding sites mutations were cloned into

pmirGLO downstream of the firefly luciferase reporter gene. pmirGLO-mSOCS5-3UTR was transiently transfected into an NIH3T3 cell line stably expressing miR-124, and luciferase activity was measured 72 hours post- transfection. Bar graphs show the means ± SEM of three independent experiments. Paired t-tests were employed to determine the statistic significance. (C&D) $CD4^+$ T cells from LLO118 TCR transgenic mice were retrovirally transfected with either mock or miR-124 overexpression vector. 72 hours after infection, $CD4^+GFP^+$ cells were sorted and their *socs5* (C) protein and (D) mRNA expression were measured by WB and qPCR, respectively. Data shown is representative of three independent experiments. (E-F) $CD4^+$ T cells from LLO118 TCR transgenic WT and KO littermates were retrovirally transfected with either mock or miR-124 overexpression vector. Previously primed T cells were stimulated with 50ng/ml IL-6 and the dynamics of STAT3 activation were monitored by Phospho-Flow analysis of Y705 phosphorylation; analysis was pre-gated on $CD4^+GFP^+$ virally-infected T cells. (E) The dynamics of STAT3 activation in WT $CD4^+$ T cells in the presence and absence of enforced miR-124 expression; (F) The dynamics of STAT3 activation in WT $CD4^+$ T cells and MeCP2 KO $CD4^+$ T cells in the presence and absence of enforced miR-124 expression; (G-H) $CD4^+$ T cells from LLO118 TCR transgenic WT and KO littermates retrovirally transfected with either mock or miR-124 overexpression vector were cultured under Th17 skewing conditions. Four to six days post-transfection, IL-17a production in $CD4^+GFP^+$ T cells was detected by intracellular staining. (G) The

percentage of IL-17a$^+$ cells among CD4$^+$GFP$^+$ cells representing six independent experiments. (H) MFI of IL-17a staining. Upper left: WT+ mock VS KO+ mock; Upper right: WT+ mock VS WT+ miR124; Bottom left: KO+ mock VS KO+ miR-124; Bottom right: WT+ mock VS KO+ miR-124.

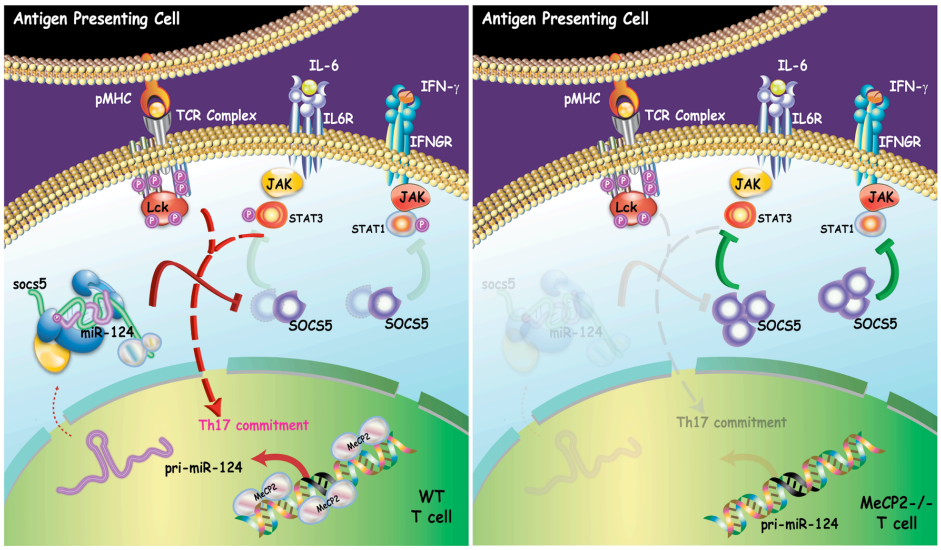

Figure 41: MeCP2-miR-124-SOCS5 axis regulates CD4⁺ T cell differentiation.

Left: in wild type CD4⁺ T cells, MeCP2 promotes pri-miR-124 transcription and, consequently, suppresses SOCS5 expression. This suppression licenses CD4⁺ T cells for efficient Th17 differentiation; Right: in MeCP2 deficient CD4⁺ T cells, the accumulation of SOCS5 attenuates STAT3 signaling and impairs the Th17 lineage commitment. Selected signaling components are depicted.

6.3 Discussion

In this chapter, we dissected the function of MeCP2 in T cells and determined that MeCP2 is required for conventional T cell differentiation (Figure 41). Mechanistically, we showed that MeCP2 plays a critical role in multiple cytokine signaling pathways by supporting miR-124 expression and restraining negative feedback that targets STAT3.

Loss-of-function mutations of *Mecp2* lead to RTT in humans, but overexpression also leads to the MECP2 duplication syndrome (MDS), a neurological disorder with remarkably similar symptoms to RTT[232]. We believe that this might reflect the dual regulatory role of MeCP2: MeCP2 is capable of recruiting machineries for both DNA methylation[171] and histone acetylation[169]. For a specific regulatory region, deletion of MeCP2 therefore results in both enhanced DNA demethylation and reduced histone acetylation, although the overall impact of loss-of-MeCP2 in this region is predominantly transcriptional inhibition. Overexpression of MeCP2, on the other hand, could potentially counteract local demethylation and result in a mechanistically distinct but phenotypically similar suppression of transcription. Therefore, we speculate that, for certain genes, the overarching role of MeCP2 in transcriptional regulation could be switchable from supportive to suppressive, depending on its dosage. This phenomenon manifests itself in the immune system as well. Clinically, patients with MDS experience recurrent respiratory tract infections [233], and it was recently reported that MeCP2-

overexpressing mice are defective in mounting efficient Th1 responses against *Leishmania major* infection [234]. Yet, immunodeficiency was not found among RTT patients. We speculate that this apparent discrepancy results from differential degrees of MeCP2 loss-of-function: immune function is intact in the majority of RTT patients bearing heterozygous mutations of *Mecp2*, and, we also failed to detect significant defects in Th1/17 differentiation in mouse T cells harboring heterozygous *Mecp2* deletion, whereas profound immune-deficiency ensued upon homozygous loss of *Mecp2*.

Because early studies identified MeCP2 as a transcriptional silencer, more recent work has largely focused on MeCP2's role in regulating gene expression at the mRNA level[169,235,236]. However, this view is somewhat at odds with expression profiling studies on samples from RTT patients, which have shown that only a limited subset of genes are mis-regulated at the mRNA level[237,238]. Using *mecp2*-deleted mouse models, expression differences were identified for additional genes, but most changes were very subtle[169,239]. In T cells, we found that the major defect associated with MeCP2 deletion was in STAT signaling, which was caused by the accumulation of SOCS5 protein: yet none of these changes were detectable at the mRNA level. Especially in wild type naïve T cells, the divergence between levels of SOCS5 mRNA and protein is striking: abundant mRNA does not result in even a modest amount of protein. This strongly indicated that active posttranscriptional suppression of SOCS5 is required for optimal and sustained T cells

responses to cytokine stimulation. We identified miR-124 as the responsible suppressive factor, whose expression is tightly controlled by MeCP2. If a similar miRNA-mediated mechanism operates in the signaling networks of neuronal and glial cells, it would likely do so without marked changes in mRNA expression, and might therefore be more difficult to detect with traditional transcriptome analyses.

7. General Discussion and Future Directions

7.1 Harnessing miRNAs in T cells for tumor immunotherapy

Our identification of miR-17-92 as a comprehensive endogenous modulator of $CD4^+$ T cells' anti-tumor response puts it forward as a putative candidate for adoptive cell transfer (ACT) based tumor immunotherapy. ACT relies on the isolation, selection, and expansion of tumor-infiltrating lymphocyte (TIL) with certain specificity *in vitro*, followed by autologous infusion back into the patient that have received "preparative lymphodepletion" by chemotherapy or irradiation[240]. Paradoxically, although this regimen is capable of generating a large number of antigen-specific T cells that enrich into the tumor, the efficacy of ACT has been just partial and majority of patients failed to respond to this therapy. This discrepancy could be largely attributed to the presence of immunosuppressive barriers existed in the tumor microenvironment. Indeed, several immunosuppressive molecules (such as PD1, CTLA4, TIM3, LAG3, IL-10) were enriched in the tumors and negatively control TIL proliferation and survival[241,242]. Importantly, TGFβ, a key cytokine involved in tumor pathogenesis, could strongly inhibit IFN-γ production from T cells[243] and promote the conversion of effector $CD4^+$ T cells into Tregs[74]. Recently, genetic engineering of T cells aiming to overcome these immunosuppressive barriers has been suggested as a promising way to improve the efficacy of ACT-based immunotherapy[240]. miRNAs are attractive targets to enhance anti-tumor responses because i) they are increasingly recognized as effective regulator of T

cell function, and ii) it is more straightforward to manipulate miRNAs as compared to traditional protein target based immune modulation.

Our findings in chapter 3 of this dissertation suggest that miR-17-92 could be such a promising miRNA target to improve the efficacy of ACT-based immunotherapy due to its multiple functions to benefit T cell anti-tumor immunity. First, we found that overexpression of miR-17-92 in $CD4^+$ T cells could significantly enhance cell proliferation and survival during T-cell recall response *in vitro*. This may lead to improved expansion and persistency of transferred T cells in the tumors. We are now testing this idea in an allograft model of B16 melanoma. Second, we showed that enhanced miR-17-92 level could effectively boost IFN-γ production from $CD4^+$ T cells, which is critical for an effective anti-tumor response through multiple pathways. Lastly, the ability of miR-17-92 to inhibit iTreg differentiation makes it a perfect candidate to overcome the immunosuppressive barrier for ACT based therapy. We previously found that when wild type antigen-specific $CD4^+$ T cells were transferred into tumor-bearing mice, majority of cells that infiltrate into tumor became Tregs (unpublished observations). This will not only blunt the intrinsic effector function of these $CD4^+$ T cells, but also harm the overall anti-tumor efficacy through suppression of other cell types. There are at least two reasons why iTreg induction is favored in the tumor microenvironment. First, many tumors antigens are weakly immunogenic and induce low-strength TCR signals, which favors iTreg induction. Secondly, the high concentration of TGFβ in the tumor

microenvironment is a strong inducer for iTreg differentiation. miR-17-92 is a good candidate to overcome both of these two tolerogenic mechanisms: by targeting PTEN, miR-17-92 enhances PI3K-Akt activation and TCR signaling strength; and, by inhibiting TGFβRII, miR-17-92 blunts TGFβ signaling. We are now actively testing whether overexpression of miR-17-92 in $CD4^+$ T cells could indeed effectively inhibit iTreg conversion in the tumor microenvironment, and ultimately, enhance the efficacy of ACT cancer immunotherapy.

In addition to miR-17-92, we are also actively pursuing for other miRNAs that control T cell anti-tumor responses. Particularly, we are currently screening for miRNAs whose expression levels are modulated by immunosuppressive cytokines (IL-10, TGFβ, and IL-35) that are enriched in the tumor microenvironment. We hypothesize that miRNAs that are universally downregulated by these cytokines may be potential "master miRNAs" controlling T cell anti-tumor response and overexpression or restoration the level of them in T cells may be an effective means to overcome the immunosuppressive barrier in the tumor microenvironment.

7.2 Regulation of global miRNA abundance by TCR signaling

Upon T cell-antigen engagement, we and others observed a global reduction of the abundance of miRNAs in CD4 T cells (data not shown and Bronevetsky et al [244]). On one hand, this unique feature prompted us to characterize the function of the few

miRNAs that are specifically upregulated by TCR stimulation, such as miR-17-92. On the other hand, it also urged us to dissect the biological meaning and molecular mechanisms underlying the global reduction of miRNA abundance upon TCR activation. It has been suggested that this global reduction of miRNA abundance is at least in part mediated through the posttranscriptional downregulation of Ago proteins[244], the key component of miRISC. It was also proposed that the high abundance of miRNAs in naïve T cells may serve as a "brake" against induction of gene expression, and upon T cell activation, they are globally suppressed to promote expression of genes that are important for T cell differentiation and effector function[244]. Consistent with this notion, cells that have a global disruption of miRNA machinery are more prone to differentiate into cytokine-producing effector T helper cells upon TCR activation. However, in addition to the intrinsic effects on T cells, the global reduction of miRNA abundance may also have other biological functions, and it may also be regulated by other mechanisms. First, the downregulation of Ago proteins by TCR signaling is less likely to account for the early changes of miRNA levels upon TCR activation. We found that as early as 6 hours after TCR activation, the global reduction of miRNA abundance was already evident. However, it was not until 48 hours of TCR stimulation that the downregulation of Ago proteins became obvious [244]. This suggests that additional mechanisms must be involved to control the early reduction of miRNA levels. Indeed, accompanying the loss of majority miRNAs in T cells upon activation, we could detect a

significant elevation of these miRNAs in the culture supernatant as early as 6 hours. More interestingly, it was recently shown that miRNA and miRISC were associated with intracellular vesicles and they could be secreted and taken up by other cells[245]. This suggests that upon TCR activation, T cells may actively exocytose or secrete miRNAs out of the cells. Why do T cells want to dump miRNAs out? One possibility is that through the immunological synapse-directed secretion, T cells may actively transfer certain miRNAs into antigen-presenting cells (APCs) to regulate their function. For example, during germinal center reactions, T follicular helper (Tfh) cells may transfer certain miRNAs into B cells. These miRNAs might be important to support B cell maturation and class switching. We are now testing this hypothesis by screening for miRNAs that are upregulated in B cells that lack endogenous miRNAs upon B cell-T cell engagement.

7.3 TCR-induced DNMT1 accumulation and its role in T helper cell differentiation

As mentioned above, it has been well recognized that iTreg favors low-strength TCR signals for optimal differentiation. However, how strong TCR signaling inhibits iTreg has been a mystery. Our studies in chapter 4 of this dissertation provided a potential molecular mechanism for this phenomenon. We found that TCR stimulation with high affinity or longer duration significantly induces the accumulation of DNMT1 and its subsequent enrichment to the *foxp3* locus, which enhances DNA methylation that

negatively controls *foxp3* transcription. As the accumulation of DNMT1 protein is a general phenomenon upon T cell activation when there are no skewing cytokines, we are curious about how the enhancement of DNMT1 level may influence the differentiation of other T helper subsets.

Similar to iTregs, Th17 cells was reported to also favor TCR signals with low strength for optimal differentiation[13]. Interestingly, in that study, it was shown that although high-strength of TCR stimulation induced similar level, or even higher NFAT activation and its nuclear translocation, it only bound to the i*l17* promoter in cells that received low-strength stimulation. We think that this is a strong indication that, like *foxp3*, the chromatin accessibility of *il17* locus could also be negatively regulated by TCR signaling strength. It is worthwhile to further examine whether the DNA methylation and DNMT1 localization in the *il17* locus could be affected by different TCR signaling strength.

Another interesting observation we made in this study is that although strong TCR stimulation led to overall accumulation of DNMT1, there is definitely certain specificity for which locus it will enrich to. For example, under strong stimulation, in contrast to *foxp3* promoter, the *ifng* locus was free of DNMT1 binding. There might be two potential mechanisms to determine this specificity. It is possible that strong TCR activation may induce the activation of certain pioneer factor that specifically binds to *foxp3* promoter, which subsequently recruits DNMT1 to complete silencing. Equally

likely, some transcription factor induced by strong TCR activation may specifically localize to the *ifng* locus to exclude DNMT1 from binding. In either case, it would be extremely interesting to further identify such pioneer factors that recruit or exclude DNMT1 from binding.

7.4 MeCP2: a general guardian for lineage stability?

In Chapter 5, we identified MeCP2 as an important safeguard to govern Treg lineage stability during inflammation. This raises the question of whether it also has any function to control the stability or plasticity of other T helper cells. The function of MeCP2 in Tregs lies in its ability to bind to *foxp3* locus and promote local histone acetylation to sustain *foxp3* transcription. However, MeCP2 has been shown to serve multifunctional roles, both as a transcription activator or repressor, presumably dependent upon the genomic context in which it operates. How then do cues in the genomic milieu control this functional switch? Genome wide analyses have suggested that for MeCP2-targeted genes, the loci activated by MeCP2 are largely unmethylated or only partially methylated, whereas repressed loci are enriched in fully methylated elements[169,172]. This suggests that the pivotal factor dictating MeCP2 function may lie in the status of local DNA methylation. Our data is consistent with this notion. CNS2, the primary region controlling the stability of Foxp3 expression[75], is completely unmethylated in naïve nTregs and becomes partially methylated upon inflammatory

stimulation. Under these conditions, MeCP2 functions as a coactivator. In contrast, the CNS2 region is fully methylated in naïve Tcon cells, a situation in which MeCP2 plays no role during iTreg induction. We speculate that, in addition to Tregs, MeCP2 may exert a much broader impact on the lineage specificity and plasticity of other $CD4^+$ T cell subsets. Following lineage commitment, MeCP2 can simultaneously serve as a transcription repressor at "closed" loci to enforce the silencing of rival cytokines, as well as an activator at fully- and/or partially- "opened" loci to support the expression of master transcription factors and signature cytokines. Using an inducible knockout system ($MeCP2^{f/y}$ ER-Cre mice), we are now actively testing whether deletion of MeCP2 after the commitment of Th1, Th2, or Th17 cells would affect their potential to "re-differentiate" into opposing lineages under skewing conditions.

7.5 MeCP2 and STAT3 signaling: implications for the pathogenesis of Rett Syndrome

Since its identification as the causal factor of RTT, MeCP2 has been extensively studied in the nervous system. However the molecular pathology stemming from this protein remains largely elusive. Therefore there is neither cure nor treatment for this disease. In Chapter 6, we dissected the function of MeCP2 in $CD4^+$ T cells and determined that MeCP2 plays a critical role in multiple cytokine signaling pathways by supporting miR-124 transcription and STAT3 activation. Interestingly, we identified that a similar mechanism operates during CNTF signaling in primary neuronal and glia cells

(data not shown). STAT3 is a necessary inflammatory signal for driving $CD4^+$ T cells differentiation into the Th17 lineage. But in the central nervous system, it is a vital neurotrophic transcription factor for neuronal survival and regeneration. STAT3 mutations are known to cause a severe immunodeficiency disease, the Job/Buckley syndrome, one symptoms of which is scoliosis[246]. Perhaps intriguingly, RTT patients are also prone to the development of scoliosis as a comorbidity[247]; coincidentally, mice with osteoblast- and osteocyte- specific *stat3* ablation develop a severe spinal deformity at 3-4 weeks of age[248]. In addition, miR-124, the direct target of MeCP2 in $CD4^+$ T cells, is also highly expressed in the central nervous system. If this miR-124-STAT3 signaling axis could be validated in the nervous systems of RTT patients, then it would provide a new molecular target for the development of therapies, or guidance for current growth-factor-based clinical trials.

7.6 Conclusions

In this dissertation, we described the function and molecular mechanism of a miRNA cluster (miR-17-92) and two epigenetic modulators (DNMT1 and MeCP2) in controlling T cell-mediated immune response. Importantly, we demonstrated how these miRNAs and epigenetic regulators could sense alterations from the environment and translate them into changes of downstream gene expression to ensure functional differentiation and stabilization. Further identification of such nodes could not only

improve our understanding of the biology underlying T cell response but also potentially benefit the development of novel treatments for patients suffering from immune-mediated diseases, such as autoimmunity, infection, and cancer.

References

1. Krammer PH, Arnold R, Lavrik IN. Life and death in peripheral T cells. *Nat Rev Immunol*. 2007;7(7):532-542.

2. Bartel DP. MicroRNAs: target recognition and regulatory functions. *Cell*. 2009;136(2):215-233.

3. Wilson CB, Rowell E, Sekimata M. Epigenetic control of T-helper-cell differentiation. *Nat Rev Immunol*. 2009;9(2):91-105.

4. Zhu J, Yamane H, Paul WE. Differentiation of effector CD4 T cell populations (*). *Annual review of immunology*. 2010;28:445-489.

5. Josefowicz SZ, Lu LF, Rudensky AY. Regulatory T cells: mechanisms of differentiation and function. *Annu Rev Immunol*. 2012;30:531-564.

6. Gallimore A, Sakaguchi S. Regulation of tumour immunity by CD25+ T cells. *Immunology*. 2002;107(1):5-9.

7. Curotto de Lafaille MA, Lafaille JJ. Natural and adaptive foxp3+ regulatory T cells: more of the same or a division of labor? *Immunity*. 2009;30(5):626-635.

8. Zhu J, Yamane H, Paul WE. Differentiation of effector CD4 T cell populations (*). *Annu Rev Immunol*. 2010;28:445-489.

9. Corse E, Gottschalk RA, Allison JP. Strength of TCR-peptide/MHC interactions and in vivo T cell responses. *J Immunol*. 2011;186(9):5039-5045.

10. Tao X, Grant C, Constant S, Bottomly K. Induction of IL-4-producing CD4+ T cells by antigenic peptides altered for TCR binding. *J Immunol*. 1997;158(9):4237-4244.

11. Constant S, Pfeiffer C, Woodard A, Pasqualini T, Bottomly K. Extent of T cell receptor ligation can determine the functional differentiation of naive CD4+ T cells. *J Exp Med*. 1995;182(5):1591-1596.

12. Yamane H, Zhu J, Paul WE. Independent roles for IL-2 and GATA-3 in stimulating naive CD4+ T cells to generate a Th2-inducing cytokine environment. *J Exp Med*. 2005;202(6):793-804.

13. Purvis HA, Stoop JN, Mann J, et al. Low-strength T-cell activation promotes Th17 responses. *Blood*. 2010;116(23):4829-4837.

14. Sauer S, Bruno L, Hertweck A, et al. T cell receptor signaling controls Foxp3 expression via PI3K, Akt, and mTOR. *Proc Natl Acad Sci U S A*. 2008;105(22):7797-7802.

15. Kretschmer K, Apostolou I, Hawiger D, Khazaie K, Nussenzweig MC, von Boehmer H. Inducing and expanding regulatory T cell populations by foreign antigen. *Nat Immunol*. 2005;6(12):1219-1227.

16. Vahedi G, Takahashi H, Nakayamada S, et al. STATs shape the active enhancer landscape of T cell populations. *Cell*. 2012;151(5):981-993.

17. Djuretic IM, Levanon D, Negreanu V, Groner Y, Rao A, Ansel KM. Transcription factors T-bet and Runx3 cooperate to activate Ifng and silence Il4 in T helper type 1 cells. *Nat Immunol*. 2007;8(2):145-153.

18. Hwang ES, Szabo SJ, Schwartzberg PL, Glimcher LH. T helper cell fate specified by kinase-mediated interaction of T-bet with GATA-3. *Science*. 2005;307(5708):430-433.

19. Afkarian M, Sedy JR, Yang J, et al. T-bet is a STAT1-induced regulator of IL-12R expression in naive CD4+ T cells. *Nat Immunol*. 2002;3(6):549-557.

20. Ansel KM, Djuretic I, Tanasa B, Rao A. Regulation of Th2 differentiation and Il4 locus accessibility. *Annu Rev Immunol*. 2006;24:607-656.

21. Amsen D, Antov A, Jankovic D, et al. Direct regulation of Gata3 expression determines the T helper differentiation potential of Notch. *Immunity*. 2007;27(1):89-99.

22. Dong C. TH17 cells in development: an updated view of their molecular identity and genetic programming. *Nat Rev Immunol*. 2008;8(5):337-348.

23. Zhou L, Lopes JE, Chong MM, et al. TGF-beta-induced Foxp3 inhibits T(H)17 cell differentiation by antagonizing RORgammat function. *Nature*. 2008;453(7192):236-240.

24. Yang XP, Ghoreschi K, Steward-Tharp SM, et al. Opposing regulation of the locus encoding IL-17 through direct, reciprocal actions of STAT3 and STAT5. *Nat Immunol*. 2011;12(3):247-254.

25. O'Shea JJ, Paul WE. Mechanisms underlying lineage commitment and plasticity of helper CD4+ T cells. *Science*. 2010;327(5969):1098-1102.

26. Wilson NJ, Boniface K, Chan JR, et al. Development, cytokine profile and function of human interleukin 17-producing helper T cells. *Nat Immunol*. 2007;8(9):950-957.

27. Lohning M, Hegazy AN, Pinschewer DD, et al. Long-lived virus-reactive memory T cells generated from purified cytokine-secreting T helper type 1 and type 2 effectors. *J Exp Med*. 2008;205(1):53-61.

28. Zhou L, Chong MM, Littman DR. Plasticity of CD4+ T cell lineage differentiation. *Immunity*. 2009;30(5):646-655.

29. Nakayamada S, Takahashi H, Kanno Y, O'Shea JJ. Helper T cell diversity and plasticity. *Curr Opin Immunol*. 2012;24(3):297-302.

30. Sakaguchi S. Naturally arising CD4+ regulatory t cells for immunologic self-tolerance and negative control of immune responses. *Annu Rev Immunol*. 2004;22:531-562.

31. Sakaguchi S, Yamaguchi T, Nomura T, Ono M. Regulatory T cells and immune tolerance. *Cell*. 2008;133(5):775-787.

32. Jordan MS, Boesteanu A, Reed AJ, et al. Thymic selection of CD4+CD25+ regulatory T cells induced by an agonist self-peptide. *Nat Immunol*. 2001;2(4):301-306.

33. Hsieh CS, Liang Y, Tyznik AJ, Self SG, Liggitt D, Rudensky AY. Recognition of the peripheral self by naturally arising CD25+ CD4+ T cell receptors. *Immunity*. 2004;21(2):267-277.

34. Fontenot JD, Rasmussen JP, Gavin MA, Rudensky AY. A function for interleukin 2 in Foxp3-expressing regulatory T cells. *Nat Immunol*. 2005;6(11):1142-1151.

35. Vang KB, Yang J, Mahmud SA, Burchill MA, Vegoe AL, Farrar MA. IL-2, -7, and -15, but not thymic stromal lymphopoeitin, redundantly govern CD4+Foxp3+ regulatory T cell development. *J Immunol*. 2008;181(5):3285-3290.

36. Burchill MA, Yang J, Vogtenhuber C, Blazar BR, Farrar MA. IL-2 receptor beta-dependent STAT5 activation is required for the development of Foxp3+ regulatory T cells. *J Immunol*. 2007;178(1):280-290.

37. Malin S, McManus S, Cobaleda C, et al. Role of STAT5 in controlling cell survival and immunoglobulin gene recombination during pro-B cell development. *Nat Immunol*. 2010;11(2):171-179.

38. Liu Y, Zhang P, Li J, Kulkarni AB, Perruche S, Chen W. A critical function for TGF-beta signaling in the development of natural CD4+CD25+Foxp3+ regulatory T cells. *Nat Immunol*. 2008;9(6):632-640.

39. Tone Y, Furuuchi K, Kojima Y, Tykocinski ML, Greene MI, Tone M. Smad3 and NFAT cooperate to induce Foxp3 expression through its enhancer. *Nat Immunol*. 2008;9(2):194-202.

40. Ouyang W, Beckett O, Ma Q, Li MO. Transforming growth factor-beta signaling curbs thymic negative selection promoting regulatory T cell development. *Immunity*. 2010;32(5):642-653.

41. Xu L, Kitani A, Fuss I, Strober W. Cutting edge: regulatory T cells induce CD4+CD25-Foxp3- T cells or are self-induced to become Th17 cells in the absence of exogenous TGF-beta. *J Immunol*. 2007;178(11):6725-6729.

42. Yang XO, Nurieva R, Martinez GJ, et al. Molecular antagonism and plasticity of regulatory and inflammatory T cell programs. *Immunity*. 2008;29(1):44-56.

43. Hori S. Stability of regulatory T-cell lineage. *Adv Immunol*. 2011;112:1-24.

44. Zhou X, Bailey-Bucktrout SL, Jeker LT, et al. Instability of the transcription factor Foxp3 leads to the generation of pathogenic memory T cells in vivo. *Nat Immunol*. 2009;10(9):1000-1007.

45. Rubtsov YP, Niec RE, Josefowicz S, et al. Stability of the regulatory T cell lineage in vivo. *Science*. 2010;329(5999):1667-1671.

46. Fabian MR, Sonenberg N, Filipowicz W. Regulation of mRNA translation and stability by microRNAs. *Annu Rev Biochem*. 2010;79:351-379.

47. Baumjohann D, Ansel KM. MicroRNA-mediated regulation of T helper cell differentiation and plasticity. *Nat Rev Immunol*. 2013;13(9):666-678.

48. Baltimore D, Boldin MP, O'Connell RM, Rao DS, Taganov KD. MicroRNAs: new regulators of immune cell development and function. *Nat Immunol*. 2008;9(8):839-845.

49. Muljo SA, Ansel KM, Kanellopoulou C, Livingston DM, Rao A, Rajewsky K. Aberrant T cell differentiation in the absence of Dicer. *J Exp Med*. 2005;202(2):261-269.

50. Steiner DF, Thomas MF, Hu JK, et al. MicroRNA-29 regulates T-box transcription factors and interferon-gamma production in helper T cells. *Immunity*. 2011;35(2):169-181.

51. Jiang S, Li C, Olive V, et al. Molecular dissection of the miR-17-92 cluster's critical dual roles in promoting Th1 responses and preventing inducible Treg differentiation. *Blood*. 2011.

52. Li QJ, Chau J, Ebert PJ, et al. miR-181a is an intrinsic modulator of T cell sensitivity and selection. *Cell*. 2007;129(1):147-161.

53. Ebert PJ, Jiang S, Xie J, Li QJ, Davis MM. An endogenous positively selecting peptide enhances mature T cell responses and becomes an autoantigen in the absence of microRNA miR-181a. *Nat Immunol*. 2009;10(11):1162-1169.

54. Jiang S, Li C, Olive V, et al. Molecular dissection of the miR-17-92 cluster's critical dual roles in promoting Th1 responses and preventing inducible Treg differentiation. *Blood*. 2011;118(20):5487-5497.

55. Rodriguez A, Vigorito E, Clare S, et al. Requirement of bic/microRNA-155 for normal immune function. *Science*. 2007;316(5824):608-611.

56. Yang L, Boldin MP, Yu Y, et al. miR-146a controls the resolution of T cell responses in mice. *J Exp Med*. 2012;209(9):1655-1670.

57. Ma F, Xu S, Liu X, et al. The microRNA miR-29 controls innate and adaptive immune responses to intracellular bacterial infection by targeting interferon-gamma. *Nat Immunol*. 2011;12(9):861-869.

58. Du C, Liu C, Kang J, et al. MicroRNA miR-326 regulates TH-17 differentiation and is associated with the pathogenesis of multiple sclerosis. *Nat Immunol*. 2009;10(12):1252-1259.

59. Cobb BS, Hertweck A, Smith J, et al. A role for Dicer in immune regulation. *J Exp Med*. 2006;203(11):2519-2527.

60. Liston A, Lu LF, O'Carroll D, Tarakhovsky A, Rudensky AY. Dicer-dependent microRNA pathway safeguards regulatory T cell function. *J Exp Med*. 2008;205(9):1993-2004.

61. Chong MM, Rasmussen JP, Rudensky AY, Littman DR. The RNAseIII enzyme Drosha is critical in T cells for preventing lethal inflammatory disease. *J Exp Med*. 2008;205(9):2005-2017.

62. Lu LF, Thai TH, Calado DP, et al. Foxp3-dependent microRNA155 confers competitive fitness to regulatory T cells by targeting SOCS1 protein. *Immunity*. 2009;30(1):80-91.

63. Lu LF, Boldin MP, Chaudhry A, et al. Function of miR-146a in controlling Treg cell-mediated regulation of Th1 responses. *Cell*. 2010;142(6):914-929.

64. Kouzarides T. Chromatin modifications and their function. *Cell*. 2007;128(4):693-705.

65. Ruthenburg AJ, Li H, Patel DJ, Allis CD. Multivalent engagement of chromatin modifications by linked binding modules. *Nat Rev Mol Cell Biol*. 2007;8(12):983-994.

66. Berger SL. The complex language of chromatin regulation during transcription. *Nature*. 2007;447(7143):407-412.

67. Ballas ZK. The use of 5-azacytidine to establish constitutive interleukin 2-producing clones of the EL4 thymoma. *J Immunol*. 1984;133(1):7-9.

68. Valapour M, Guo J, Schroeder JT, et al. Histone deacetylation inhibits IL4 gene expression in T cells. *J Allergy Clin Immunol*. 2002;109(2):238-245.

69. Li C, Ebert PJ, Li QJ. T Cell Receptor (TCR) and Transforming Growth Factor beta (TGF-beta) Signaling Converge on DNA (Cytosine-5)-methyltransferase to Control forkhead box protein 3 (foxp3) Locus Methylation and Inducible Regulatory T Cell Differentiation. *J Biol Chem*. 2013;288(26):19127-19139.

70. Wei G, Wei L, Zhu J, et al. Global mapping of H3K4me3 and H3K27me3 reveals specificity and plasticity in lineage fate determination of differentiating CD4+ T cells. *Immunity*. 2009;30(1):155-167.

71. Zheng Y, Josefowicz SZ, Kas A, Chu TT, Gavin MA, Rudensky AY. Genome-wide analysis of Foxp3 target genes in developing and mature regulatory T cells. *Nature*. 2007;445(7130):936-940.

72. Kim HP, Leonard WJ. CREB/ATF-dependent T cell receptor-induced FoxP3 gene expression: a role for DNA methylation. *J Exp Med*. 2007;204(7):1543-1551.

73. Mantel PY, Ouaked N, Ruckert B, et al. Molecular mechanisms underlying FOXP3 induction in human T cells. *J Immunol*. 2006;176(6):3593-3602.

74. Tone Y, Furuuchi K, Kojima Y, Tykocinski ML, Greene MI, Tone M. Smad3 and NFAT cooperate to induce Foxp3 expression through its enhancer. *Nature immunology*. 2008;9(2):194-202.

75. Zheng Y, Josefowicz S, Chaudhry A, Peng XP, Forbush K, Rudensky AY. Role of conserved non-coding DNA elements in the Foxp3 gene in regulatory T-cell fate. *Nature*. 2010;463(7282):808-812.

76. Tran DQ, Ramsey H, Shevach EM. Induction of FOXP3 expression in naive human CD4+FOXP3 T cells by T-cell receptor stimulation is transforming growth factor-beta dependent but does not confer a regulatory phenotype. *Blood*. 2007;110(8):2983-2990.

77. Polansky JK, Schreiber L, Thelemann C, et al. Methylation matters: binding of Ets-1 to the demethylated Foxp3 gene contributes to the stabilization of Foxp3 expression in regulatory T cells. *J Mol Med (Berl)*. 2010;88(10):1029-1040.

78. Wang Y, Su MA, Wan YY. An essential role of the transcription factor GATA-3 for the function of regulatory T cells. *Immunity*. 2011;35(3):337-348.

79. Maines LW, Fitzpatrick LR, French KJ, et al. Suppression of ulcerative colitis in mice by orally available inhibitors of sphingosine kinase. *Dig Dis Sci*. 2008;53(4):997-1012.

80. Szabo SJ, Kim ST, Costa GL, Zhang X, Fathman CG, Glimcher LH. A novel transcription factor, T-bet, directs Th1 lineage commitment. *Cell*. 2000;100(6):655-669.

81. Ikeda H, Chamoto K, Tsuji T, et al. The critical role of type-1 innate and acquired immunity in tumor immunotherapy. *Cancer Sci*. 2004;95(9):697-703.

82. Dighe AS, Richards E, Old LJ, Schreiber RD. Enhanced in vivo growth and resistance to rejection of tumor cells expressing dominant negative IFN gamma receptors. *Immunity*. 1994;1(6):447-456.

83. Hung K, Hayashi R, Lafond-Walker A, Lowenstein C, Pardoll D, Levitsky H. The central role of CD4(+) T cells in the antitumor immune response. *J Exp Med*. 1998;188(12):2357-2368.

84. Dunn GP, Old LJ, Schreiber RD. The immunobiology of cancer immunosurveillance and immunoediting. *Immunity*. 2004;21(2):137-148.

85. Coughlin CM, Salhany KE, Gee MS, et al. Tumor cell responses to IFNgamma affect tumorigenicity and response to IL-12 therapy and antiangiogenesis. *Immunity*. 1998;9(1):25-34.

86. Shankaran V, Ikeda H, Bruce AT, et al. IFNgamma and lymphocytes prevent primary tumour development and shape tumour immunogenicity. *Nature*. 2001;410(6832):1107-1111.

87. Street SE, Cretney E, Smyth MJ. Perforin and interferon-gamma activities independently control tumor initiation, growth, and metastasis. *Blood*. 2001;97(1):192-197.

88. Street SE, Trapani JA, MacGregor D, Smyth MJ. Suppression of lymphoma and epithelial malignancies effected by interferon gamma. *J Exp Med*. 2002;196(1):129-134.

89. Leen AM, Rooney CM, Foster AE. Improving T cell therapy for cancer. *Annu Rev Immunol*. 2007;25:243-265.

90. Shevach EM. Mechanisms of foxp3+ T regulatory cell-mediated suppression. *Immunity*. 2009;30(5):636-645.

91. Curiel TJ. Regulatory T cells and treatment of cancer. *Curr Opin Immunol*. 2008;20(2):241-246.

92. Zou W. Regulatory T cells, tumour immunity and immunotherapy. *Nat Rev Immunol*. 2006;6(4):295-307.

93. Koralov SB, Muljo SA, Galler GR, et al. Dicer ablation affects antibody diversity and cell survival in the B lymphocyte lineage. *Cell*. 2008;132(5):860-874.

94. Cobb BS, Nesterova TB, Thompson E, et al. T cell lineage choice and differentiation in the absence of the RNase III enzyme Dicer. *J Exp Med*. 2005;201(9):1367-1373.

95. Zhou X, Jeker LT, Fife BT, et al. Selective miRNA disruption in T reg cells leads to uncontrolled autoimmunity. *J Exp Med*. 2008;205(9):1983-1991.

96. Tanzer A, Stadler PF. Molecular evolution of a microRNA cluster. *J Mol Biol*. 2004;339(2):327-335.

97. He L, Thomson JM, Hemann MT, et al. A microRNA polycistron as a potential human oncogene. *Nature*. 2005;435(7043):828-833.

98. Ventura A, Young AG, Winslow MM, et al. Targeted deletion reveals essential and overlapping functions of the miR-17 through 92 family of miRNA clusters. *Cell*. 2008;132(5):875-886.

99. Dews M, Homayouni A, Yu D, et al. Augmentation of tumor angiogenesis by a Myc-activated microRNA cluster. *Nat Genet*. 2006;38(9):1060-1065.

100. Fontana L, Pelosi E, Greco P, et al. MicroRNAs 17-5p-20a-106a control monocytopoiesis through AML1 targeting and M-CSF receptor upregulation. *Nat Cell Biol*. 2007;9(7):775-787.

101. Xiao C, Srinivasan L, Calado DP, et al. Lymphoproliferative disease and autoimmunity in mice with increased miR-17-92 expression in lymphocytes. *Nat Immunol*. 2008;9(4):405-414.

102. Olive V, Jiang I, He L. mir-17-92, a cluster of miRNAs in the midst of the cancer network. *Int J Biochem Cell Biol*. 2010;42(8):1348-1354.

103. Chen W, Jin W, Hardegen N, et al. Conversion of peripheral CD4+CD25- naive T cells to CD4+CD25+ regulatory T cells by TGF-beta induction of transcription factor Foxp3. *J Exp Med*. 2003;198(12):1875-1886.

104. Li MO, Wan YY, Sanjabi S, Robertson AK, Flavell RA. Transforming growth factor-beta regulation of immune responses. *Annu Rev Immunol*. 2006;24:99-146.

105. Gade P, Roy SK, Li H, Nallar SC, Kalvakolanu DV. Critical role for transcription factor C/EBP-beta in regulating the expression of death-associated protein kinase 1. *Mol Cell Biol*. 2008;28(8):2528-2548.

106. Buckler JL, Liu X, Turka LA. Regulation of T-cell responses by PTEN. *Immunol Rev*. 2008;224:239-248.

107. Okkenhaug K, Patton DT, Bilancio A, Garcon F, Rowan WC, Vanhaesebroeck B. The p110delta isoform of phosphoinositide 3-kinase controls clonal expansion and differentiation of Th cells. *J Immunol*. 2006;177(8):5122-5128.

108. Soond DR, Bjorgo E, Moltu K, et al. PI3K p110delta regulates T-cell cytokine production during primary and secondary immune responses in mice and humans. *Blood*. 2010;115(11):2203-2213.

109. Haxhinasto S, Mathis D, Benoist C. The AKT-mTOR axis regulates de novo differentiation of CD4+Foxp3+ cells. *J Exp Med*. 2008;205(3):565-574.

110. Olive V, Bennett MJ, Walker JC, et al. miR-19 is a key oncogenic component of mir-17-92. *Genes Dev*. 2009;23(24):2839-2849.

111. Huppa JB, Gleimer M, Sumen C, Davis MM. Continuous T cell receptor signaling required for synapse maintenance and full effector potential. *Nat Immunol*. 2003;4(8):749-755.

112. Muranski P, Restifo NP. Adoptive immunotherapy of cancer using CD4(+) T cells. *Curr Opin Immunol*. 2009;21(2):200-208.

113. Mu P, Han YC, Betel D, et al. Genetic dissection of the miR-17~92 cluster of microRNAs in Myc-induced B-cell lymphomas. *Genes Dev*. 2009;23(24):2806-2811.

114. Frisch SM, Mymryk JS. Adenovirus-5 E1A: paradox and paradigm. *Nat Rev Mol Cell Biol*. 2002;3(6):441-452.

115. La Thangue NB. The yin and yang of E2F-1: balancing life and death. *Nat Cell Biol*. 2003;5(7):587-589.

116. Meyer N, Penn LZ. Reflecting on 25 years with MYC. *Nat Rev Cancer*. 2008;8(12):976-990.

117. Liu G, Min H, Yue S, Chen CZ. Pre-miRNA loop nucleotides control the distinct activities of mir-181a-1 and mir-181c in early T cell development. *PLoS One*. 2008;3(10):e3592.

118. Mestdagh P, Bostrom AK, Impens F, et al. The miR-17-92 microRNA cluster regulates multiple components of the TGF-beta pathway in neuroblastoma. *Molecular cell*. 2010;40(5):762-773.

119. Dews M, Fox JL, Hultine S, et al. The myc-miR-17~92 axis blunts TGF{beta} signaling and production of multiple TGF{beta}-dependent antiangiogenic factors. *Cancer research*. 2010;70(20):8233-8246.

120. Yamane H, Zhu J, Paul WE. Independent roles for IL-2 and GATA-3 in stimulating naive CD4+ T cells to generate a Th2-inducing cytokine environment. *The Journal of experimental medicine*. 2005;202(6):793-804.

121. Tao X, Grant C, Constant S, Bottomly K. Induction of IL-4-producing CD4+ T cells by antigenic peptides altered for TCR binding. *Journal of immunology*. 1997;158(9):4237-4244.

122. Constant S, Pfeiffer C, Woodard A, Pasqualini T, Bottomly K. Extent of T cell receptor ligation can determine the functional differentiation of naive CD4+ T cells. *The Journal of experimental medicine*. 1995;182(5):1591-1596.

123. Fontenot JD, Gavin MA, Rudensky AY. Foxp3 programs the development and function of CD4+CD25+ regulatory T cells. *Nature immunology*. 2003;4(4):330-336.

124. Hori S, Nomura T, Sakaguchi S. Control of regulatory T cell development by the transcription factor Foxp3. *Science*. 2003;299(5609):1057-1061.

125. Khattri R, Cox T, Yasayko SA, Ramsdell F. An essential role for Scurfin in CD4+CD25+ T regulatory cells. *Nature immunology*. 2003;4(4):337-342.

126. Williams LM, Rudensky AY. Maintenance of the Foxp3-dependent developmental program in mature regulatory T cells requires continued expression of Foxp3. *Nature immunology*. 2007;8(3):277-284.

127. Bennett CL, Christie J, Ramsdell F, et al. The immune dysregulation, polyendocrinopathy, enteropathy, X-linked syndrome (IPEX) is caused by mutations of FOXP3. *Nature genetics*. 2001;27(1):20-21.

128. Brunkow ME, Jeffery EW, Hjerrild KA, et al. Disruption of a new forkhead/winged-helix protein, scurfin, results in the fatal lymphoproliferative disorder of the scurfy mouse. *Nature genetics*. 2001;27(1):68-73.

129. Mantel PY, Ouaked N, Ruckert B, et al. Molecular mechanisms underlying FOXP3 induction in human T cells. *Journal of immunology*. 2006;176(6):3593-3602.

130. Kim HP, Leonard WJ. CREB/ATF-dependent T cell receptor-induced FoxP3 gene expression: a role for DNA methylation. *The Journal of experimental medicine*. 2007;204(7):1543-1551.

131. Long M, Park SG, Strickland I, Hayden MS, Ghosh S. Nuclear factor-kappaB modulates regulatory T cell development by directly regulating expression of Foxp3 transcription factor. *Immunity*. 2009;31(6):921-931.

132. Sauer S, Bruno L, Hertweck A, et al. T cell receptor signaling controls Foxp3 expression via PI3K, Akt, and mTOR. *Proceedings of the National Academy of Sciences of the United States of America*. 2008;105(22):7797-7802.

133. Kretschmer K, Apostolou I, Hawiger D, Khazaie K, Nussenzweig MC, von Boehmer H. Inducing and expanding regulatory T cell populations by foreign antigen. *Nature immunology*. 2005;6(12):1219-1227.

134. Huehn J, Polansky JK, Hamann A. Epigenetic control of FOXP3 expression: the key to a stable regulatory T-cell lineage? *Nature reviews Immunology*. 2009;9(2):83-89.

135. Lal G, Bromberg JS. Epigenetic mechanisms of regulation of Foxp3 expression. *Blood*. 2009;114(18):3727-3735.

136. Janson PC, Winerdal ME, Marits P, Thorn M, Ohlsson R, Winqvist O. FOXP3 promoter demethylation reveals the committed Treg population in humans. *PloS one*. 2008;3(2):e1612.

137. Floess S, Freyer J, Siewert C, et al. Epigenetic control of the foxp3 locus in regulatory T cells. *PLoS biology*. 2007;5(2):e38.

138. Seder RA, Paul WE, Davis MM, Fazekas de St Groth B. The presence of interleukin 4 during in vitro priming determines the lymphokine-producing potential of CD4+ T cells from T cell receptor transgenic mice. *The Journal of experimental medicine*. 1992;176(4):1091-1098.

139. Davis MM, Boniface JJ, Reich Z, et al. Ligand recognition by alpha beta T cell receptors. *Annual review of immunology*. 1998;16:523-544.

140. Reay PA, Kantor RM, Davis MM. Use of global amino acid replacements to define the requirements for MHC binding and T cell recognition of moth cytochrome c (93-103). *Journal of immunology*. 1994;152(8):3946-3957.

141. Huppa JB, Gleimer M, Sumen C, Davis MM. Continuous T cell receptor signaling required for synapse maintenance and full effector potential. *Nature immunology*. 2003;4(8):749-755.

142. Haxhinasto S, Mathis D, Benoist C. The AKT-mTOR axis regulates de novo differentiation of CD4+Foxp3+ cells. *The Journal of experimental medicine*. 2008;205(3):565-574.

143. Smith-Garvin JE, Koretzky GA, Jordan MS. T cell activation. *Annual review of immunology*. 2009;27:591-619.

144. Josefowicz SZ, Rudensky A. Control of regulatory T cell lineage commitment and maintenance. *Immunity*. 2009;30(5):616-625.

145. Josefowicz SZ, Wilson CB, Rudensky AY. Cutting edge: TCR stimulation is sufficient for induction of Foxp3 expression in the absence of DNA methyltransferase 1. *Journal of immunology*. 2009;182(11):6648-6652.

146. Kim GD, Ni J, Kelesoglu N, Roberts RJ, Pradhan S. Co-operation and communication between the human maintenance and de novo DNA (cytosine-5) methyltransferases. *The EMBO journal*. 2002;21(15):4183-4195.

147. Rhee I, Bachman KE, Park BH, et al. DNMT1 and DNMT3b cooperate to silence genes in human cancer cells. *Nature*. 2002;416(6880):552-556.

148. Schoenborn JR, Dorschner MO, Sekimata M, et al. Comprehensive epigenetic profiling identifies multiple distal regulatory elements directing transcription of the gene encoding interferon-gamma. *Nature immunology*. 2007;8(7):732-742.

149. Cohen P, Frame S. The renaissance of GSK3. *Nature reviews Molecular cell biology*. 2001;2(10):769-776.

150. Cross DA, Alessi DR, Cohen P, Andjelkovich M, Hemmings BA. Inhibition of glycogen synthase kinase-3 by insulin mediated by protein kinase B. *Nature*. 1995;378(6559):785-789.

151. Goode N, Hughes K, Woodgett JR, Parker PJ. Differential regulation of glycogen synthase kinase-3 beta by protein kinase C isotypes. *The Journal of biological chemistry*. 1992;267(24):16878-16882.

152. Sun L, Zhao H, Xu Z, et al. Phosphatidylinositol 3-kinase/protein kinase B pathway stabilizes DNA methyltransferase I protein and maintains DNA methylation. *Cellular signalling*. 2007;19(11):2255-2263.

153. Fabian MR, Sonenberg N, Filipowicz W. Regulation of mRNA translation and stability by microRNAs. *Annual review of biochemistry*. 2010;79:351-379.

154. Pan W, Zhu S, Yuan M, et al. MicroRNA-21 and microRNA-148a contribute to DNA hypomethylation in lupus CD4+ T cells by directly and indirectly targeting DNA methyltransferase 1. *Journal of immunology*. 2010;184(12):6773-6781.

155. Huang J, Wang Y, Guo Y, Sun S. Down-regulated microRNA-152 induces aberrant DNA methylation in hepatitis B virus-related hepatocellular carcinoma by targeting DNA methyltransferase 1. *Hepatology*. 2010;52(1):60-70.

156. Li MO, Wan YY, Sanjabi S, Robertson AK, Flavell RA. Transforming growth factor-beta regulation of immune responses. *Annual review of immunology*. 2006;24:99-146.

157. Luo X, Zhang Q, Liu V, Xia Z, Pothoven KL, Lee C. Cutting edge: TGF-beta-induced expression of Foxp3 in T cells is mediated through inactivation of ERK. *Journal of immunology*. 2008;180(5):2757-2761.

158. Chen W, Jin W, Hardegen N, et al. Conversion of peripheral CD4+CD25- naive T cells to CD4+CD25+ regulatory T cells by TGF-beta induction of transcription factor Foxp3. *The Journal of experimental medicine*. 2003;198(12):1875-1886.

159. Pillai V, Ortega SB, Wang CK, Karandikar NJ. Transient regulatory T-cells: a state attained by all activated human T-cells. *Clinical immunology*. 2007;123(1):18-29.

160. Wang J, Ioan-Facsinay A, van der Voort EI, Huizinga TW, Toes RE. Transient expression of FOXP3 in human activated nonregulatory CD4+ T cells. *European journal of immunology*. 2007;37(1):129-138.

161. Mukasa R, Balasubramani A, Lee YK, et al. Epigenetic instability of cytokine and transcription factor gene loci underlies plasticity of the T helper 17 cell lineage. *Immunity*. 2010;32(5):616-627.

162. Youngblood B, Oestreich KJ, Ha SJ, et al. Chronic virus infection enforces demethylation of the locus that encodes PD-1 in antigen-specific CD8(+) T cells. *Immunity*. 2011;35(3):400-412.

163. Vijayanand P, Seumois G, Simpson LJ, et al. Interleukin-4 Production by Follicular Helper T Cells Requires the Conserved Il4 Enhancer Hypersensitivity Site V. *Immunity*. 2012;36(2):175-187.

164. Ebert PJ, Ehrlich LI, Davis MM. Low ligand requirement for deletion and lack of synapses in positive selection enforce the gauntlet of thymic T cell maturation. *Immunity*. 2008;29(5):734-745.

165. Mempel TR, Henrickson SE, Von Andrian UH. T-cell priming by dendritic cells in lymph nodes occurs in three distinct phases. *Nature*. 2004;427(6970):154-159.

166. Quaderi NA, Meehan RR, Tate PH, et al. Genetic and physical mapping of a gene encoding a methyl CpG binding protein, Mecp2, to the mouse X chromosome. *Genomics*. 1994;22(3):648-651.

167. Lewis JD, Meehan RR, Henzel WJ, et al. Purification, sequence, and cellular localization of a novel chromosomal protein that binds to methylated DNA. *Cell*. 1992;69(6):905-914.

168. Meehan RR, Lewis JD, Bird AP. Characterization of MeCP2, a vertebrate DNA binding protein with affinity for methylated DNA. *Nucleic Acids Res*. 1992;20(19):5085-5092.

169. Chahrour M, Jung SY, Shaw C, et al. MeCP2, a key contributor to neurological disease, activates and represses transcription. *Science*. 2008;320(5880):1224-1229.

170. Nan X, Ng HH, Johnson CA, et al. Transcriptional repression by the methyl-CpG-binding protein MeCP2 involves a histone deacetylase complex. *Nature*. 1998;393(6683):386-389.

171. Kimura H, Shiota K. Methyl-CpG-binding protein, MeCP2, is a target molecule for maintenance DNA methyltransferase, Dnmt1. *J Biol Chem*. 2003;278(7):4806-4812.

172. Yasui DH, Peddada S, Bieda MC, et al. Integrated epigenomic analyses of neuronal MeCP2 reveal a role for long-range interaction with active genes. *Proc Natl Acad Sci U S A*. 2007;104(49):19416-19421.

173. Guy J, Cheval H, Selfridge J, Bird A. The role of MeCP2 in the brain. *Annu Rev Cell Dev Biol*. 2011;27:631-652.

174. Amir RE, Van den Veyver IB, Wan M, Tran CQ, Francke U, Zoghbi HY. Rett syndrome is caused by mutations in X-linked MECP2, encoding methyl-CpG-binding protein 2. *Nat Genet*. 1999;23(2):185-188.

175. Neul JL, Fang P, Barrish J, et al. Specific mutations in methyl-CpG-binding protein 2 confer different severity in Rett syndrome. *Neurology*. 2008;70(16):1313-1321.

176. Neul JL, Kaufmann WE, Glaze DG, et al. Rett syndrome: revised diagnostic criteria and nomenclature. *Ann Neurol*. 2010;68(6):944-950.

177. Sawalha AH, Webb R, Han S, et al. Common variants within MECP2 confer risk of systemic lupus erythematosus. *PLoS One*. 2008;3(3):e1727.

178. Webb R, Wren JD, Jeffries M, et al. Variants within MECP2, a key transcription regulator, are associated with increased susceptibility to lupus and differential gene expression in patients with systemic lupus erythematosus. *Arthritis Rheum*. 2009;60(4):1076-1084.

179. Cobb BL, Fei Y, Jonsson R, et al. Genetic association between methyl-CpG binding protein 2 (MECP2) and primary Sjogren's syndrome. *Ann Rheum Dis*. 2010;69(9):1731-1732.

180. Reichelt KL, Skjeldal O. IgA antibodies in Rett syndrome. *Autism*. 2006;10(2):189-197.

181. Derecki NC, Cronk JC, Lu Z, et al. Wild-type microglia arrest pathology in a mouse model of Rett syndrome. *Nature*. 2012;484(7392):105-109.

182. Chatila TA, Blaeser F, Ho N, et al. JM2, encoding a fork head-related protein, is mutated in X-linked autoimmunity-allergic disregulation syndrome. *J Clin Invest*. 2000;106(12):R75-81.

183. Brunkow ME, Jeffery EW, Hjerrild KA, et al. Disruption of a new forkhead/winged-helix protein, scurfin, results in the fatal lymphoproliferative disorder of the scurfy mouse. *Nat Genet*. 2001;27(1):68-73.

184. Wildin RS, Ramsdell F, Peake J, et al. X-linked neonatal diabetes mellitus, enteropathy and endocrinopathy syndrome is the human equivalent of mouse scurfy. *Nat Genet*. 2001;27(1):18-20.

185. Bennett CL, Christie J, Ramsdell F, et al. The immune dysregulation, polyendocrinopathy, enteropathy, X-linked syndrome (IPEX) is caused by mutations of FOXP3. *Nat Genet*. 2001;27(1):20-21.

186. Khattri R, Cox T, Yasayko SA, Ramsdell F. An essential role for Scurfin in CD4+CD25+ T regulatory cells. *Nat Immunol*. 2003;4(4):337-342.

187. Fontenot JD, Gavin MA, Rudensky AY. Foxp3 programs the development and function of CD4+CD25+ regulatory T cells. *Nat Immunol*. 2003;4(4):330-336.

188. Williams LM, Rudensky AY. Maintenance of the Foxp3-dependent developmental program in mature regulatory T cells requires continued expression of Foxp3. *Nat Immunol*. 2007;8(3):277-284.

189. Yao Z, Kanno Y, Kerenyi M, et al. Nonredundant roles for Stat5a/b in directly regulating Foxp3. *Blood*. 2007;109(10):4368-4375.

190. Mouly E, Chemin K, Nguyen HV, et al. The Ets-1 transcription factor controls the development and function of natural regulatory T cells. *J Exp Med*. 2010;207(10):2113-2125.

191. Ouyang W, Beckett O, Ma Q, Paik JH, DePinho RA, Li MO. Foxo proteins cooperatively control the differentiation of Foxp3+ regulatory T cells. *Nat Immunol*. 2010;11(7):618-627.

192. Rudra D, Egawa T, Chong MM, Treuting P, Littman DR, Rudensky AY. Runx-CBFbeta complexes control expression of the transcription factor Foxp3 in regulatory T cells. *Nat Immunol*. 2009;10(11):1170-1177.

193. Huehn J, Polansky JK, Hamann A. Epigenetic control of FOXP3 expression: the key to a stable regulatory T-cell lineage? *Nat Rev Immunol*. 2009;9(2):83-89.

194. Lal G, Zhang N, van der Touw W, et al. Epigenetic regulation of Foxp3 expression in regulatory T cells by DNA methylation. *J Immunol*. 2009;182(1):259-273.

195. Kim JM, Rasmussen JP, Rudensky AY. Regulatory T cells prevent catastrophic autoimmunity throughout the lifespan of mice. *Nat Immunol*. 2007;8(2):191-197.

196. Cretney E, Xin A, Shi W, et al. The transcription factors Blimp-1 and IRF4 jointly control the differentiation and function of effector regulatory T cells. *Nat Immunol*. 2011;12(4):304-311.

197. Kerdiles YM, Stone EL, Beisner DR, et al. Foxo transcription factors control regulatory T cell development and function. *Immunity*. 2010;33(6):890-904.

198. Ouyang W, Liao W, Luo CT, et al. Novel Foxo1-dependent transcriptional programs control T(reg) cell function. *Nature*. 2012;491(7425):554-559.

199. Kukreja A, Cost G, Marker J, et al. Multiple immuno-regulatory defects in type-1 diabetes. *J Clin Invest*. 2002;109(1):131-140.

200. Feuerer M, Shen Y, Littman DR, Benoist C, Mathis D. How punctual ablation of regulatory T cells unleashes an autoimmune lesion within the pancreatic islets. *Immunity*. 2009;31(4):654-664.

201. Ohkura N, Hamaguchi M, Morikawa H, et al. T cell receptor stimulation-induced epigenetic changes and Foxp3 expression are independent and complementary events required for Treg cell development. *Immunity*. 2012;37(5):785-799.

202. Laurence A, Amarnath S, Mariotti J, et al. STAT3 transcription factor promotes instability of nTreg cells and limits generation of iTreg cells during acute murine graft-versus-host disease. *Immunity*. 2012;37(2):209-222.

203. Chijiwa T, Mishima A, Hagiwara M, et al. Inhibition of forskolin-induced neurite outgrowth and protein phosphorylation by a newly synthesized selective inhibitor of cyclic AMP-dependent protein kinase, N-[2-(p-bromocinnamylamino)ethyl]-5-isoquinolinesulfonamide (H-89), of PC12D pheochromocytoma cells. *J Biol Chem*. 1990;265(9):5267-5272.

204. Chrivia JC, Kwok RP, Lamb N, Hagiwara M, Montminy MR, Goodman RH. Phosphorylated CREB binds specifically to the nuclear protein CBP. *Nature*. 1993;365(6449):855-859.

205. Nan X, Campoy FJ, Bird A. MeCP2 is a transcriptional repressor with abundant binding sites in genomic chromatin. *Cell*. 1997;88(4):471-481.

206. Hite KC, Adams VH, Hansen JC. Recent advances in MeCP2 structure and function. *Biochem Cell Biol*. 2009;87(1):219-227.

207. Young JI, Hong EP, Castle JC, et al. Regulation of RNA splicing by the methylation-dependent transcriptional repressor methyl-CpG binding protein 2. *Proc Natl Acad Sci U S A*. 2005;102(49):17551-17558.

208. Georgel PT, Horowitz-Scherer RA, Adkins N, Woodcock CL, Wade PA, Hansen JC. Chromatin compaction by human MeCP2. Assembly of novel secondary chromatin structures in the absence of DNA methylation. *J Biol Chem*. 2003;278(34):32181-32188.

209. Horike S, Cai S, Miyano M, Cheng JF, Kohwi-Shigematsu T. Loss of silent-chromatin looping and impaired imprinting of DLX5 in Rett syndrome. *Nat Genet*. 2005;37(1):31-40.

210. Rett A. [On a unusual brain atrophy syndrome in hyperammonemia in childhood]. *Wien Med Wochenschr*. 1966;116(37):723-726.

211. Laurvick CL, de Klerk N, Bower C, et al. Rett syndrome in Australia: a review of the epidemiology. *J Pediatr*. 2006;148(3):347-352.

212. Hagberg B. Rett's syndrome: prevalence and impact on progressive severe mental retardation in girls. *Acta Paediatr Scand*. 1985;74(3):405-408.

213. Chen RZ, Akbarian S, Tudor M, Jaenisch R. Deficiency of methyl-CpG binding protein-2 in CNS neurons results in a Rett-like phenotype in mice. *Nat Genet*. 2001;27(3):327-331.

214. Lioy DT, Garg SK, Monaghan CE, et al. A role for glia in the progression of Rett's syndrome. *Nature*. 2011;475(7357):497-500.

215. Armstrong DD. Neuropathology of Rett syndrome. *J Child Neurol*. 2005;20(9):747-753.

216. Jellinger K, Seitelberger F. Neuropathology of Rett syndrome. *Am J Med Genet Suppl*. 1986;1:259-288.

217. Saleh M, Elson CO. Experimental inflammatory bowel disease: insights into the host-microbiota dialog. *Immunity*. 2011;34(3):293-302.

218. Weber KS, Li QJ, Persaud SP, Campbell JD, Davis MM, Allen PM. Distinct CD4+ helper T cells involved in primary and secondary responses to infection. *Proc Natl Acad Sci U S A*. 2012;109(24):9511-9516.

219. Sospedra M, Martin R. Immunology of multiple sclerosis. *Annu Rev Immunol*. 2005;23:683-747.

220. Luger D, Silver PB, Tang J, et al. Either a Th17 or a Th1 effector response can drive autoimmunity: conditions of disease induction affect dominant effector category. *J Exp Med*. 2008;205(4):799-810.

221. Yang XO, Panopoulos AD, Nurieva R, et al. STAT3 regulates cytokine-mediated generation of inflammatory helper T cells. *J Biol Chem*. 2007;282(13):9358-9363.

222. Harris TJ, Grosso JF, Yen HR, et al. Cutting edge: An in vivo requirement for STAT3 signaling in TH17 development and TH17-dependent autoimmunity. *J Immunol*. 2007;179(7):4313-4317.

223. Korn T, Bettelli E, Oukka M, Kuchroo VK. IL-17 and Th17 Cells. *Annu Rev Immunol*. 2009;27:485-517.

224. O'Shea JJ, Murray PJ. Cytokine signaling modules in inflammatory responses. *Immunity*. 2008;28(4):477-487.

225. Seki Y, Hayashi K, Matsumoto A, et al. Expression of the suppressor of cytokine signaling-5 (SOCS5) negatively regulates IL-4-dependent STAT6 activation and Th2 differentiation. *Proc Natl Acad Sci U S A*. 2002;99(20):13003-13008.

226. Brender C, Columbus R, Metcalf D, et al. SOCS5 is expressed in primary B and T lymphoid cells but is dispensable for lymphocyte production and function. *Mol Cell Biol*. 2004;24(13):6094-6103.

227. Nicholson SE, Willson TA, Farley A, et al. Mutational analyses of the SOCS proteins suggest a dual domain requirement but distinct mechanisms for inhibition of LIF and IL-6 signal transduction. *EMBO J*. 1999;18(2):375-385.

228. Guo H, Ingolia NT, Weissman JS, Bartel DP. Mammalian microRNAs predominantly act to decrease target mRNA levels. *Nature*. 2010;466(7308):835-840.

229. Lagos-Quintana M, Rauhut R, Yalcin A, Meyer J, Lendeckel W, Tuschl T. Identification of tissue-specific microRNAs from mouse. *Curr Biol*. 2002;12(9):735-739.

230. Sanuki R, Onishi A, Koike C, et al. miR-124a is required for hippocampal axogenesis and retinal cone survival through Lhx2 suppression. *Nat Neurosci*. 2011;14(9):1125-1134.

231. Ledderose C, Mohnle P, Limbeck E, et al. Corticosteroid resistance in sepsis is influenced by microRNA-124--induced downregulation of glucocorticoid receptor-alpha. *Crit Care Med*. 2012;40(10):2745-2753.

232. Chahrour M, Zoghbi HY. The story of Rett syndrome: from clinic to neurobiology. *Neuron*. 2007;56(3):422-437.

233. Friez MJ, Jones JR, Clarkson K, et al. Recurrent infections, hypotonia, and mental retardation caused by duplication of MECP2 and adjacent region in Xq28. *Pediatrics*. 2006;118(6):e1687-1695.

234. Yang T, Ramocki MB, Neul JL, et al. Overexpression of Methyl-CpG Binding Protein 2 Impairs TH1 Responses. *Sci Transl Med*. 2012;4(163):163ra158.

235. Tudor M, Akbarian S, Chen RZ, Jaenisch R. Transcriptional profiling of a mouse model for Rett syndrome reveals subtle transcriptional changes in the brain. *Proc Natl Acad Sci U S A*. 2002;99(24):15536-15541.

236. Ballestar E, Ropero S, Alaminos M, et al. The impact of MECP2 mutations in the expression patterns of Rett syndrome patients. *Hum Genet*. 2005;116(1-2):91-104.

237. Traynor J, Agarwal P, Lazzeroni L, Francke U. Gene expression patterns vary in clonal cell cultures from Rett syndrome females with eight different MECP2 mutations. *BMC Med Genet*. 2002;3:12.

238. Gibson JH, Slobedman B, K NH, et al. Downstream targets of methyl CpG binding protein 2 and their abnormal expression in the frontal cortex of the human Rett syndrome brain. *BMC Neurosci*. 2010;11:53.

239. Ben-Shachar S, Chahrour M, Thaller C, Shaw CA, Zoghbi HY. Mouse models of MeCP2 disorders share gene expression changes in the cerebellum and hypothalamus. *Hum Mol Genet*. 2009;18(13):2431-2442.

240. Restifo NP, Dudley ME, Rosenberg SA. Adoptive immunotherapy for cancer: harnessing the T cell response. *Nat Rev Immunol*. 2012;12(4):269-281.

241. Fourcade J, Sun Z, Benallaoua M, et al. Upregulation of Tim-3 and PD-1 expression is associated with tumor antigen-specific CD8+ T cell dysfunction in melanoma patients. *J Exp Med*. 2010;207(10):2175-2186.

242. Woo SR, Turnis ME, Goldberg MV, et al. Immune inhibitory molecules LAG-3 and PD-1 synergistically regulate T-cell function to promote tumoral immune escape. *Cancer Res*. 2012;72(4):917-927.

243. Thomas DA, Massague J. TGF-beta directly targets cytotoxic T cell functions during tumor evasion of immune surveillance. *Cancer Cell*. 2005;8(5):369-380.

244. Bronevetsky Y, Villarino AV, Eisley CJ, et al. T cell activation induces proteasomal degradation of Argonaute and rapid remodeling of the microRNA repertoire. *J Exp Med*. 2013;210(2):417-432.

245. Hoy AM, Buck AH. Extracellular small RNAs: what, where, why? *Biochem Soc Trans*. 2012;40(4):886-890.

246. Freeman AF, Holland SM. Clinical manifestations, etiology, and pathogenesis of the hyper-IgE syndromes. *Pediatr Res*. 2009;65(5 Pt 2):32R-37R.

247. Percy AK, Lee HS, Neul JL, et al. Profiling scoliosis in Rett syndrome. *Pediatr Res*. 2010;67(4):435-439.

248. Zhou H, Newnum AB, Martin JR, et al. Osteoblast/osteocyte-specific inactivation of Stat3 decreases load-driven bone formation and accumulates reactive oxygen species. *Bone*. 2011;49(3):404-411.

Biography

I was born on June 15, 1986 in Huinan, Jilin Province of People's Republic of China. I went to Peking University in 2004 and earned a Bachelor degree of Science in Biological Science in 2008. I was then accepted to the Immunology Ph.D program at Duke University, where I spent the past five years studying T cell-mediated immune response with Dr. Qi-Jing Li.

I have published and/or submitted the following manuscripts in peer-reviewed journals:

1. **Chaoran Li*,** Shan Jiang*, Si-Qi Liu, Erik Lykken, Lin-Tao Zhao, Jose Sevilla, Bo Zhu and Qi-Jing Li. **(* equal contribution)**. MeCP2 enforces Foxp3 expression to determine natural regulatory T cells' resilience to inflammation. 2013 (Submitted)
2. Shan Jiang*, **Chaoran Li***, Gabrielle McRae, Erik Lykken, Jose Sevilla, Siqi Liu, Ying Wan & Qi-Jing Li. **(* equal contribution and listed in an alphabetic order)**. MeCP2 reinforces STAT3 signaling and effector T cell differentiation by controlling miR-124-mediated suppression of SOCS5. 2013 (In revision at *Science Signaling*)
3. Yun Zhang, Pengyuan Yang, Tao Sun, Dong Li, Xin Xu, Yaocheng Rui, **Chaoran Li**, Mengyang Chong, Toni Ibrahim, Laura Mercatali, Dino Amadori, Xincheng Lu, Dong Xie, Qi-Jing Li & Xiao-Fan Wang. miR-126 and miR-126* repress recruitment of mesenchymal stem cells and inflammatory monocytes to inhibit breast cancer metastasis. *Nat Cell Biol*. 15(3):284-94. (2013).
4. **Chaoran Li,** Peter J.R. Ebert & Qi-Jing Li. T Cell Receptor (TCR) and Transforming Growth Factor β (TGF-β) Signaling Converge on DNA (Cytosine-5)-methyltransferase to Control forkhead box protein 3 (foxp3) Locus Methylation and Inducible Regulatory T Cell Differentiation. *J Biol Chem*. 288(26):19127-392012. (2013).
5. Shan Jiang*, **Chaoran Li***, Virginie Olive, Erik Lykken, Feng Feng, Jose Sevilla, Ying wan, Lin He & Qi-Jing Li **(* equal contribution and listed in an alphabetic order)**. Molecular dissection of the miR-17-92 cluster's critical dual roles in promoting Th1 responses and preventing inducible Treg differentiation. *Blood* 118(20):5487-5497. (2011)

6. **Li, Chaoran**, BIEKE Tu-er-xun, CAI Hong, ZHU Yu-xian. Prokaryotic Expression of CFP-10 Protein Secreted by *Mycobacterium bovis* and Its Application in the Diagnosis of Bovine Tuberculosis. *Progress in Veterinary Medicine*. 28(8):21-26. (2007) (Chinese)

I have received the following awards and honors:

Travel Award for Immunology 2013 (Annual AAI meeting), Honolulu, Hawaii. May. 2013.

1st place, D. Bernard Amos Research Awards, Duke University. May. 2012.

2012-2013 Duke Scholars in Infectious Diseases. Apr. 2012.

Travel Award for Research Center for Allergy and Immunology (RCAI). International Summer Program 2012, RIKEN, Japan. Feb. 2012.

Nominee of Howard Hughes Medical Institute-International Student Research Fellowships. Duke University. Nov. 2010.

Chancellor's Scholarship, Duke University. Sept. 2008.

President's Research Fellowship for Undergraduates, Peking University. Jun. 2006.